Master Thesis in Geosciences

Northeastern Brazilian margin: regional tectonic evolution based on integrated analysis of seismic reflection and potential field data and modelling

by

Olav Antonio Blaich

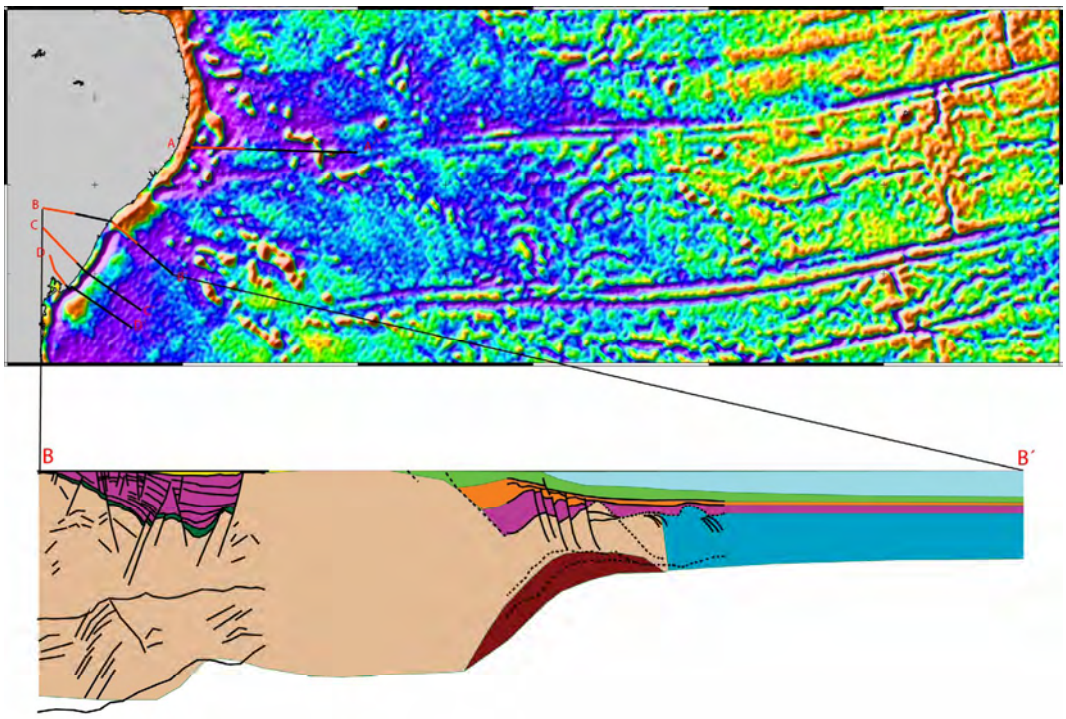

UNIVERSITY OF OSLO

FACULTY OF MATHEMATICS AND NATURAL SCIENCES

Northeastern Brazilian margin: regional tectonic evolution based on integrated analysis of seismic reflection and potential field data and modelling

by

Olav Antonio Blaich

Master Thesis in Geosciences

Discipline: Petroleum Geology and Geophysics

Department of Geosciences

Faculty of Mathematics and Natural Sciences

UNIVERSITY OF OSLO

[June 2006]

Contents

Preface

The Master Thesis presents results derived from an integrated analysis of seismic reflection and potential field data and modelling on the Northeastern Brazilian margin. The work was carried out at the Department of Geosciences, University of Oslo under the supervision of Prof. Jan Inge Faleide and Assoc. Prof. Filippos Tsikalas.

Acknowledgements

First of all, I would like to thank my beautiful and beloved Ingerid Elgesem Bjelland for all support and encouragement during this work.

I owe special thanks to Prof. Jan Inge Faleide for supervising me during this work, and providing constructive and very interesting discussions. I also owe special thanks to Assoc. Prof. Filippos Tsikalas for the very hard work providing me with technical support and continuous feedback. He is responsible for the long, hardworking days at the Department.

Thanks to Oliver Ritzmann, Jonas Wilson, Asbjørn Breivik, Øyvind Marcussen and Ivar Midtkandal for technical support and discussions. Thanks also to my fellow students for all the fun and company during these years.

University of Oslo, June 2006

Olav Antonio Blaich

Chapter 1
Introduction

The South Atlantic rift system developed during the Mesozoic breakup of Africa and South America. These continental masses belonged to the Gondwana Palaeozoic super-continent. Rifting started in the south, and propagated toward the north. Lithospheric stretching and rifting in northeastern Brazil culminated with the onset of sea floor spreading, which probably occured in late Aptian to early Albian times and took place along transform fractures in the equatorial rift zone (Chang et al., 1992).

The South Atlantic rift system created two very different margins around Brazil: the North and East Brazilian margins. The North Brazilian Equatorial margin evolved in response to strike-slip motion between Brazil and Africa, resulting in complex shear-dominated basins. In contrast, the East Brazilian margin, evolved into a passive margin, as a consequence of orthogonal crustal extension (Chang et al., 1992). This part of the margin, also called the East Brazil Rift system (EBRIS) consists of rifted continental margin basins, which include from south to north the Pelotas, Santos, Campos, Espírito Santo, Mucuri, Cumuruxatiba, Jequitinhonha, Camamu/Almada, Jacuípe, and Sergipe-Alagoas basins. The Recôncavo, Tucano and Jatobá intra-continental (aulacogene) rift basins are also included in EBRIS. In this thesis, the study is primarily concentrated in the offshore Jacuípe, Sergipe-Alagoas Basins and the onshore Recôncavo, Tucano and Jatobá basins (Fig. 1.1 and Fig. 1.2).

Rift-related volcanism was voluminous along the southern margin of Brazil (Pelotas, Santos, Campos and Espírito Santos basins), but almost absent during the Neocomian-Barremian rift phase of the northeastern margin (Chang et al., 1992).

The reconstruction of plate motion during the early stage of seafloor spreading and demarcation of the boundary between continental and oceanic crust is controversial for the South Atlantic margins. This is due to the presence of a wide magnetic quiet zone from early

Aptian to Campanian times, preventing the studies of seafloor spreading anomalies immediately adjacent to the continental margin (Chang et al., 1992). Another problem in imaging and analysing the syn-rift structures and the continent-ocean boundary location and character is the presence of diapiric salt along much of the South Atlantic margins, complicating and obliterating seismic imaging (Katz et al., 2000).

The integration of potential field and regional deep seismic data has been extensively applied in many sedimentary basins worldwide as a refinement of structural and stratigraphic studies. Potential field data are powerful resources for reducing costs and interpretation risks when petroleum exploration advances towards new frontiers. It helps to characterize the transition between continental and oceanic crust, refine the crustal architecture of sedimentary basins, locate major depocenters, and identify master fault zones, all of which are crucial in the evaluation of new exploratory frontiers in the ultra-deep water province of the petroleum system in the South Atlantic (Mohriak et al., 2000).

The sedimentary basins along the South American and African margins are traditionally considered to be independent basins. With an expanding knowledge of the area, especially with geophysical data, including both seismic and satellite-derived gravity data, both margins and their associated basins have been viewed as having a common, conjugate tectonostratigraphic evolution, upon which local characteristics can be overlain (Katz et al., 2000).

Based on integrated analysis of seismic reflection, potential field data and modelling the aims of this thesis are to: (1) study and model the crustal structure; (2) refine the continent-ocean boundary/transition; (3) refine the tectonic and structural setting; (4) refine the margin segmentation due to a number of transfer systems and within a framework of simplified plate reconstruction; and finally (5) discuss the architecture and development of the conjugate margins.

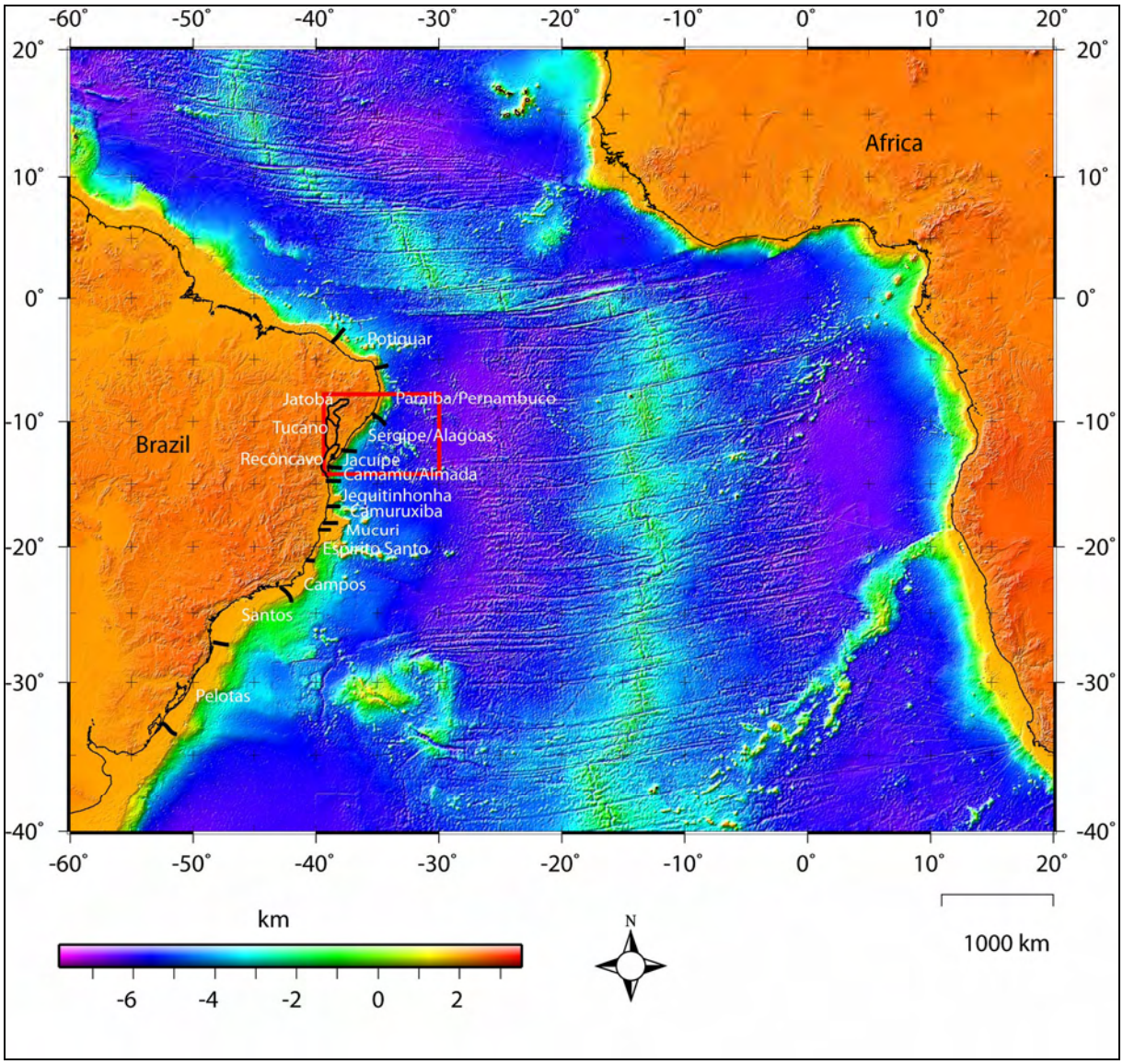

Fig. 1.1: 1x1 minute elevation grid (GEBCO, General Bathymetric Chart of the Oceans; Jakobsson et al., 2000). Rectangular outlines the study area. The location of sedimentary basins along the East Brazilian margin is also indicated.

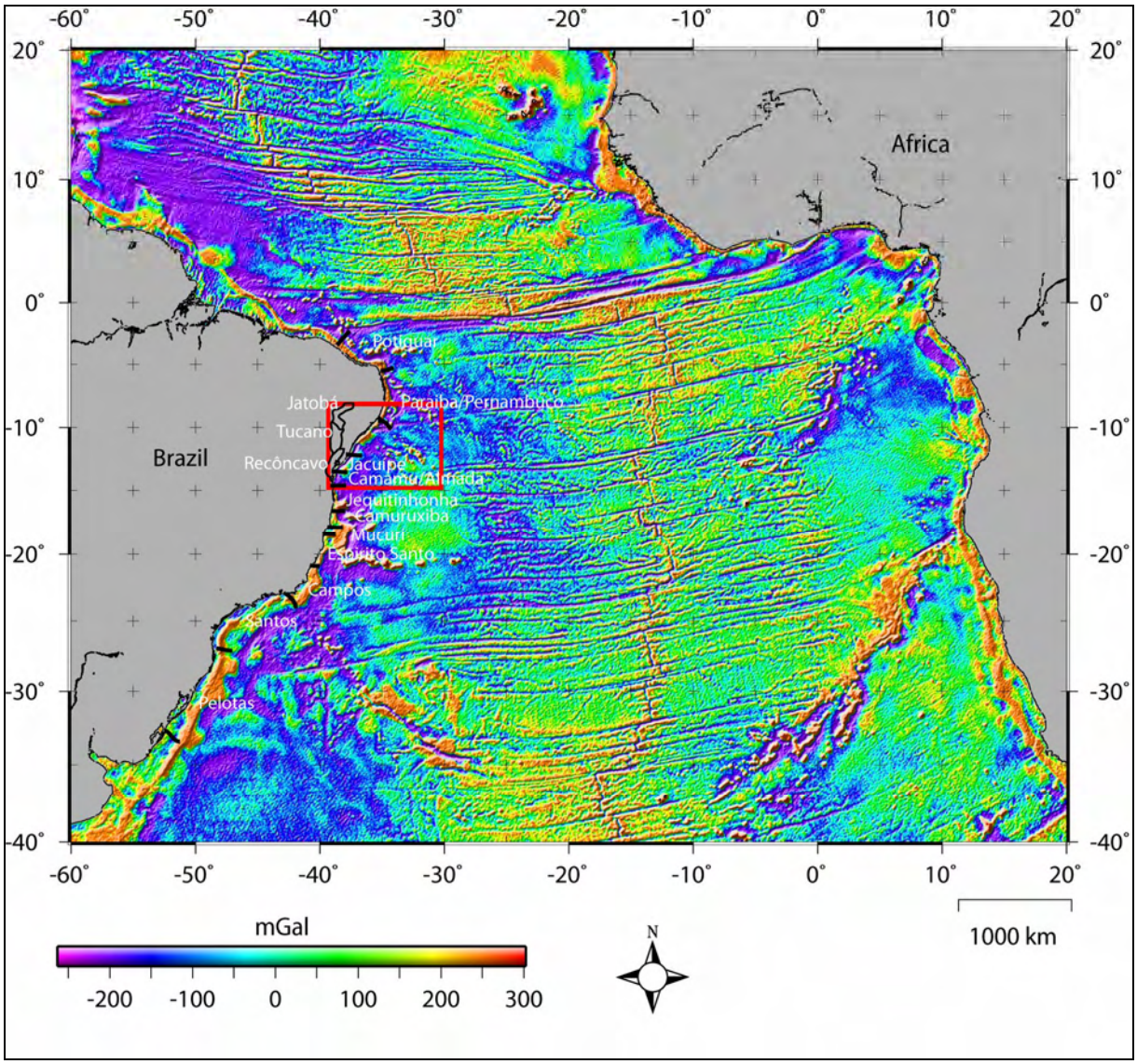

Fig. 1.2: 1x1 minute gridded satellite-radar-altimeter free-air gravity anomaly field (Sandwell & Smith, 1997; version 10.1). Rectangular outlines the study area.

Chapter 2

Geological framework

The Gondwana super-continent formed in Neoproterozoic time as a result of the Braziliano/Pan-African orogeny. The São Francisco-Congo craton is interpreted as being the interior and stable portion of the tectonic plates that by a serious of collisions formed the western part of the Gondwana continent (Alkmim, 2004). In the Precambrian, the Braziliano orogeny reached a climax in which the northeastern region of Brazil was affected by lithospheric convergence. During the Paleozoic, the northeastern region was affected by a relatively small but regional intracratonic subsidence creating accommodation space for deposition of sediments (Mohriak et al., 2000).

The South Atlantic rift system developed in the Mesozoic time due to the breakup of the Gondwana Palaeozoic supper-continent. Regionally, the South American divergent continental margin is limited to the north by transcurrent movements associated with oceanic fracture zones located in the equatorial segment of the Atlantic, and to the south by fracture zones in the Malvinas (Falkland) Plateau. Due to the presence of a wide magnetic quiet zone (constant magnetic polarity) from early Aptian to Campanian times, preventing construction of distinct and recognizable seafloor spreading magnetic anomalies, reconstruction of plate motion during the early drift stage, and the continent-ocean boundary (COB) location are subjects of a long-lasting debate (Chang et al., 1992). This setting is further complicated due to the presence of diapiric salt and syn-rift volcanic rocks along much of the South Atlantic margin blurring seismic reflection imaging and resolution.

Based on mapping of Mesozoic linear magnetic anomalies along the continental margins south of the Walvis-São Paulo ridges, Rabinowitz & La Brecque (1979) suggested a model of a rigid plate motion with a minimum stretching of continental crust during the early opening of the southern South Atlantic Ocean. They suggested a rotation pole for South Atlantic

located at 2.5° S, 45.0 ° W, and an angular rotation of Africa with respect to South America of 11° counter-clockwise. The linear magnetic anomalies were modelled as edge effect anomalies separating oceanic from continental basement. This model predicted a Neocomian E-W motion of the continents south of the Walvis-São Paulo ridges, progressively more NE-SW motion to the north of these ridges, shear-extension in the Sergipe-Alagoas/Niger rift system, and transtension along the eastern- and compression in the western-Equatorial margin. Initiation of seafloor spreading in the South Atlantic was thought to have started during the Late Berriasian-Early Valanginian in the southern part and propagated towards the north, which means that the COB gets progressively younger northward (Fig. 2.1).

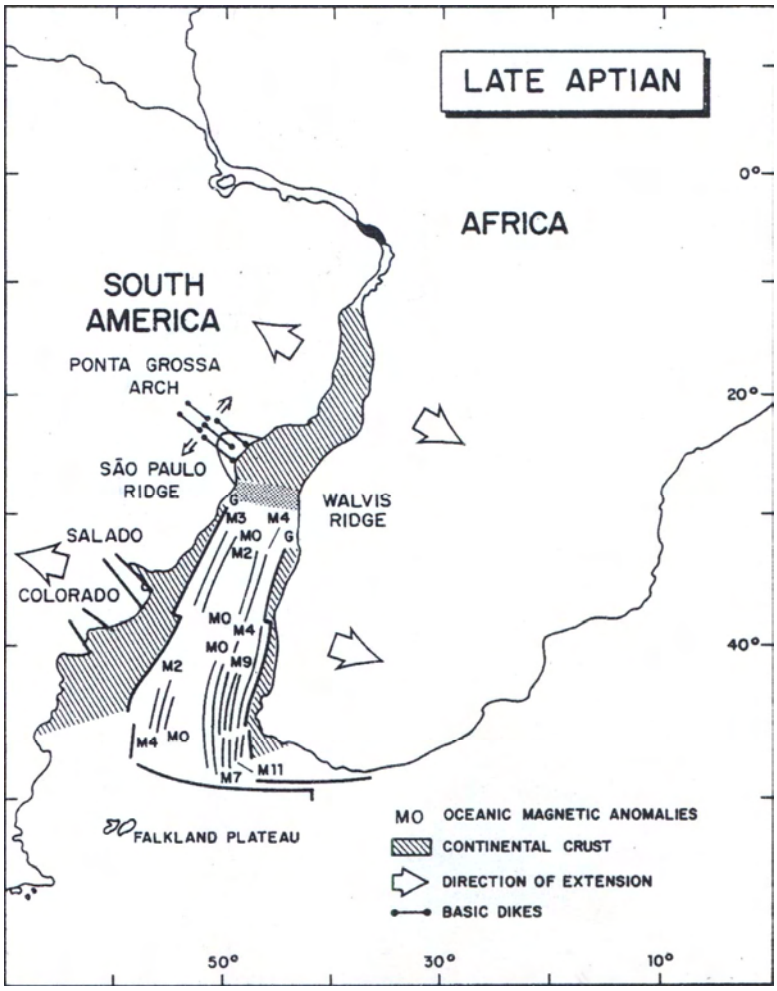

Fig. 2.1: Reconstruction of the South Atlantic in the late Aptian with Mesozoic magnetic lineaments described by Rabinowitz & La Brecque (1979) (Chang et al., 1992).

Based on reflection seismic data, Austin & Uchupi (1982) suggested that the presence of several lineated magnetic anomalies were caused by rifting and local dike intrusion and not to

sea-floor spreading as described by Rabinowitz & La Brecque (1979). The seafloor spreading in the South Atlantic was predicted to have initiated around Valangian-Early Hauterivian to the south of Walvis-São Paulo ridges whereas to the north of it oceanic crust was initially emplaced near Aptian/Albian times, i.e. much later than previously proposed by Rabinowitz & La Brecque (1979). Furthermore, Chang et al. (1992) proposed a model where intraplate deformation due to strain accommodation caused by rotation of South America relative to Africa was not necessary if sea-floor spreading south of the Walvis-São Paulo ridges is accompanied by continental crustal stretching north of it. In this case, intraplate deformation would be only needed to account for the differences in the seafloor spreading rate south of the Walvis-São Paulo ridges and the amount of crustal extension north of it.

By applying an integrated basin modelling approach, combining quantitative kinematic and isostatic basin modelling, Karner & Driscoll (1999) proposed that Mesozoic rifting occurred in three phases: Berriasian-Hauterivian, Hauterivian-late Barremian, and late Barremian-early Aptian. The extension was responsible for the development of two major tectonic hinge zones, an inner-onshore and an outer-offshore hinge zone, both subparallel to the continental margin. The individual rift basins located seaward of the offshore hinge zone, tend to show an en-echelon arrangement. The width of the offshore rift zone, which is defined within the western hinge zone and the continent-ocean boundary, changes dramatically along the Brazilian margin. It is very narrow between the Jequitinhonha to Sergipe-Alagoas basins and abruptly widens across the Maceió Fracture zone (Fig. 2.2). These areas with accentuated rift-zone-width along the Brazilian margin are conjugate to areas with reduced rift-zone-width along the West African Margin (Karner & Driscoll, 1999).

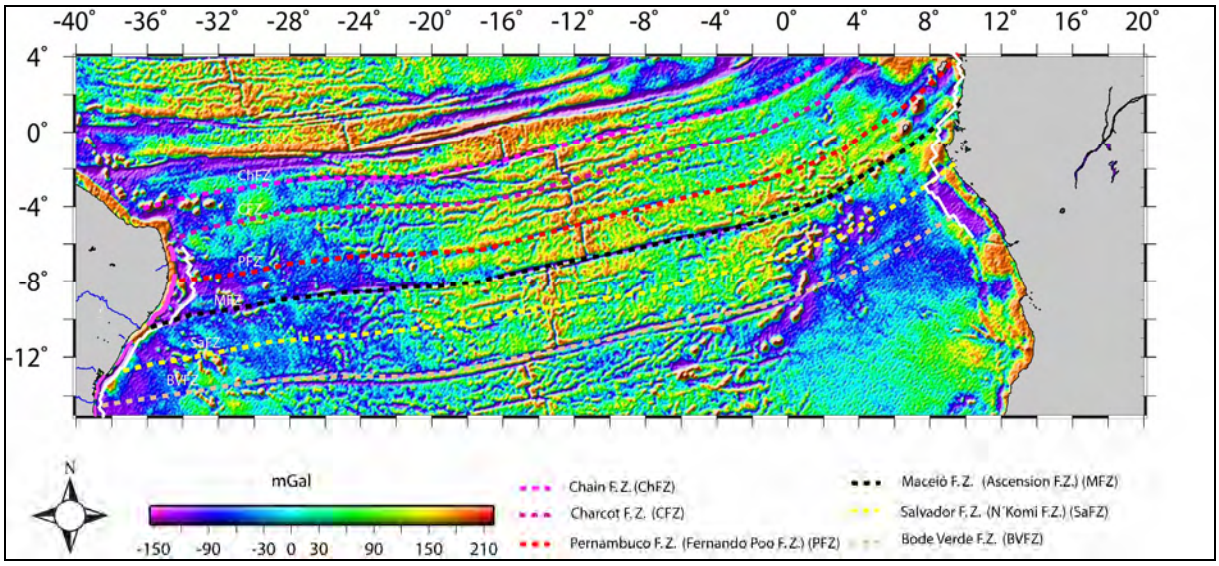

Fig. 2.2: Gravity map showing main continental rift zones. Observe that areas with accentuated rift-zone-width along the Brazilian margin are conjugate to areas with reduced rift-zone-width along the West African Margin. The COT/COB (white line) of the Brazilian side is from Karner & Driscoll (1999) and of the African side from Wilson et al. (2003). Fracture zones are interpreted based on Mohriak et al. (2000); Gomes et al. (1997) and Davison (1999).

2.1. Recôncavo-Tucano-Jatobá and Jacuípe-Alagoas-Sergipe basins

The onshore Recôncavo-Tucano-Jatobá, and the offshore Jacuípe and Alagoas-Sergipe basins are located in the northeastern part of the EBRIS (East Brazil Rift System) and are considered, together with the Campos Basin, to account for the largest hydrocarbon accumulation of the eastern Brazilian margin.

The structural framework of the Sergipe-Alagoas Basin is controlled by fault systems trending NE-SW, interpreted as normal faults, and subsidiary E-W and NW-SE, interpreted as transfer faults (Mohriak et al., 2000). Synthetic normal planar step-faults predominate the basement structure (Chang et al., 1992). A series of small and unconnected en-echelon basins are formed.

The Recôncavo-Tucano-Jatobá rift consists of a series of five asymmetric grabens: Recôncavo, South and Central Tucano, North Tucano and Jatobá (Fig 2.3). Several NW oriented dextral transfer zones segment the Recôncavo, Tucano and Jatobá rift. The opening

of the Recôncavo, Tucano and Jatobá rift took place in a NW direction, oblique to the N-S rift trend. Well defined transfer faults parallel the opening direction and are responsible for the offsetting en-echelon depocenters in the Tucano and Recôncavo basins. The N-S trending South Tucano Graben is separated from the SW-trending Recôncavo Graben by the Aporá, Boa União and Dom João basement-highs. The latter continues to the south and divides the Recôncavo into an eastern and western part (Figs. 2.3 and 2.4). The South and Central Tucano grabens have similar tectonic style and are separated by the Itapicuru transfer fault. The depocenters of these grabens are situated along the eastern border of the rift (Figs. 2.3 and 2.5). The North Tucano Graben is separated from the Central Tucano Graben by an NW-SE trending transfer zone called the Vaza-Barris Arch. The bouguer gravity anomaly of the area indicates that the asymmetry of the grabens flips across the Vaza-Barris Arch, and the depocenter located on the eastern side of the Central Tucano Graben switches to the western side on the North Tucano Graben (Fig. 2.5). The North Tucano Graben is separated from the NE-trending Jatobá Graben by the São Francisco Arch. The depocenter shallows to the northeast where its northern border faults merges with a major basement shear zone (Pernambuco lineament) (Milani & Davison, 1988).

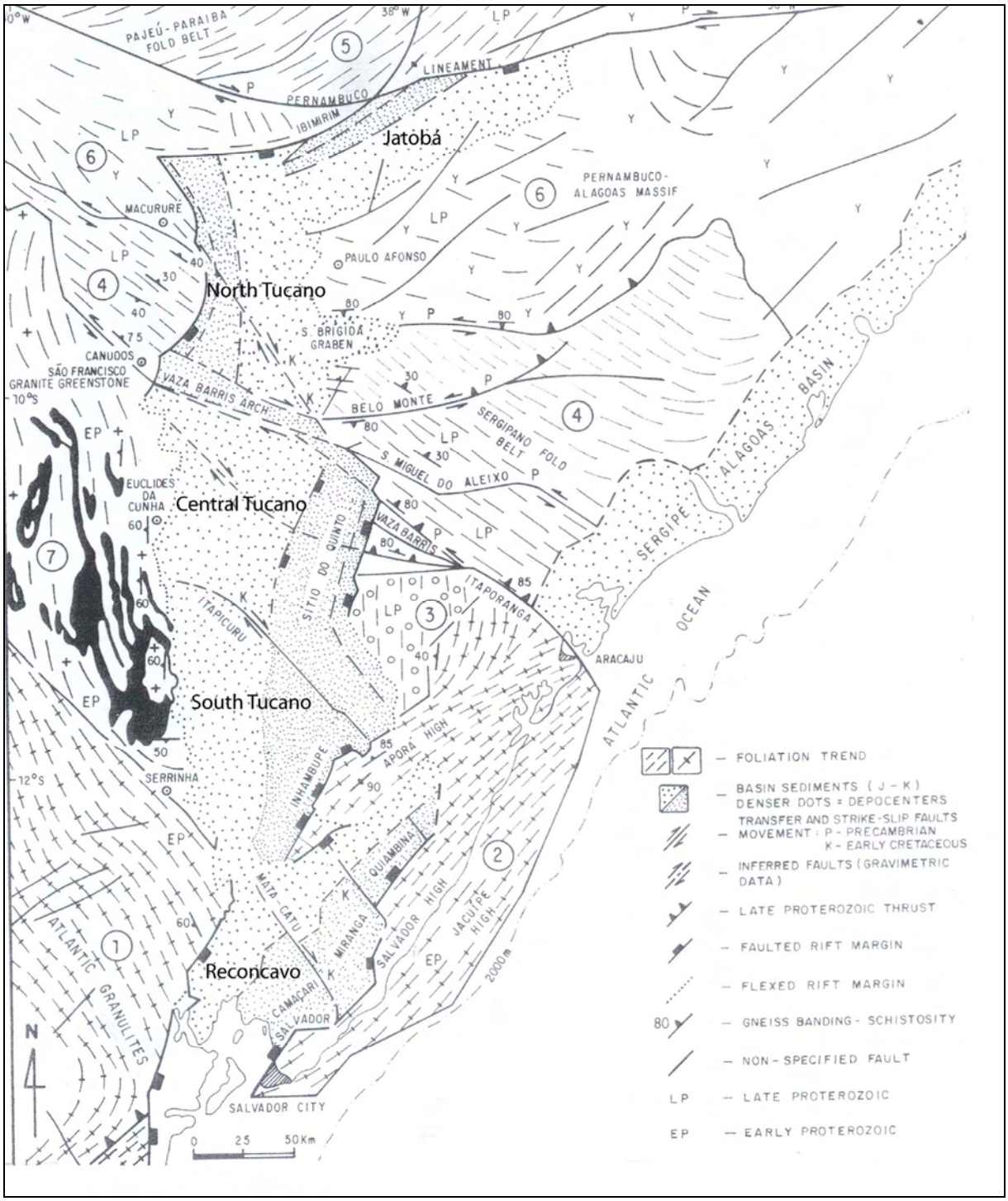

Fig. 2.3: Structural map of the basement surrounding the rift. 1 and 2 – Lower Proterozoic granulites. 3 – Upper Proterozoic sediments. 4 and 5 – Late Proterozoic fold belt. 6 – Reworked gneisses and granulites. 7 – Lower Proterozoic granulite-greenstone terrain. Black areas correspond to the Rio Itapicuru Greenstone Belt (modified from Milani & Davison, 1988).

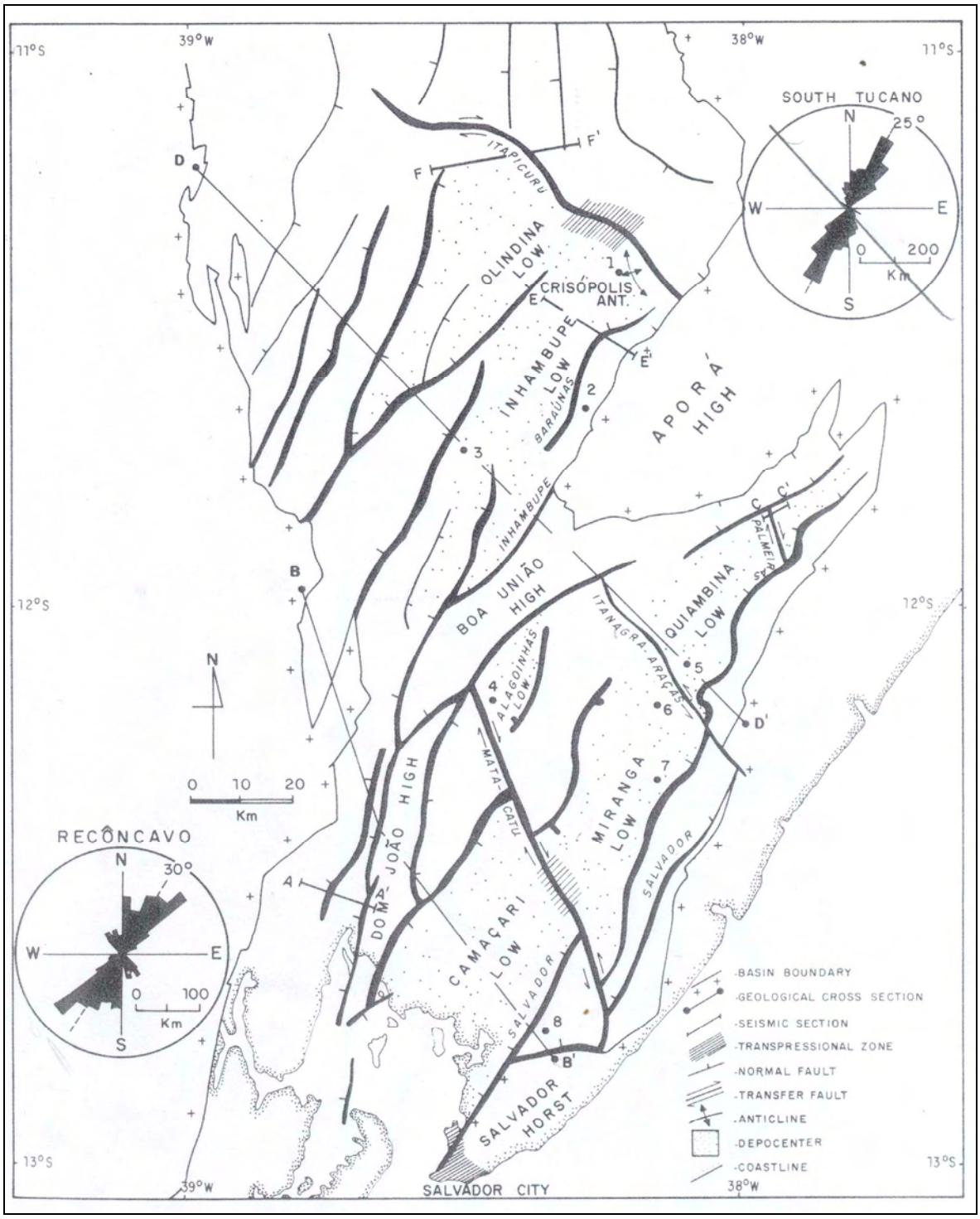

Fig. 2.4: Structure map of the Recôncavo and South Tucano grabens (Milani & Davison, 1988).

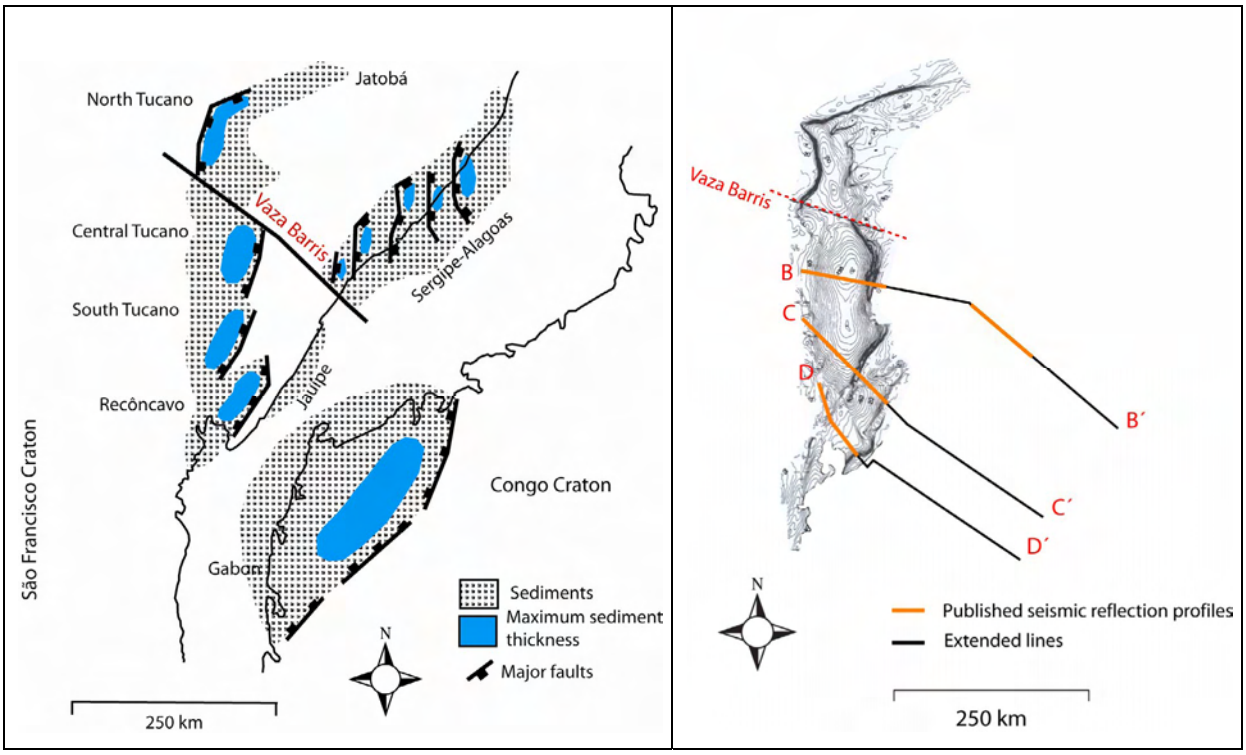

Fig. 2.5: To the left, map showing major fault activity during the Neocomian and depocenter of the grabens (modified from Castro, 1987). To the right, Bouguer anomaly map (Chang et al., 1992), showing strong gradient along the major faults. These pictures indicate that the asymmetry of the grabens flips across the Vaza-Barris Arch, and the depocenter located on the eastern side of the Central Tucano Graben switches to the western side on the North Tucano Graben. The dashed line represents the Vaza-Barris transfer zone.

Two basic models have been proposed for the structural configuration of the Recôncavo, Tucano, Jatobá, Sergipe-Alagoas and Jacuípe basins (Chang et al., 1992). Milani & Davison (1988) proposed that these rifts delimit a microplate which underwent a rigid rotation anticlockwise relative to the São Francisco Craton around a pole located near the eastern termination of the Jatobá Graben (Fig. 2.6). The microplate model implies a concentric extensional stress field, acting upon the Recôncavo, Tucano and Jatobá rift system, thereby generating a set of NE striking normal faults; at the same time sinistral strike-slip motions are activated in the Sergipe-Alagoas Basin. A problem with the microplate rotational model is the lack of the Neocomian strike-slipe motion in the Sergipe-Alagoas Basin (Chang et al., 1992).

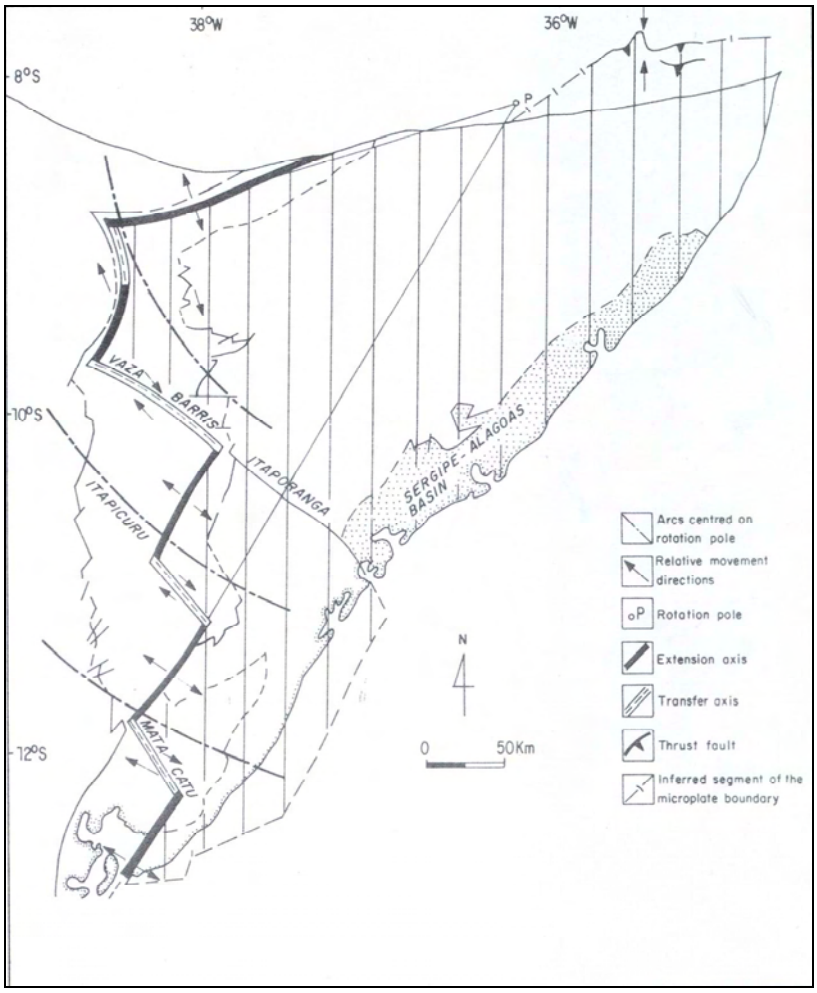

Fig. 2.6: The East Brazilian microplate with rotation pole (Milani & Davison, 1988).

An alternative model accounts for a single homogeneous NW-SE oriented extension, and it is compatible with the structural style of the Sergipe-Alagoas Basin. The general N-S and E-W trend of the major normal faults, separating the deep parts of the basin from the shallow ones, are interpreted as pre-existing crustal weakness zones, which were reactivated under an oblique extensional stress field. This single, rather homogeneous extensional stress field is also compatible with the direction of extension during the Barremian/ earliest Aptian final pulse of rifting (Fig. 2.7) (Chang et al., 1992).

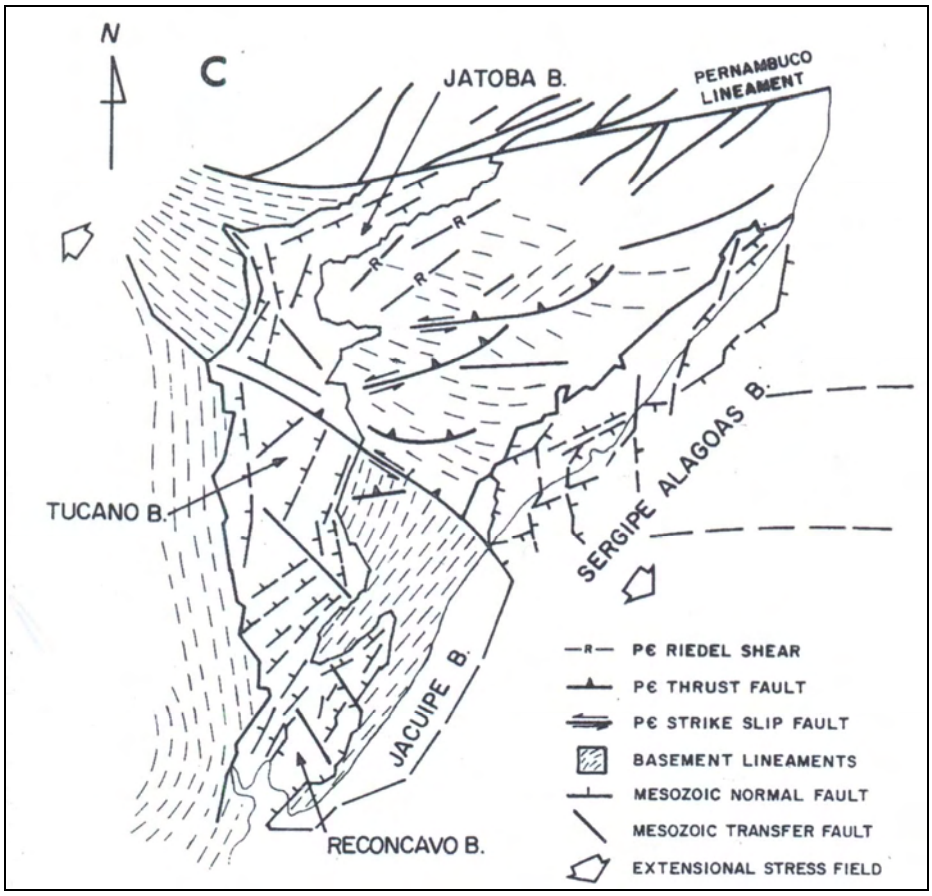

Fig. 2.7: Kinematic model of the northeast EBRIS evolution, proposing a single homogeneous NW-SE extension (Chang et al., 1992).

Based on detailed regional mapping, Mohriak et al. (2000) suggested that the Tucano and the Sergipe basins evolved as a result of regional lithospheric extension during the Neocomian. Extension was first distributed over a wide region, perhaps forming rifts along pre-existing zones of weakness in the crust caused by the Brasiliano tectonic event, and subsequently, focussed along a deeper mantle weak zone, the locus of a posterior plate rupture (Fig. 2.8). Furthermore, Mohriak et al. (2000) proposed a bifurcation of the rift system, associated with a ridge-ridge-ridge (RRR) triple junction. In this model, it is proposed that the rift axis in the offshore region abruptly changes to a more northerly direction near the triple junction. The western branch of the rift system forms the aulacogene onshore Recôncavo, Tucano and Jatobá basins. The eastern branch evolved to form the continental passive margin basins along the South Atlantic margins which include the Jacuípe-Sergipe-Alagoas rift system along the northeastern Brazilian margin and the Gabon-Rio Muni basins in western Africa (Fig. 2.9).

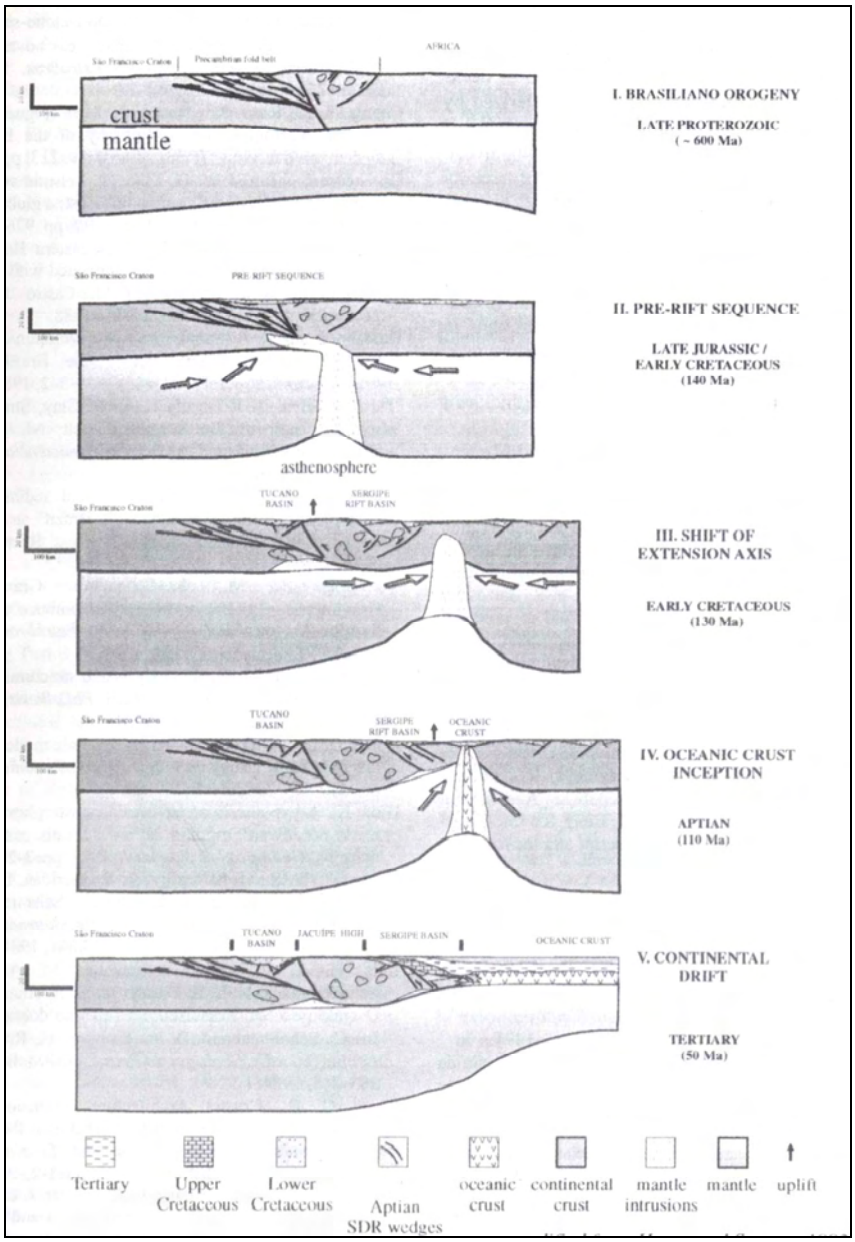

Fig. 2.8: Schematic geodynamic model for the tectonic evolution of the Tucano-Sergipe basins (Mohriak et al., 2000).

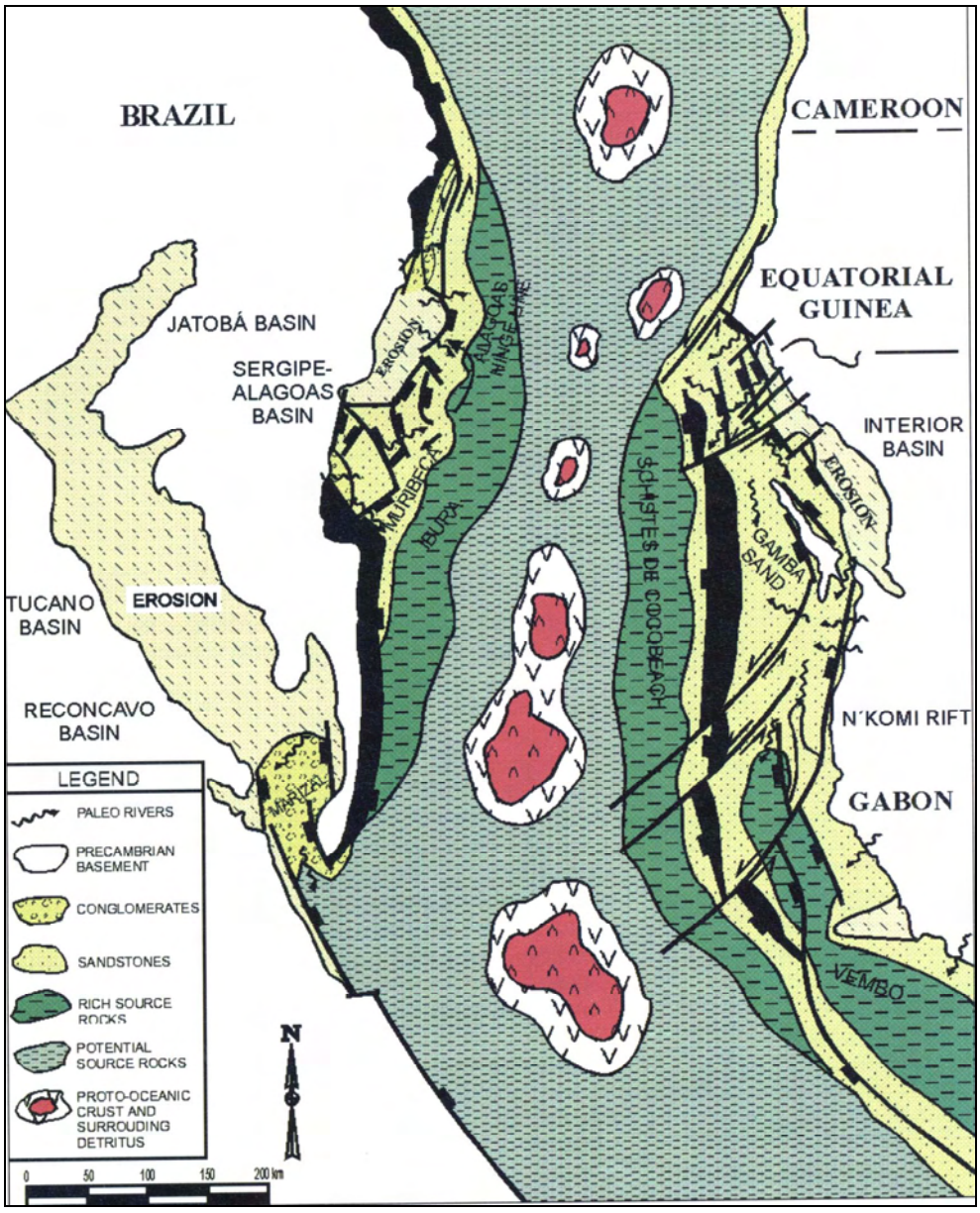

Fig. 2.9: Reconstruction of the rift system between northeastern Brazil and western Africa at the time of oceanic crust inception (late Aptian), showing bifurcation of the spreading axis in two branches (Mohriak et al., 2000).

Ussami et al. (1986) used the simple shear model of Wernicke (1985) to model the East Brazilian continental margin. They proposed that all basins were formed by lithospheric extension during the rifting phase of South Atlantic breakup. Upper crustal extension affected both onshore and offshore basins, but extension at deeper lithospheric levels was concentrated beneath the offshore basins, as evidenced by the degree of thermal subsidence in this area. The offshore and onshore regions were connected by a low angle, crustal detachment surface. In this way, the Tucano aborted rift was located on the lower plate, while the offshore Jacuípe and Gabon basins rode on the upper plate. The asthenospheric rise and the future zone of crustal separation were located between the Jacuípe and Gabon basins, where gravity

modelling suggests considerable crustal extension and Moho upwarp. The Bouguer gravity anomaly map for this area shows that the Recôncavo, Tucano and Jatobá basins are characterized by large-amplitude local negative gravity anomalies indicating low-density sediment infill. There is no indication of upwarping of the underlying Moho immediately beneath these basins (Fig. 2.10).

Castro (1987) proposed a model were the Recôncavo, Tucano, and Sergipe-Alagoas basins in the northeastern Brazil and the Gabon basin in West Africa originated in a double rifting system associated with multiple crustal detachment surfaces, where the direction of detachment dip was reversed at the Vaza-Barris fault system. It was proposed that the rifting geometry in the basins is defined by major extensional stresses, controlled by crustal weakness zones which were affected by the Brasiliano tectonic event. The Gabon-Recôncavo, and southern Tucano half-grabens were characterized by westward dipping master faults whereas the northern Tucano-Sergipe-Alagoas half grabens were characterized by eastward dipping master faults. The Vaza-Barris fault system formed the transition zone between the two half graben systems (Fig. 2.10) (Castro, 1987).

The model proposed by Rabinowitz and La Brecque (1979) requires compression along the northeastern part of South American margin, however, interpretation of seismic data indicates extension facilitated with blocks along normal faults rather than compression in these areas (Castro, 1987). Castro (1987) proposed that the marginal basins in the South Atlantic were formed under a regime of predominantly extensional stresses. Finally, the pure shear extensional model of McKenzie (1978) has been proposed by Guimarães (1988) as the basic mechanism to explain the formation of the passive margin sedimentary basins along the northeastern margin of Brazil.

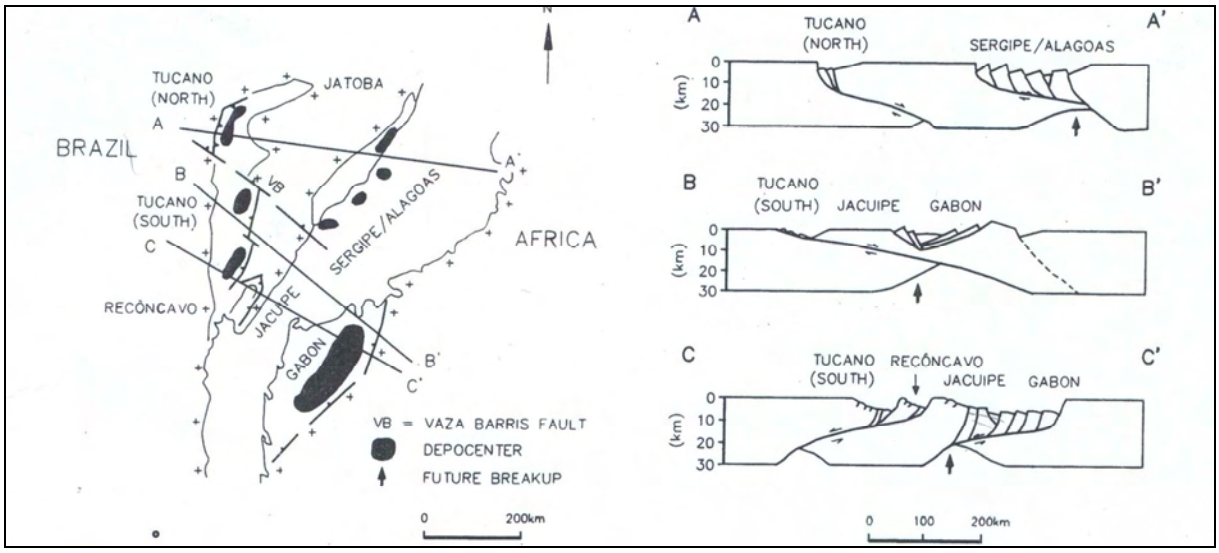

Fig. 2.10: Suggested evolution history of the Tucano-Gabon basin system. Section A-A´ and C-C´ are after Castro (1987) and B-B´ after Ussami et al. (1986) (Chang et al., 1992).

2.2 Magmatism

A volcanic passive margin is characterized by having volcanic activity at the transition between rift and sea-floor spreading and by showing domal uplift during extension. A non-volcanic margin is characterized by little or no-volcanic activity during sea-floor spreading and rapid initial subsidence. Volcanic activity along the Brazilian continental margin is essentially restricted to areas south of 16° S. Syn-rift volcanic rocks are abundant in the Pelotas, Santos, Campos and Espirito Santo basins and also in the conjugate West African Moçamedes and Cuanza basins (Chang et al., 1992). Volcanic activity is thought to have commenced in the Paraná Basin around 150 Ma and peaked around 125-135 Ma.

White & McKenzie (1989) proposed that the production and flow of basaltic magmas onto the adjacent continents can be explained by a simple model of decompression melting of hot asthenospheric mantle as it rises passively beneath the stretched and thinned lithosphere. A hot spot is not always by itself the cause of continental breakup, neither continental rifting always occurs above hot spots. Nevertheless, the presence of a hot spot causes considerable dynamic uplift and additional tensional forces in the lithosphere. White & MacKenzie (1989) proposed that the opening of the South Atlantic occurred right across a mantle plume and its

associated thermal anomaly, generating extensive syn-rift igneous activity on the conjugate margins of both southern Africa and South America.

The northern part of EBRIS is characterized by negligible magmatism, where highly stretched crust is limited to a relative narrow zone. EBRIS is subdivided in two rifting domains, where Campos and Santos are characterized by major domal uplift of the rift flanks evolved by active rifting, while the northern part is characterized by inter-domal areas evolved by passive rifting (Chang et al., 1992).

Mohriak et al. (2000) modelled the Sergipe-Alagoas Basin and found indication of emplacement of seaward dipping reflection (SDR) wedges and volcanic mounds in the deep water region probably located close to the continent-ocean boundary, indicating that this part of EBRIS was also influenced by intense magmatic activity.

The continent-ocean transition changes considerably from the Sergipe-Alagoas basin and up to the Potiguar Basin further north. While the Sergipe-Alagoas basin exhibits indication of intense magmatic activity (Mohriak et al., 2000), the Pernambuco-Paraiba basin evolved without the presence of volcanic-related activity as the ones observed further to the south. This area is located very close to a transform continental margin, where shearing stresses are expected to play an important role reducing the probabilities for the occurrence of SDR sequences at the Pernambuco plateau and adjoining areas (Gomes et al., 1997). Emplacement of SDR sequences is a strong evidence of the occurrence of a typical volcanic margin. Similarly, the Sergipe-Alagoas basin is part of a volcanic margin, characterized by rapid crustal thinning and emplacement of SDR sequences succeeded by a non-volcanic rifted margin, on the Pernambuco Plateau. The latter is marked by a more gradual crustal thinning and no evidence of SDR sequence emplacement (Gomes et al., 1997).

2.3 Generalized stratigraphy of the northeastern Brazilian continental margin

Only pre-rift and syn-rift sediments have been deposited in the Recôncavo, Tucano and Jatobá basins and in the onshore parts of the Sergipe-Alagoas Basin, whereas in the Campos Basin and the offshore part of Sergipe-Alagoas Basin post-rift sedimentary sequences were deposited as well (Fig. 2.14). This means that subsidence of the Recôncavo, Tucano and Jatobá and the onshore part of the Sergipe-Alagoas rift was completed by Early Aptian time, whereas the offshore Sergipe-Alagoas and Campos basins have continued to subside until present time (Chang et al., 1992). Pre-rift (Upper Jurassic to Lower Cretaceous) red beds of the Brotas Group (Itaparica Fm and Tauá Member of the Candeias Fm) reach thicknesses of 1.5 km in the southern Recôncavo Graben and thin progressively north to the Jatobá Graben. Syn-rift sediments, consisting of thick fanglomerates sequences (Salvador Fm), was deposited during the Valanginian when faulting occurred along the eastern margin of the Recôncavo and Tucano grabens. With increase in subsidence rate, a deep-lacustrine environment developed in the basins and shales of the Gomo and Maracangalha units were deposited along with occasional turbidite and fan depositions. The shale units represent the main hydrocarbon source rock in these areas. In Hauterivian, subsidence rates declined and prograding delta fans filled the lakes (Ilhas Fm). The rift phase terminated with fluvial deposits of the Marfim and São Sebastião Fm. The Marizal Fm (fluvial conglomerates deposits) was deposited during the Aptian, and it is interpreted as a veneer of a post-rift depositional sequence (Milani & Davison, 1988) (Fig. 2.11).

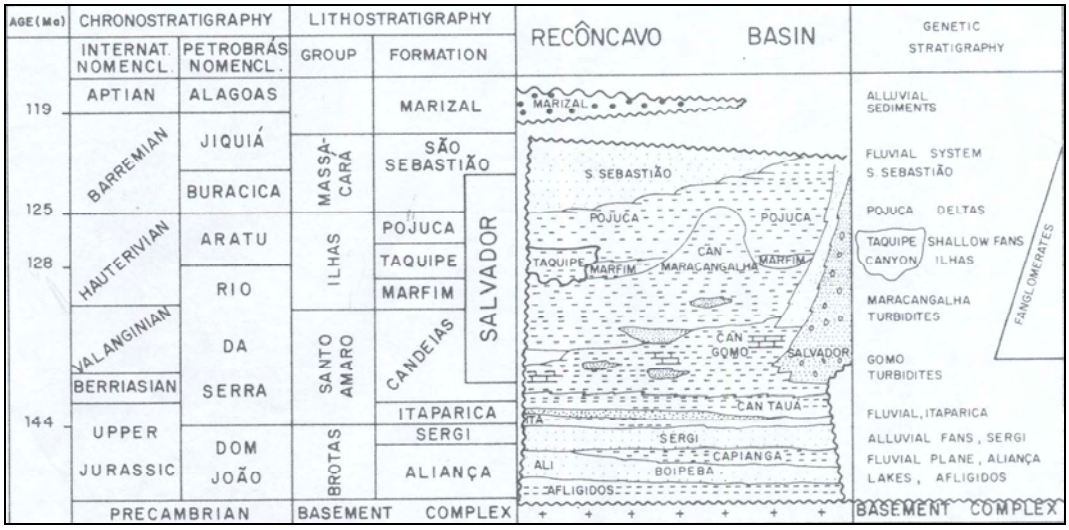

Fig. 2.11: Stratigraphy of the Recôncavo Graben (Milani & Davison, 1988).

The evolution of the northeastern Brazilian basins is best described if the sedimentation record is subdivided into five mega-sequences namely the pre-rift; the syn-rift (or continental); the transitional (or evaporitic); the transgressive marine; and the regressive marine (Mohriak et al., 2000; Chang et al., 1992):

- The pre-rift mega-sequence outcrops onland along the borders of the rift system. It consists of strata ranging from Paleozoic (mainly Carboniferous-Permian) to Mesozoic (mainly Late Jurassic-Early Cretaceous). The Permian-Carboniferous sequence includes a siliciclastic section with glacial sediments (Batinga Formation). The Upper Jurassic sequence is dominated by red beds at its base (Bananeiras Formation) and grading upward into fluvial-eolian sedimentary rocks (Serraria Formation). A Jurassic unconformity is dividing the sequences (Mohriak et al., 2000).

- The syn-rift mega-sequence is best known in the Campos, Recôncavo and Sergipe-Alagoas basins. It was deposited in a large depression known as the African-Brazilian Depression. These huge N-S trending topographic lows were rapidly filled by a complex package of coarse-grained fluvial and alluvial fan deposits (Chang et al., 1992). This mega-sequence is composed by a prograding lacustrine sequence (Barra de Itiúpia Formation) grading into a siliciclastic-carbonate sequence (Morro do Chaves Formation) and culminating in a predominantly siliciclastic sequence (Coqueiro Seco and Maceió Formation). Coarser siliciclastic deposit associated with major border faults are typical for this mega-sequence and are represented by the Rio Pitanga Formation and the Penedo Formation (Mohriak et al., 2000). To the south of Jequitinhonha Basin, time equivalent sedimentary rocks are replaced by basaltic lava flows (Chang et al., 1992).

- The transitional mega-sequence corresponds to a proto-oceanic stage in the South Atlantic basins. It is characterized by widespread deposition of siliciclastics, carbonates and evaporites (Muribeca Formation) during the first marine incursion in the basin. The Sergipe-Alagoas Basin in the Brazilian margin and its conjugate Rio Muni Basin have been considered to be devoid of salt tectonics. However, elusive structures in the deep-water region may be associated with salt tectonics (Mohriak et al., 2000). In most of the marginal and interior basins, the syn-rift mega-sequence is covered by Aptian sediments of the transitional mega-sequence. An angular unconformity separates these two mega-sequences, marking the

rift/post-rift boundary. Progressive transgression, initiated from the south, led to the development of a narrow seaway along the entire East Brazilian margin north of the Pelotas Basin. The existence of a barrier to water circulation at the Walvis-São Paulo Ridge led to the existence of a very restrictive, euxinic and saline environment along the East Brazilian margin. Massive halites and anhydrites accumulated in the most rapidly subsiding parts of the proto-South Atlantic Basin (Fig. 2.12) (Chang et al., 1992).

- The transgressive marine mega-sequence may be subdivided into an earlier phase I (Aptian-Early Albian) characterized by restricted environments and predominantly carbonate deposition (Riachuelo Formation), with facies variation from proximal siliciclastic (Angico Member) to lagoonal and distal pelitic (Taquari Formation). The subsequent phase II (Late Albian-early Tertiary) was characterized by rising sea level and predominantly siliciclastic depositional environment. The proximal facies are characterized by sandstones (Cotingua Formation), while the platform facies by carbonate rocks (Sapucari Member), and the distal facies by pelagic rocks (Aracaju Formation). This mega-sequence was affected by salt tectonics, which started to play a leading role in the development of different petroleum systems on both sides of the Atlantic by Albian time and strongly influenced Upper Cretaceous sequences (Mohriak et al., 2000).

- The regression marine mega-sequence coincides with the eustatic sea level fall in the early Tertiary. This mega-sequence is made up of three facies: the proximal facies, along the coastal region (Marituba Formation), with predominantly coarse sandstones; the platform facies (Mosqueiro Formation) with mainly limestones; and the distal facies (Calumbi Formation) with mostly shales and interbedded turbidites (Figs. 2.13 and 2.14).

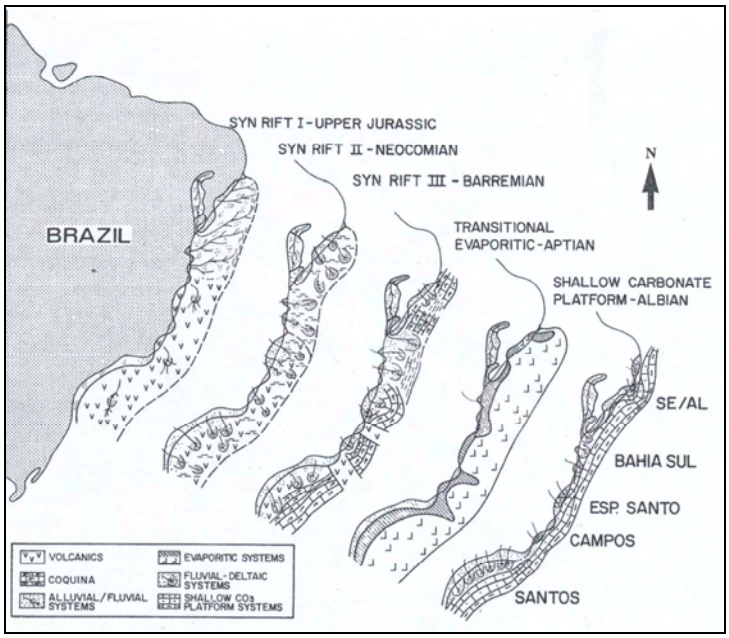

Fig. 2.12: Paleogeographic reconstruction of the syn-rift, post-rift, transitional and transgressive mega-sequences (Chang et al., 1992).

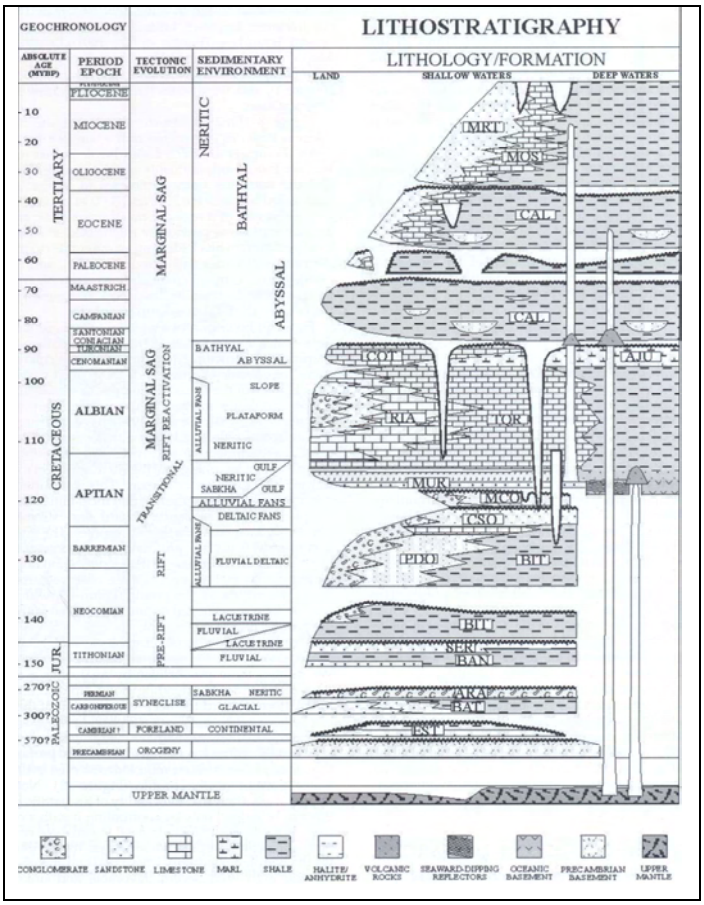

Fig. 2.13: Tectono-stratigraphic column for the Sergipe subbasin. Abreviations of units: EST, Estância; BAT, Batinga; ARA, Aracaré; BAN, Bananeiras; SER, Serraria; BIT, Barra de Itiúba; PDO, Penedo; CSO, Coqueiro Seco; MAC, Maceió; MUR, Muribeca; RIA, Riachuelo; TQR, Taquari; COT, Cotinguaba; AJU, Aracaju; CAL, Calumbi; MOS, Mosquero; MRT, Marituba. To the right, Tucano and Sergipe-Alagoas basins (Mohriak et al., 2000).

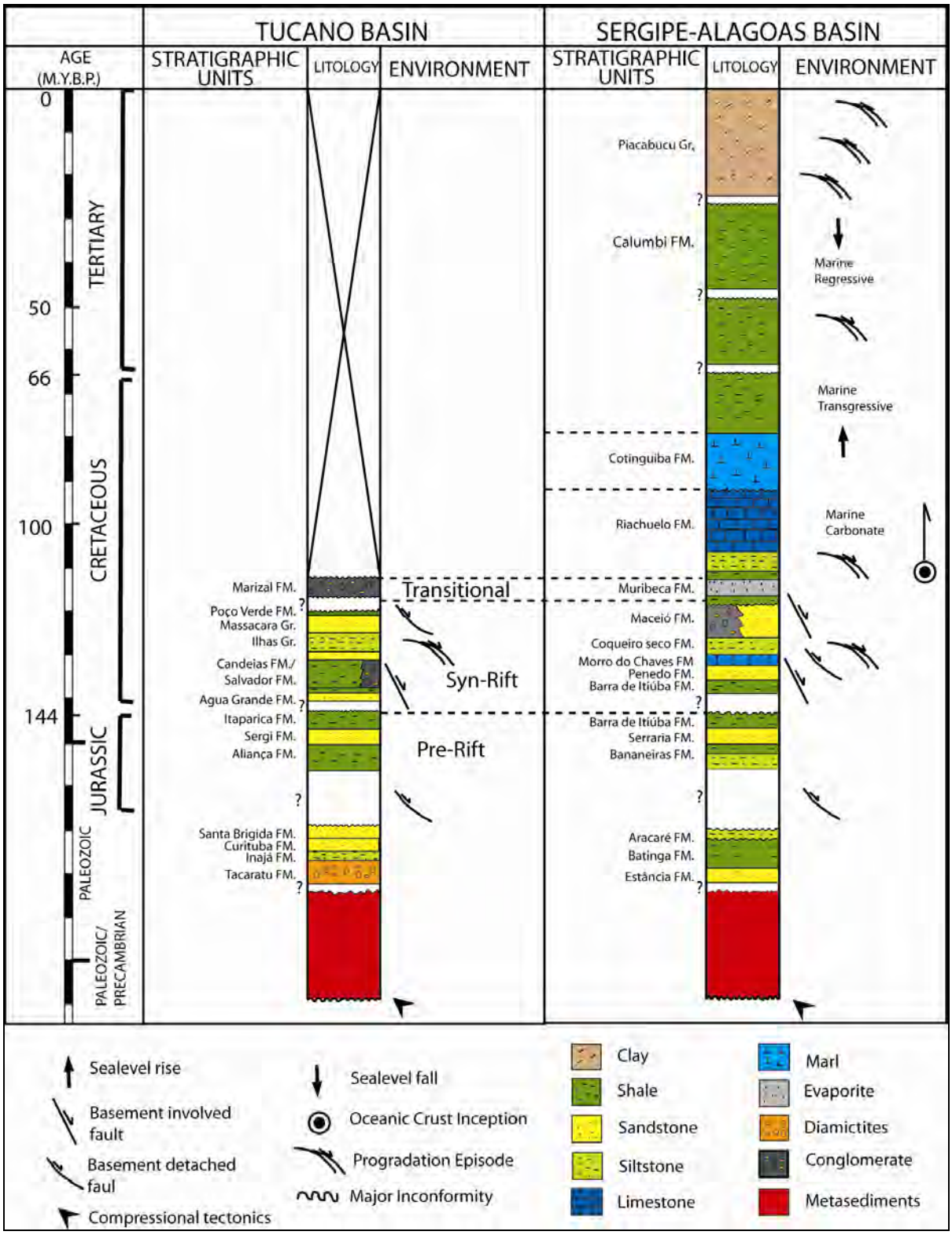

Fig. 2.14: Correlation of the tectono-sedimentary columns of the Tucano/Sergipe-Alagoas basins (modified from Mohriak et al., 2000).

Chapter 3
Data

The geophysical and geological data used in this study include: published seismic reflection data and line-drawing profiles; regional seismic velocity-depth functions; magnetic, gravity and bathymetry from academic ship-tracks (LDEO, Lamont-Doherty Earth Observatory); 1x1 minute gridded satellite-radar-altimeter free-air gravity anomalies (Sandwell & Smith, 1997; version 10.1); 1x1 minute elevation grid (GEBCO, General Bathymetric Chart of the Oceans; Jakobsson et al., 2000); and Bouguer-corrected gravity anomalies extracted from gridded data. Basemaps with location of the published profiles, the coastline of the study area, location of academic ship-tracks and potential field grids were created using GMT (Generic Mapping Tools; Wessel & Smith, 1998) at a Mercator projection. GMT is an academic, interactive software package used in the reduction, management, and visualization of geophysical data. GMT was also used to extract bathymetric, gravity and magnetic data along academic ship-tracks and to extract bathymetric and gravity data along any defined profile in the gridded maps.

3.1 Margin setting

The margin setting of the study area is defined in a series of basemaps. Potential field data can be a powerful supplement to the seismic interpretation, delineating both upper and lower crustal structural trends. In addition, such an integrated approach contributes to the better study and refinement of the COT/COB (continent-ocean transition/boundary) and to the characterization of the basin architecture. The use of potential field data can be crucial in the evaluation of new exploratory frontiers, especially in the ultra-deep water provinces. Potential field data extracted from academic ship-tracks have a better resolution providing a more realistic picture of the causative anomaly. Academic track c1611 provided the bathymetric and potential field data used in the modelling of the offshore part of line C-C´ and D-D´.

Since line B-B´ and A-A´ are not parallel with any academic track, bathymetric and potential field data were extracted from the gridded maps (Fig. 3.1).

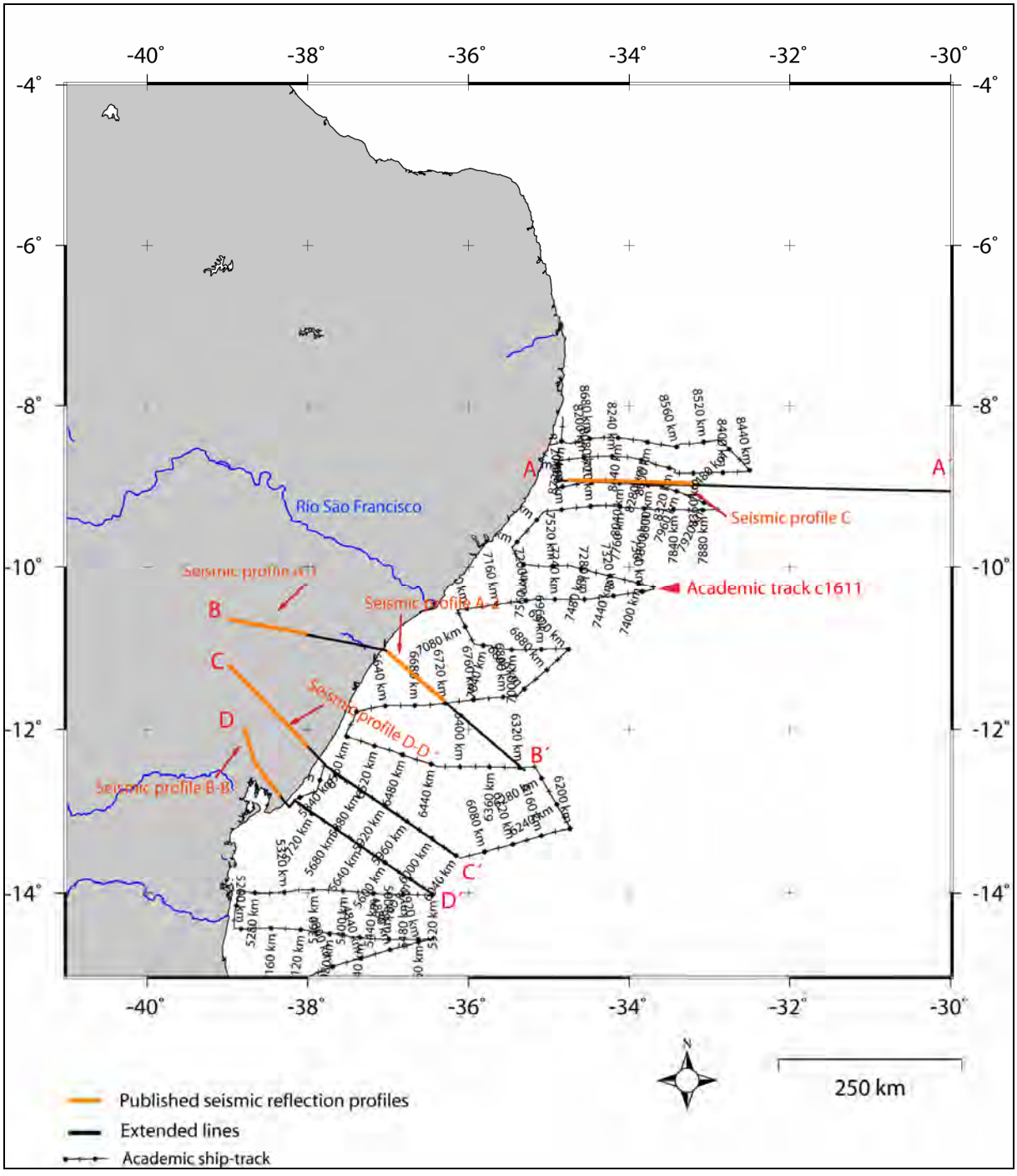

Fig. 3.1: Location of the published seismic reflection profiles, extended lines/profiles and academic track c1611.

In this study, bathymetric and potential field data were used to define an initial Moho relief that was further utilized to gravity model the profiles and to refine the overall structural features of the area and the COT/COB.

3.1.1 Bathymetry

Bathymetric/elevation information, generally for the study area and specifically along the modelled profiles, was extracted both from ship-borne tracks and gridded data. In particular, bathymetric data extracted from academic ship-tracks that are part of the worldwide LDEO database were used to define the exact position of the published profiles along the extended lines and as input in the process of defining an initial Moho relief along the modelled profiles. Furthermore, bathymetry/elevation for the entire study area was extracted from the 1x1 minute GEBCO elevation grid. The bathymetry/elevation basemap (Fig. 3.2) is very useful to define the morphological features in the study area. By comparing it with the free-air gravity anomaly map, many conclusions about the structural trends of the area can be made. Comparing Figures 1.1 and 1.2 it is very clear that the continental margin is delimited by many fracture zones associated with shear movements. Several morphological features are observed along the eastern Brazilian margin. Among the most prominent ones are local elevations located in the ultra deep-water provinces. These features are interpreted as oceanic basement highs (seamounts) (Mohriak, 2004). The continental platform is very shallow in the southern-part (Jacuípe Basin) as indicated by Figure 3.2 and gets progressively wider northward (Alagoas Basin). The Pernambuco Plateau, located northward of line A-A´, is a typical marginal plateau situated at the continental slope and visualized by the bathymetry map (Fig. 3.2). The outer hinge interpreted by Karner et al. (1999) is shown by the bathymetry map (Fig. 3.2) to correspond to the shelf-edge. The bathymetry basemap was also used as input to generate the Bouguer-corrected gravity anomaly map.

Oceanic fracture zones are not visible on bathymetry maps of marginal areas (Fig. 3.2) as they are probably covered by sediments. The fracture zones interpreted on Figure 3.2 are extrapolated from free-air gravity anomaly map and bathymetry map that covered larger areas (Figs. 1.1 and 1.2). These interpretations are also based on publications by Mohriak et al. (2000); Gomes et al. (1997) and Davison (1999).

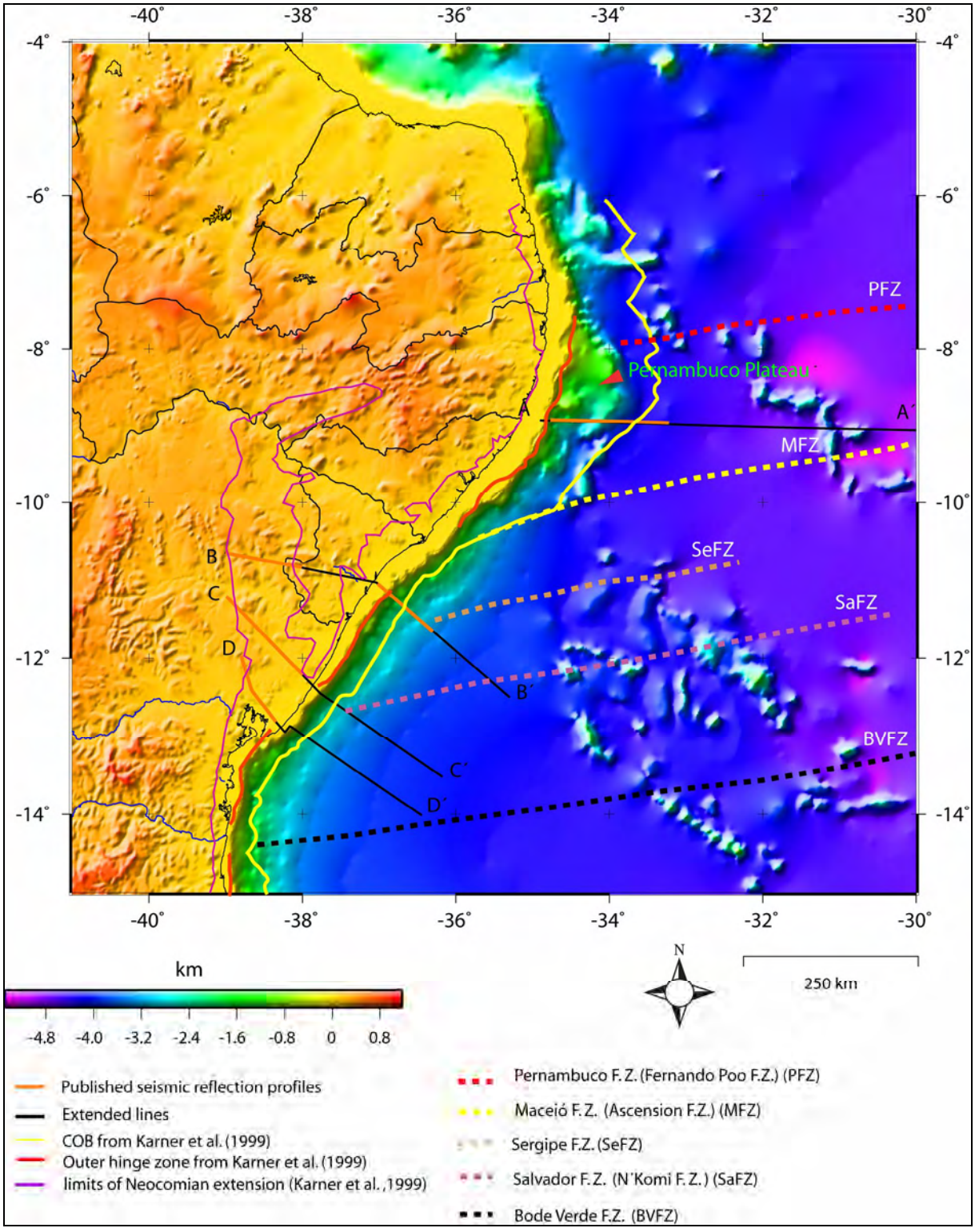

Fig. 3.2: 1x1 minute elevation grid (GEBCO, General Bathymetric Chart of the Oceans; Jakobsson et al., 2000). The outer hinge interpreted by Karner et al. (1999) probably corresponds to the shelf-edge.

3.1.2 Gravity

Gravity data were also derived both from ship-borne profiles and gridded maps. In particular, the gravity data extracted from LDEO academic ship-tracks were used in the process of Moho relief definition and for the gravity modelling of lines C-C´ and D-D´. Furthermore, the 1x1 minute gridded free-air gravity, based on satellite-radar-altimeter (Sandwell & Smith, 1997; version 10.1) was used to generate the gravity basemap for the study area (Fig. 3.3), to define an initial Moho relief and to gravity model line A-A´ and line B-B´. The gridded gravity basemap was also used as input for the Bouguer-corrected gravity anomaly. A comparison between satellite free-air gravity and ship-borne (LDEO) gravity images was proposed by Karner (2000). The analysis showed that the shape, trend and amplitude of the satellite free-air gravity data are in a good agreement with the ship-borne gravity, giving confidence in interpreting crustal structure using satellite free-air gravity (Fig. 3.3).

Gravity anomalies derived from measurements of the variation in acceleration due to gravity pull down over the surface of the Earth. The variation in gravity is produced by lateral variation in subsurface densities and is used to investigate subsurface bodies and structures. Free-air gravity anomaly maps are used to study the morphology and structure configuration of the basement. Gravity anomalies reflects lateral density variations from the surface to the upper mantle. A high/strong gravity anomaly describes a high/strong lateral density variation and can reflect, for example, the geometry of the basement in a faulted area, where the shoulders of the fault block exhibit lateral mass excess (high densities), while the grabens filled with sediments exhibits mass deficiency (low densities). The basement geometry is described by the short wavelength components of the observed gravity anomalies while the overall Moho relief is described by the longer wavelength components.

For Bouguer correction, in the offshore areas, a density of 2.20 g/cm^3 was utilized as infill to the bathymetric relief (Fig. 3.4). A density of 2.67 g/cm^3 was also tested and gave approximately the same result in a regional sense. The purpose of Bouguer-correction is to eliminate the gravity anomaly effect of the bathymetric relief, meaning that the Bouguer-corrected anomalies are not affected by the strong lateral density variation between the water-layer and top-sediments or basement. The result is a better picture of the basement and Moho geometry (Fig. 3.4).

Onshore Bouguer gravity anomalies (Chang et al., 1992) are used in the gravity modelling of the onshore part of line C-C´ and D-D´ in the Recôncavo, Tucano and Jatobá basins. Bouguer gravity anomalies values were picked at each 5 km through the contour map. The data used in the gravity modelling of the onshore part of line B-B´ were based on Bouguer gravity anomalies published by Mohriak et al. (2000).

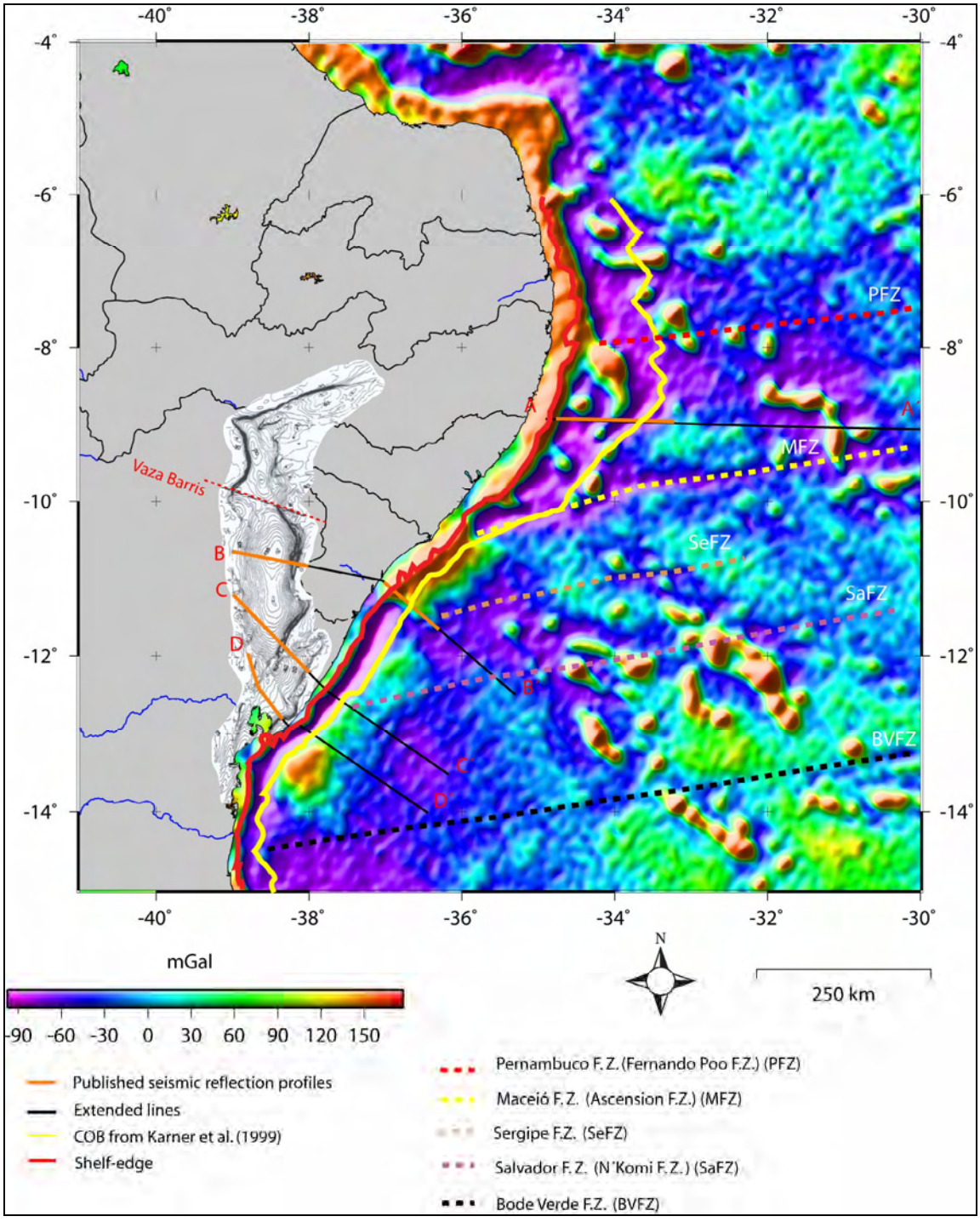

Fig. 3.3: 1x1 minute gridded satellite-radar-altimeter free-air gravity anomaly field (Sandwell & Smith, 1997; version 10.1) and onshore Bouguer gravity anomalies from Chang et al. (1992).

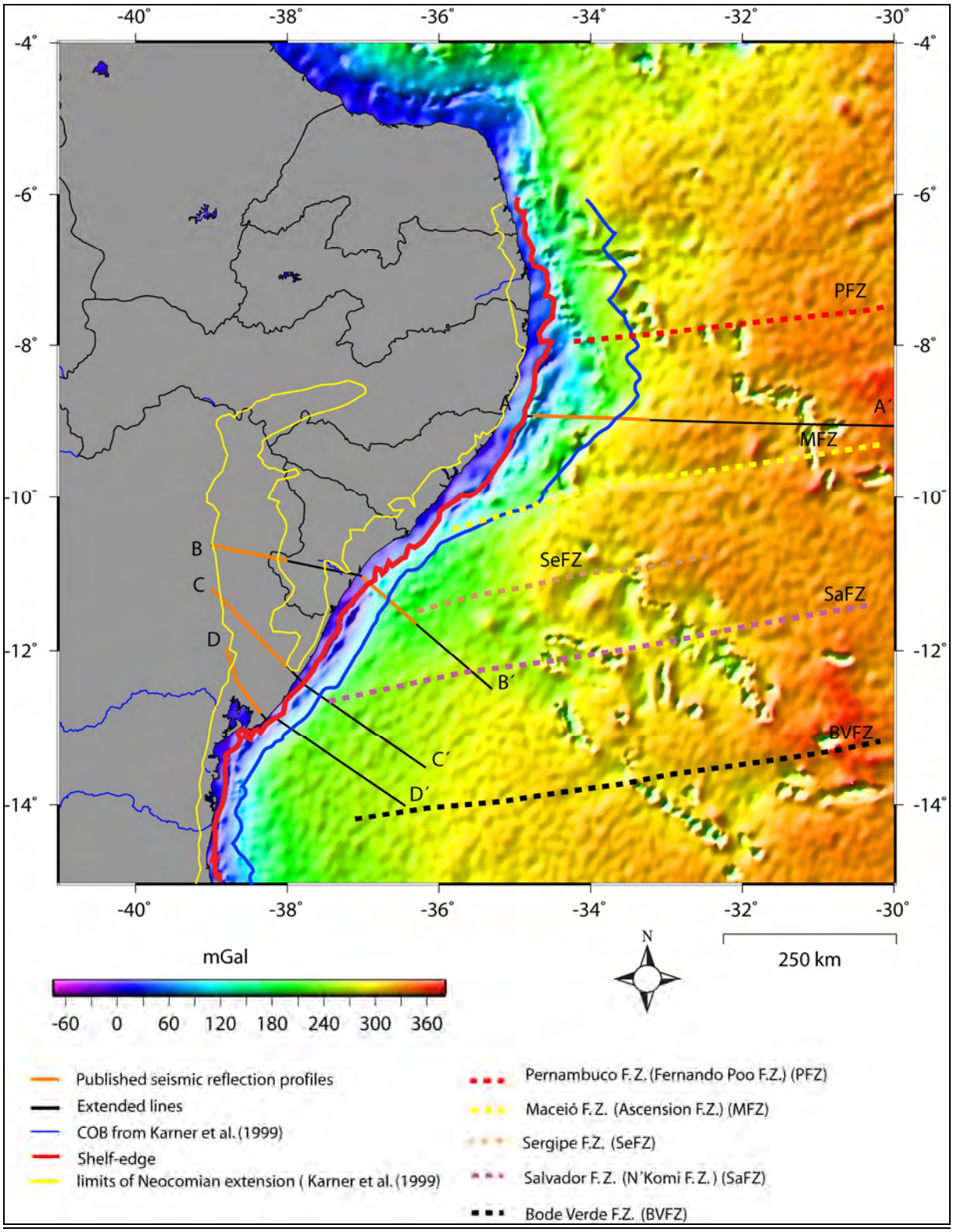

Fig. 3.4: Bouguer-corrected gravity anomaly. COT/COB is indicated by the blue line (from Karner & Driscoll, 1999) and is consistent with the high gradient on the Bouguer anomaly map. Location map showing the major tectonic and structural features along the eastern Brazilian margin. The onshore western Hinge Zone, indicated by a yellow line, demarcates the limit of Neocomian extension and separates continental margin sediments from Precambrian basement.

Two tectonic hinge zones, trending subparallel to the continental margin are presented in Figure 3.4. The trend is only broken by the Recôncavo, Tucano and Jatobá rift system. A hinge zone represents the boundary between a region of negligible deformation from a region characterized by significant normal faulting and accommodation generation (Karner & Driscoll, 1999). The offshore hinge zone (Fig. 3.4, bold red line) consists of a series of high-standing blocks that separate onshore-nearshore basins from deeper water offshore equivalents (Karner & Driscoll, 1999). The same features are interpreted in this study as corresponding to the shelf-edge. The width between the outer hinge zone (shelf-edge) and the continent-ocean boundary changes dramatically along the northeastern Brazilian margin. It is very narrow in the southern areas of Figure 3.4 (Jacuípe Basin) widening abruptly across the Maceió Fracture Zone (Alagoas Basin). The continent-ocean boundary is delineated by a strong positive-negative gradient in the Bouguer anomaly map (Fig. 3.4).

The Maceió Fracture Zone is also clearly identified on the gravity anomaly map (Fig 3.3). Another prominent feature observed on this map is the high amplitude anomalies characterizing the seamounts. The submarine volcanic highs (seamounts) located in the oceanic crust domain are aligned in a E-W and NW-SE directions. These volcanic ridges are related, in one way or another to the oceanic fracture zones (Gomes et al., 1997). During the drift phase, oceanic fracture zones may leak magmas from the mantle which may underplate the lower crust or extrude as seamounts. Finally, the prominent high amplitude anomalies observed parallel and close to the continental margin are “edge-effect” anomalies that characterize the shelf break.

3.1.3 Magnetic

Magnetic data were available along the LDEO ship-tracks. Gridding of all available tracks within the study area resulted in Figure 3.5, exhibiting a complex pattern of magnetic anomalies.

Magnetic anomalies are more complex than gravity ones, due to the fact that they depend on the orientation and latitude of the source-body as well as its geometry and magnetic properties. Rocks that have high contents of the mineral magnetite and are cooled at lower temperatures than the Curie temperature will retain remanent magnetisation, meaning that the rock will retain its magnetisation even in the absence of the causative magnetic field or in the presence of a different magnetic field. Magnetic susceptibility is the ability of a rock to

become temporarily magnetised while a magnetic field is applied. This temporary magnetisation is called induced magnetisation. The value of susceptibility of a rock depends on the type of magnetic minerals and their concentration. The magnetic susceptibility is higher for igneous rocks (Alan et al., 2000). The total magnetisation, representing the magnetic anomaly, will be a vector-summation of the remanent and induced magnetisation. Magnetic anomaly can be used to establish stratigraphic horizons, to identify igneous intrusion, to define the COT/COB and to estimate the depth to the basement. The high-amplitude and narrow magnetic anomalies will usually represent shallow basement, or magmatic intrusions, in contrast to the wide magnetic lows that will usually represent thick sedimentary deposit. However, the chaotic patterns of magnetic anomalies (Fig. 3.5) shows little similarity with the free-air gravity anomaly map (Fig.3.3) and prominent features are not visible on the magnetic anomaly map.

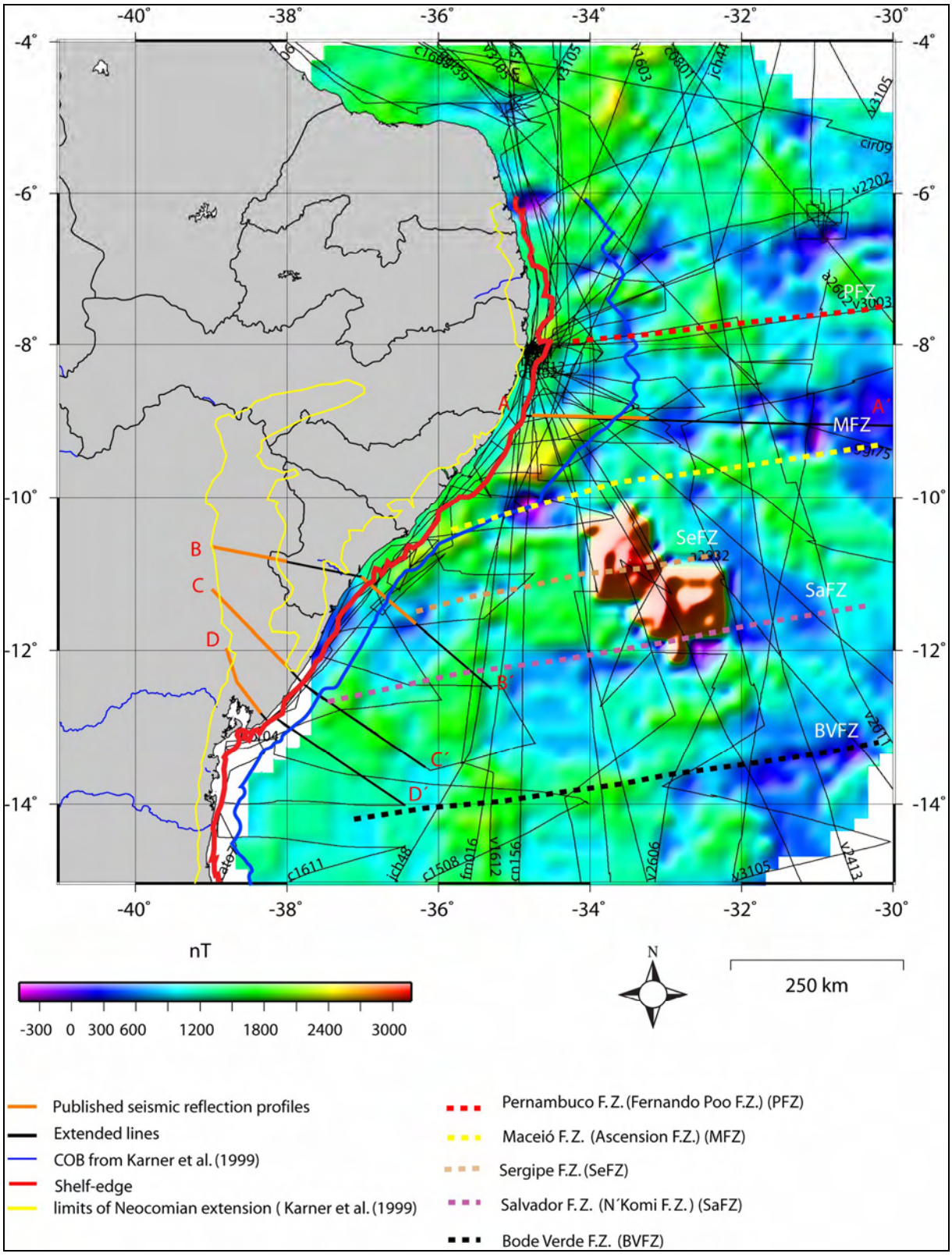

Fig. 3.5: Magnetic anomaly map resulted from gridding all LDEO ship-track.

3.2 Published seismic profiles

Published seismic reflection profiles within the study area were used, and they were extended from mainland all the way to oceanic crust. These profiles were further used for gravity modelling aiming at achieving a broader understanding of the study area. The published profiles are presented in Table 3.1. The location of the published profiles, academic ship-track and the extended lines are presented on Figure 3.1. The published profiles were digitised using the "in-house" software package SECTION (Planke, 1993).

Seismic reflection profile	**Reference**
C (offshore part of line A-A´)	Gomes et al. (1997)
A-1 (onshore part of line B-B´)	Mohriak et al. (2000)
A-2 (offshore part of line B-B´)	Mohriak et al. (2000) Mohriak et al. (2000)
D-D´ (onshore part of line C-C´)	Milani & Davison (1988)
B-B´ (onshore part of Line D-D´)	Milani & Davison (1988)

Table 3.1: Published seismic reflection profiles used in this study.

3.2.1 Seismic profile C

This seismic profile (Fig. 3.6) was collected by LEPLAC ("Brazilian Continental Continental Shelf Survey Plan"). It was acquired in offshore areas of the northern part of Alagoas Basin (Fig. 3.1). The seismic section extends for about 170 km and it was performed with a shot interval of 50 m, using high-pressure air guns as seismic source. The collected seismic data were processed at PETROBRAS, using standard processing sequence for deep-seismic profiling to a time length of 9 s TWT (two-way traveltime). Deterministic source-receiver deconvolution was applied to minimize/eliminate multiples (Fig. 3.6).

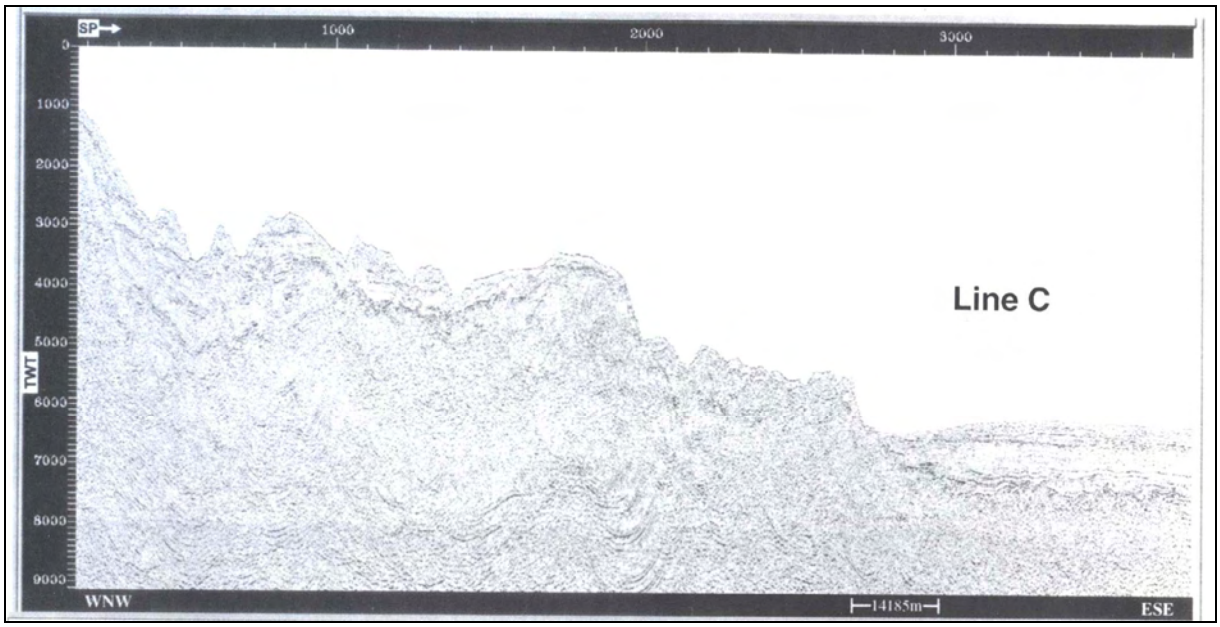

Fig. 3.6: Regional deep seismic profile C, located basinward of the shelf edge (Gomes et al., 1997).

3.2.2 Seismic profile A-1

The seismic profile A-1 (Fig. 3.7) is a deep, onshore reflection seismic line, located in the Central Tucano Graben, south of the Vaza Barris Fault Zone (Figs. 3.1 and 3.3). It was acquired with the use of powerful explosives with the purpose of imaging the deeper portion of the basin. The seismic section extends for ~108.5 km with a shotpoint interval of 35 m. It was processed by PETROBRAS to a time length of 16 s TWT using standard migration techniques.

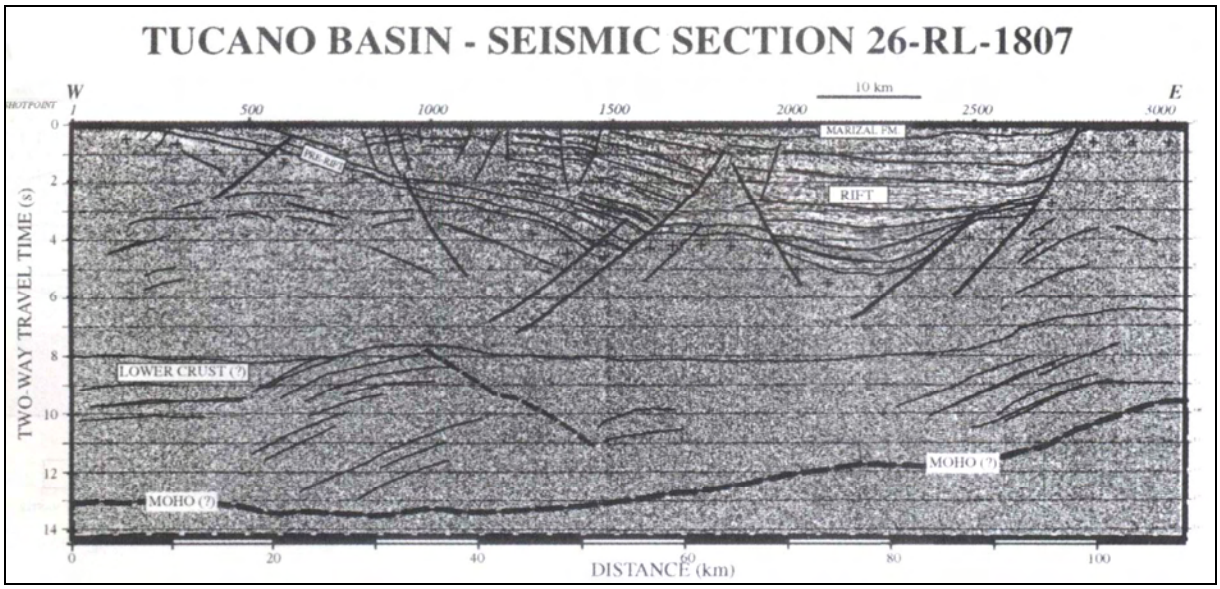

Fig. 3.7: Regional deep seismic profile A-1, located on the Central Tucano Basin (Mohriak et al., 2000).

3.2.3 Seismic profile A-2

Seismic profile A-2 (Fig. 3.8) is a deep reflection seismic line located in the offshore part of the Sergipe-Alagoas Basin (Figs. 3.1 and 3.2). This seismic profile is ~104 km long and it was recorded and processed to a time length of 11 s TWT (Fig. 3.8).

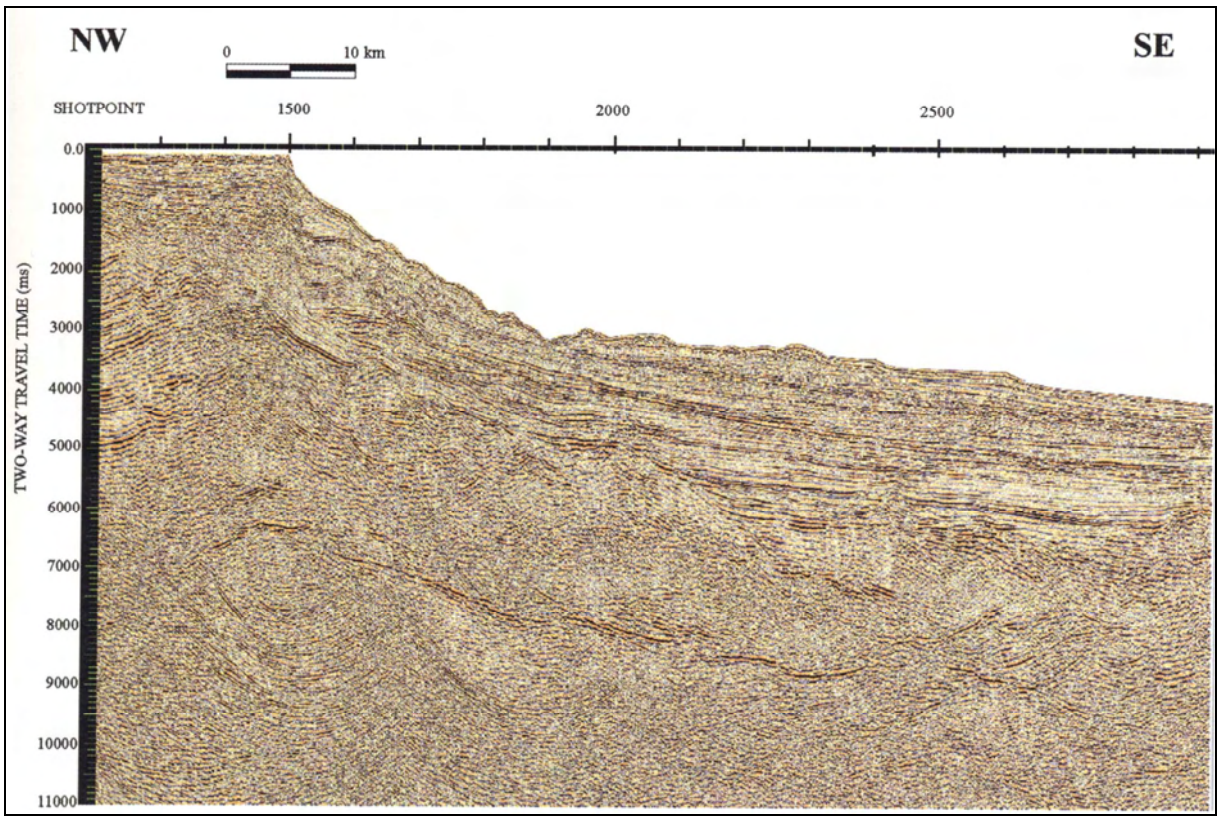

Fig. 3.8: Regional deep seismic profile A-2, located basinward of the shelf edge. The profile exhibits high amplitude reflections extending from about 6.5 to 9 s TWT.

3.2.4 Seismic profile D-D´ and B-B´

Seismic profiles D-D´ and B-B´ are located onshore across the South Tucano and Recôncavo grabens. Both are located to the south of the Vaza Barris Fault Zone (Figs. 3.1 and 3.3). Profile D-D´, ~156-km-long and 9-km-deep extends across the South Tucano and Recôncavo basins, while profile B-B´, ~152-km-long and 9-km-deep extends across the Recôncavo Graben. Depth-conversion of these profiles was completed by Milani & Davison (1988).

Chapter 4
Methods and approach

4.1 Seismic interpretation and depth-conversion

As mentioned earlier the seismic interpretation of the profiles was mainly based on publications described in Table 3.1. However, the seismic interpretation has been refined and homogenized, and it will be discussed individually for each of the seismic profiles.

4.1.1 General stratigraphic characteristics

The stratigraphic interpretation of all seismic transects is divided into three main sedimentary sequence units: pre-rift, syn-rift, and post-rift (Nøttvedt et al., 1995). The pre-rift sedimentary units are deposited in a wide slowly subsiding basin with minor fault activity during early flexural subsidence, and they are generally characterized by uniform thickness. The subsidence may be interrupted by domal uplift associated with increased heat flow caused by the asthenospheric material flow beneath the basin. Syn-rift sedimentary units are deposited during a phase of active stretching and fault-block rotation. Subsidence is controlled by lithospheric thinning and the upwelling of asthenospheric material. This sequence is characterised by extensive erosion on the fault-block shoulders. Rotation of the fault-blocks and local footwall uplift causes the overall geometry of the syn-rift sedimentary sequences to be wedge-shaped, i.e. thinning away from the graben-bounding-fault onto the hanging wall. Following the latter, less developed wedge-shaped sequences suggest relatively small rates of tilting. Finally, post-rift sedimentary sequences are characterized by thick deposition in the depocenter of the basin that gradually thins toward the flanks. Basins which have suffered some degree of sediment starvation are characterized by remnant topography at the post-rift stage, giving to the post-rift sediment sequence a wedge-shaped geometry. This phenomenon complicates the distinction between syn-rift and post-rift sequences. The main criteria that can be used in distinguishing them apart is the divergence of the syn-rift strata against the active footwall, in contrast to the parallel build-up and onlap of post-rift strata against the footwall after cessation of fault-movement. Subsidence is caused by thermal contraction and relaxation

of the heated crust and it is likely to be greatest at an early stage of cooling due to the exponential nature of thermal decay.

Some of the seismic reflection profiles used in this study were published as two-way traveltime sections. As depth-sections were needed for gravity modelling and further analyses depth-conversion had to be performed. Depth-conversion is done by using velocity functions along the individual profiles with the "in-house" software DEPTH (Breivik, 1995). The input file used to perform depth-conversion consists of the digitized transect and the velocity function parameter file. The program requires that the distance along the x-axis is given in kilometres and that velocity functions are added beyond the profile boundaries to avoid edge-effects. DEPTH also requires that each velocity layer is continuous through the profile. Each point along the digitized profile is depth-converted using the two closest velocity functions. Velocity-depth functions used for depth-conversion were constructed based on publications, regional considerations and inversion of the world ocean-floor sediment thickness map (NGDC, National Geophysical Data Center). Velocity functions are discussed individually for each published profile. The published profiles D-D´ and B-B´ (Milani & Davison, 1988) were already depth-converted.

4.1.2 Seismic profile C

The interpretation of the seismic profile C indicates a typical rifted continental crust, characterized by synthetic tilted fault blocks. The maximum sedimentary thickness is encountered along the westernmost tilted block, around shotpoint (sp) 450 (Fig. 3.6) [~10-20 km distance, Fig 4.1]. The interpreted structural geometry resembles that of detachment faulting, involving crustal extension along shear zones (Gomes et al., 1997). The detachment surface was interpreted to be located at the termination of the faults, at 20 km distance and ~6.5 s TWT. Seaward-dipping reflection sequences (SDRs) were not interpreted in this profile. The relative proximity to a transform margin could reduce the probabilities for the occurrence of SDRs (Gomes et al., 1997). Another possibility for the absence of the SDRs could be poor seismic resolution.

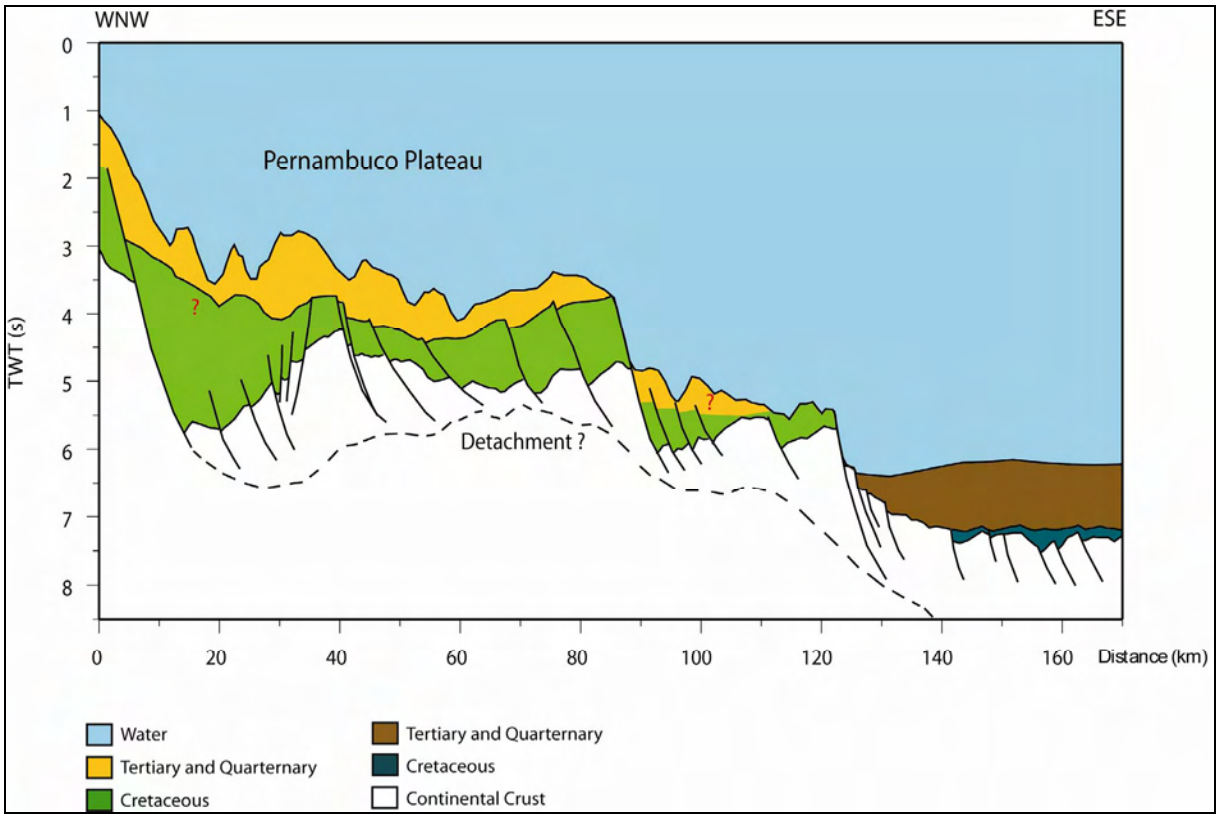

Fig.4.1: Digitised published profile C in TWT. Seismic interpretations is based on Gomes et al. (1997).

Velocities used for depth-conversion were mainly based on regional velocity functions derived from the study of Gomes et al. (1997) and from inversion of the world ocean-floor sediment thickness map. A total of 42 velocities stations have been constructed along the profile. These were positioned every 5 km distance along the profile. Five main velocity layers are used through the seismic profile, and Table 4.1 shows the interval velocities used for the different units.

Unit	**Average interval velocity (km/s)**
Water	1.48
Quaternary/Tertiary (ocean crust)	2.20
Quaternary/Tertiary	2.50
Rift (Cretaceous)	3.60
Basement	6.00

Table 4.1: Velocities for the different seismic units used in the depth-conversion of seismic profile C.

The depth-converted profile is presented in Figure 4.2. This seismic profile is not deep enough to image and resolve the Moho discontinuity. The dashed line is interpreted as a possible detachment surface.

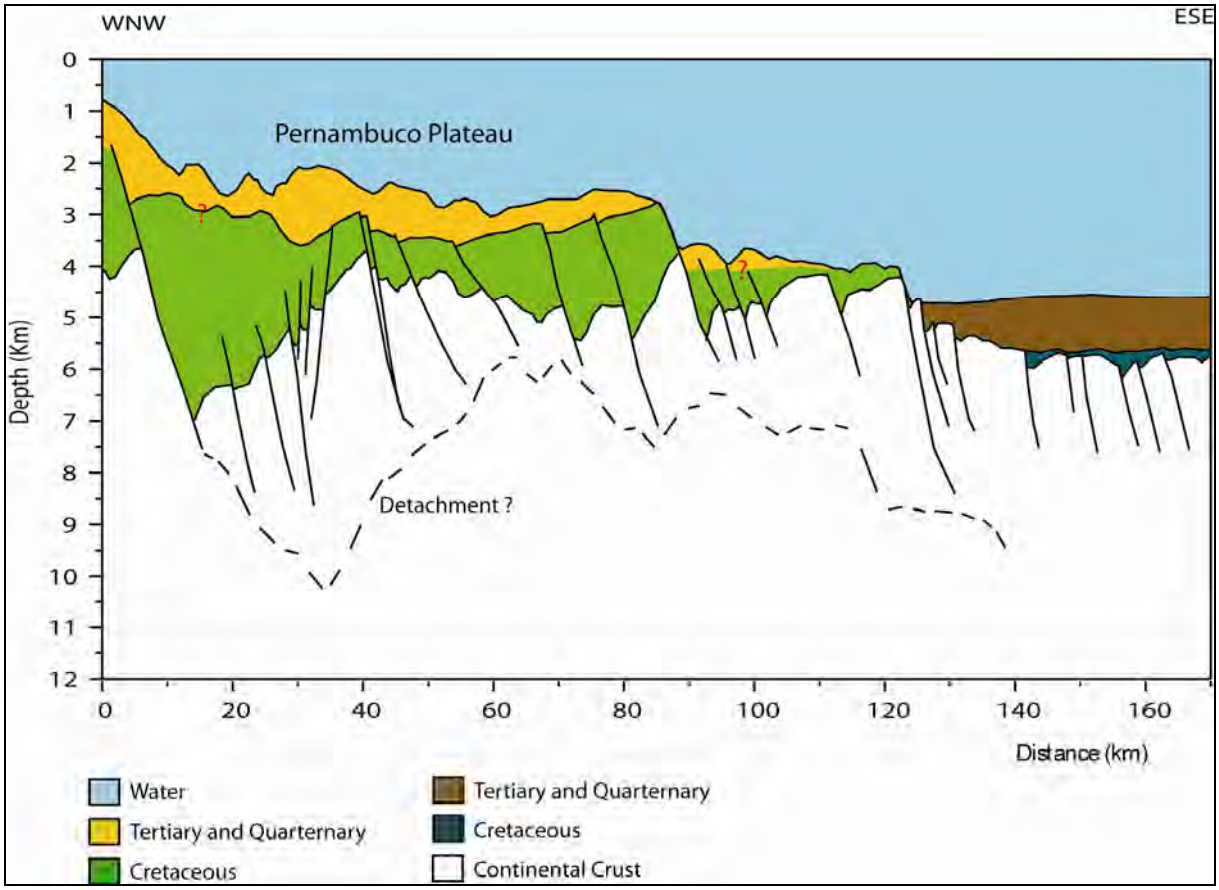

Fig.4.2: Depth-converted seismic profile C. The irregularity on the proposed detachment is caused by velocity effect during depth conversion.

4.1.3 Seismic profile A-1

The profile exhibits good resolution at large depth. In particular, at a depth of about 13 s TWT a western-dipping array of reflectors are observed clearly traversed by a subhorizontal band of reflectors that extend from 10-30 km distance from the western edge of the profile (Figs. 3.7 and 4.3). This image was interpreted by Mohriak et al. (2000) as being a possible seismic Moho candidate.

Mohriak et al. (2000) interpreted the stratigraphy and divided it in three units: pre-rift, syn-rift (Neocomian/Barremian) and a veneer of post-rift sediments of Aptian age (Fig. 4.3).The

depocenter of the Tucano Basin is located at ~70 to 90 km distance from the origin of the profile on the eastern side of the basin. This area is considerable less faulted in the upper section of the sedimentary succession, in comparison to the profile segment westward of the 55-km-distance. The lower sedimentary layer sequences in the depocenter are distinguished by the presence of sigmoidal reflections, forming a sag basin that pinchs-out towards a west-dipping fault. Younger sequences onlap the lower sequences towards the easternmost boundary of the basin which is controlled by a major east-dipping fault. This fault is formed at a later time/stage than the inner normal fault which controlled the first subsidence phase. The Marizal Fm, interpreted as being a veneer of post-rift sediments of Aptian age, is not affected by faulting (Mohriak et al., 2000). The detailed litho-stratigraphic column is provided in Figures 2.11 and 2.14.

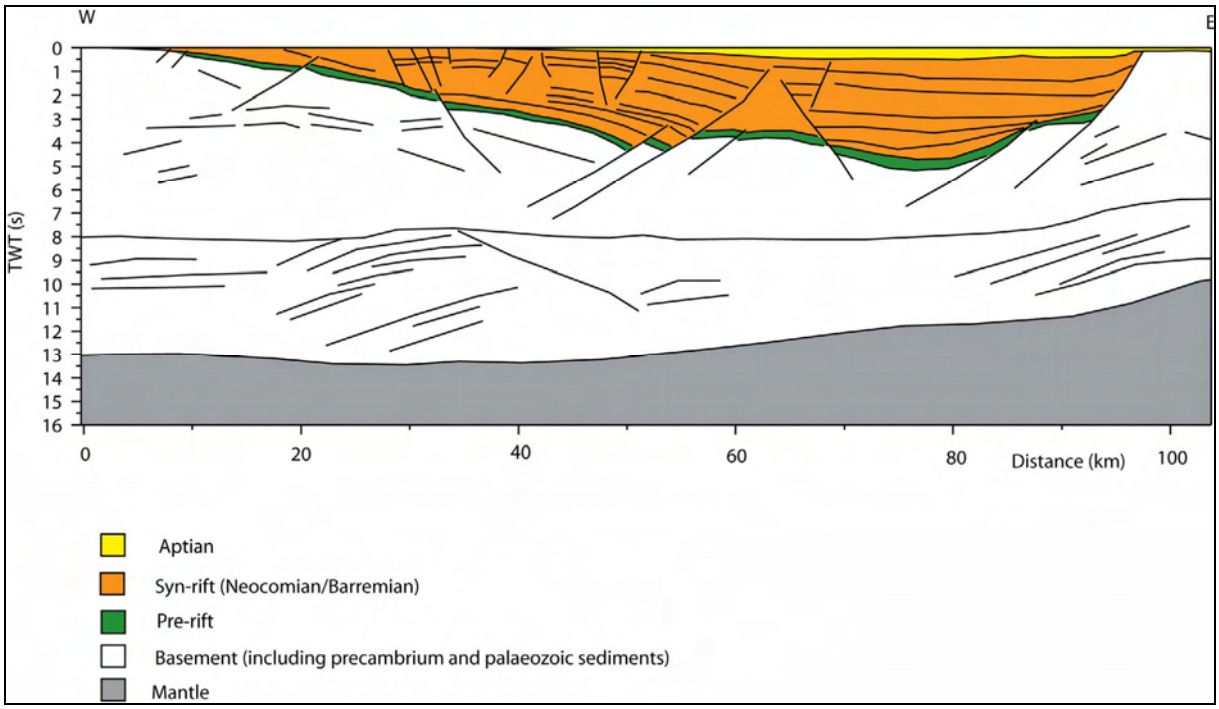

Fig. 4.3: Digitised published profile A-1 in TWT. Seismic interpretations is based on Mohriak et al. (2000).

There is a lack of well-data information in the area, and the velocities used for depth-conversion were mainly based on regional velocity functions derived from the study of Mohriak et al. (2000). A total of 16 velocities stations have been constructed along the profile. These were positioned every 5 km distance along the profile, and every 10 km distance in less faulted areas. Four main velocity layers are used through the seismic profile and Table 4.2 shows the interval velocities used for the different units.

Unit	Average interval velocity (km/s)
Aptian	3.20
Syn-rift	4.10
Pre-rift	4.90
Basement	6.00

Table 4.2: Velocities for the different seismic units used in the depth-conversion of seismic profile A-1.

Depth-conversion resulted in a lower crust/mantle transition (Moho discontinuity) at a depth of about 39 km on the western side and about 29 km on the eastern side of transect A-1 (Fig. 4.4). This result is consistent with worldwide observations of Moho depths in cratonic regions, where the thickness of the crust in Archean provinces is generally found to be ~35 km (Durrheim & Mooney, 1991). Besides the difficulty in identifying Moho in the seismic section (probably due to attenuation) Mohriak et al. (2000) interpreted Moho to be steadily stepwise shallowing towards the eastern side.

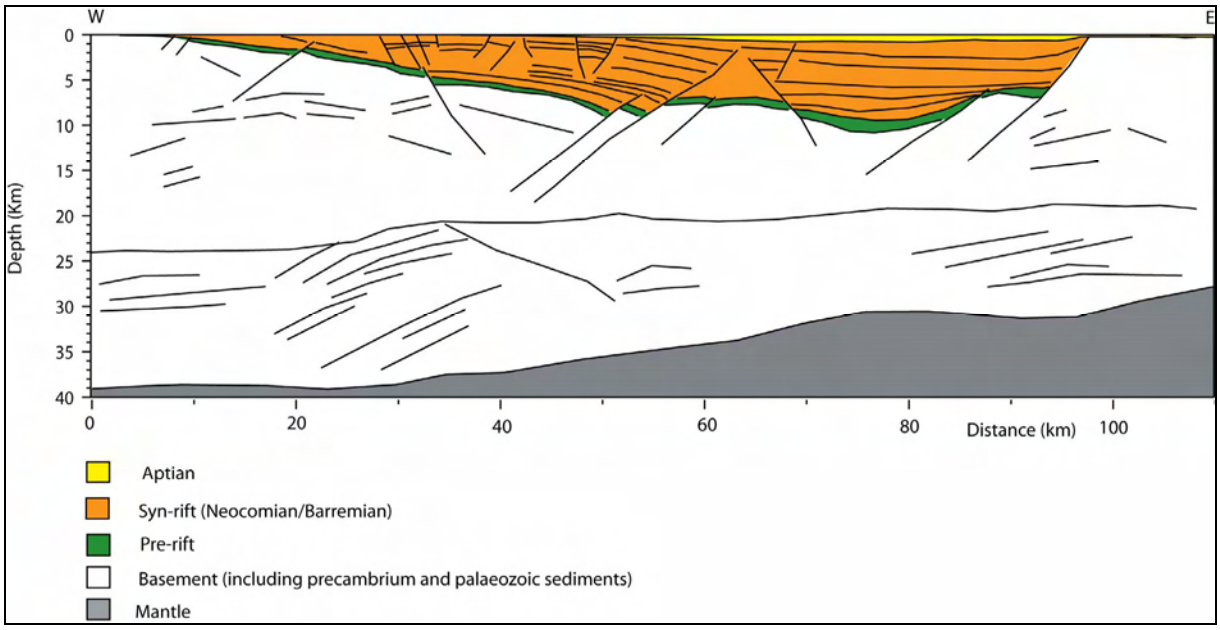

Fig. 4.4: Depth-converted seismic profile A-1.

4.1.4 Seismic profile A-2

The profile exhibits eastward dipping reflections located around 4-5 s TWT at sp 1200-1400 (Fig. 3.8) [~15-45 km distance, Fig. 4.5] that are interpreted to indicate major faults that control syn-rift deposition. Furthermore, the profile exhibits high-amplitude reflectivity from ~6.5 to 9 s TWT (Fig. 3.8). Mohriak et al. (2000) interpreted these seismic reflections as representing intracrustal horizons (underplating) that, further eastward in the deep water regions of the continental margin, merge with the seismic Moho. The same deep seismic reflections were interpreted by Pontes et al. (1991) as representing the transition between a thick syn-rift sedimentary sequence and Precambrian basement.

There is a remarkable lack of volcanic features in the platform, as confirmed by boreholes drilled through the syn-rift sequences. However, there are some structures that might have an igneous origin, such as the volcanic plug near sp 2900 (Fig. 3.8) [~85-90 km distance, Fig. 4.5]. This feature is interpreted as a post-rift volcanic intrusion, located near the continent-ocean boundary. The packages of reflections with sigmoidal geometry, dip mostly basinward. Nevertheless, locally seaward dipping reflectors is also observed, e.g. between sp 2500-2800 at a depth of 8-9 s TWT (Fig. 3.8) [~65-100 km distance, Fig. 4.5] that are suggested to be magmatic features. These probably correspond to SDRs formed mainly by volcanic rock extruded during an early phase of oceanic ridge spreading (Mutter, 1985). Seaward of the volcanic plug (sp 2900, Fig. 3.8) [~90 km distance, Fig. 4.5], the basement is probably made of volcanic igneous rocks intercalated with volcanoclastic rocks, forming the SDR wedges that grade seawards into pure oceanic crust. The magmatic underplating and the massive SDR wedges are interpreted as being contemporaneous with the emplacement of oceanic crust, post-dating the syn-rift sequences. Moho shallows rapidly along the profile (Figs. 3.8 and 4.5) and a very thin continental crust extends for only a few tens of km beyond the shelf edge. The transition to proto-oceanic crust is interpreted to coincide with the western limits of the SDRs while the transition to a pure oceanic crust is interpreted to be at the eastern limits of the SDRs, basinward of the volcanic plug (Figs. 3.8 and 4.5).

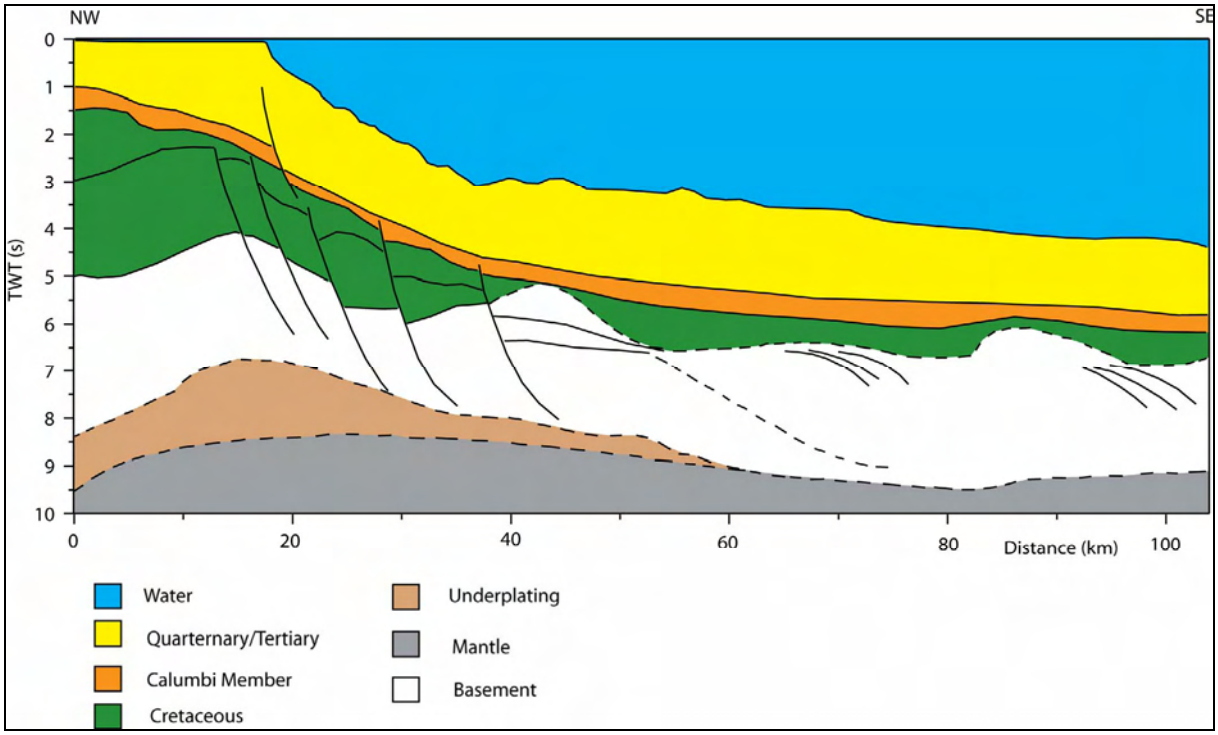

Fig. 4.5: Digitised published profile A-2 in TWT showing seismic interpretations based on Mohriak et al. (2000). For a detailed litho-stratigraphic column see Fig. 2.14.

Regional velocity functions based on Mohriak et al. (2000) were used for depth conversion. A total of 22 velocity stations have been constructed along profile A-2. They were positioned every 5 km along the profile. Five main velocity layers are used through the profile and Table 4.3 shows the interval velocities used for the different units.

Unit	**Average interval velocity (km/s)**
Water	1.48
Quaternary/Tertiary	2.26
Calumbi Member	4.10
Cretaceous	4.90
Basement	6.00

Table 4. 3: Velocities for the different seismic units used in the depth-conversion of the seismic profile A-2.

The depth-converted profile is presented in Figure 4.6. Moho depth shallows very rapidly eastward of the depocenter, were it reaches a depth of about 20-15 km near the shelf edge. This resulted in a highly-attenuated lower crust, which was probably extended considerable in

a ductile manner. The upper crust, characterised by brittle behaviour, has also suffered large degree of thinning due to extensional processes (Mohriak et al., 2000).

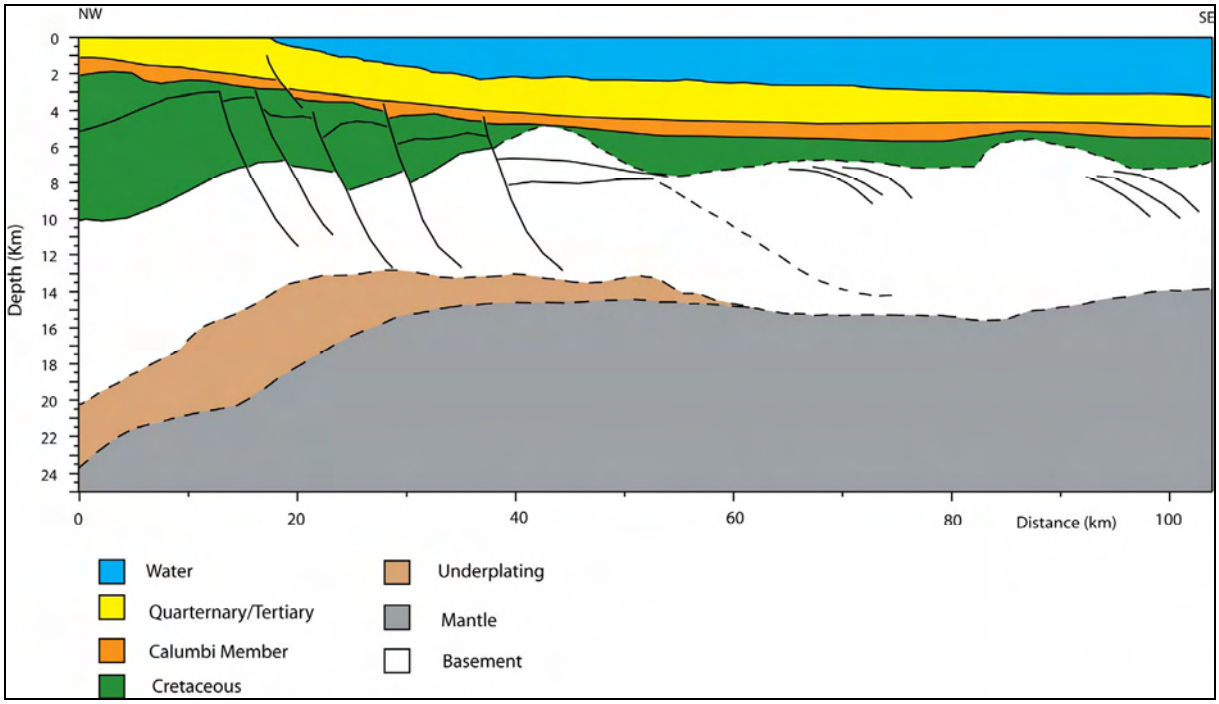

Fig. 4.6: Depth-converted seismic profile A-2.

4.1.5 Seismic profile D-D´ and B-B´

Seismic interpretation and depth-conversion of these profiles are based on Milani & Davison, (1988) (Figs. 4.7 and 4.8). Since these profiles are also located south of the Vaza Barris Fault Zone, the observed depocenters are located on the eastern side of the basins. As indicated in the detailed litho-stratigraphic column for the region (Fig 2.11), the pre-rift (Upper Jurassic to Lower Cretaceous) Brotas Group consists of red beds deposited in a fluvial system. Syn-rift deposits consist of the Santo Amaro, Ilhas and Massacará groups, and these sequences were deposited as turbidites, deltas and conglomerates. Note, as earlier mentioned, that no post-rift sequences were deposited in these basins.

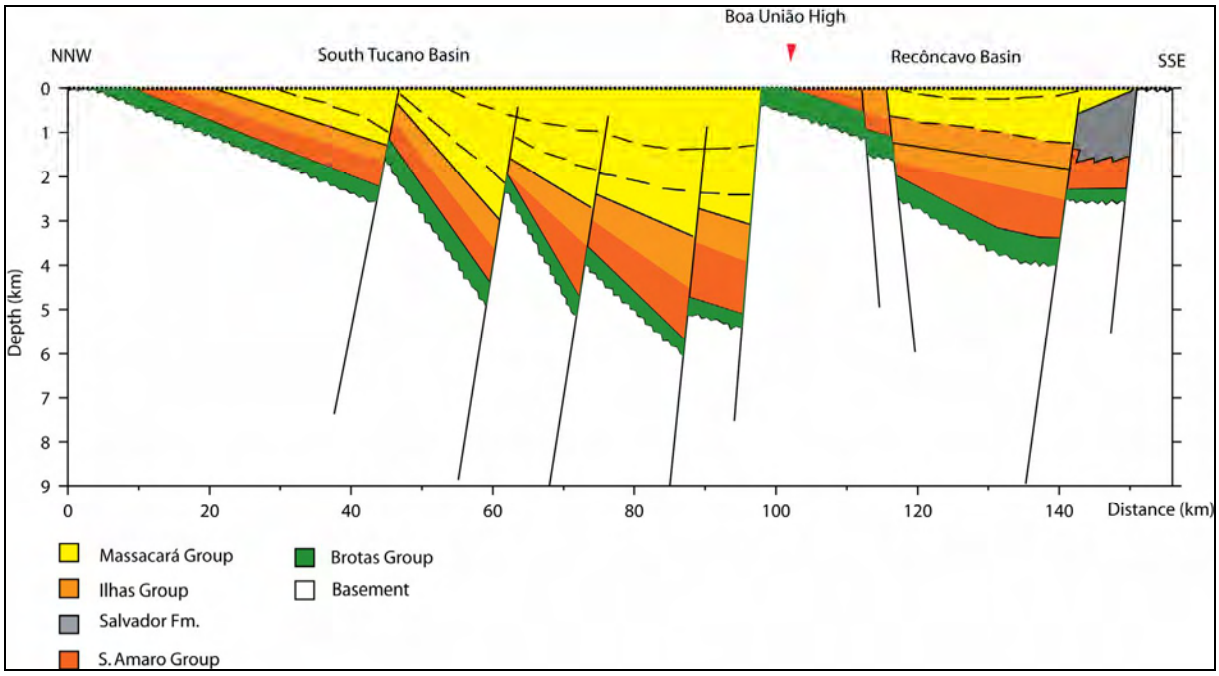

Fig. 4.7: Depth converted seismic profile D-D´ (after Milani & Davison, 1988).

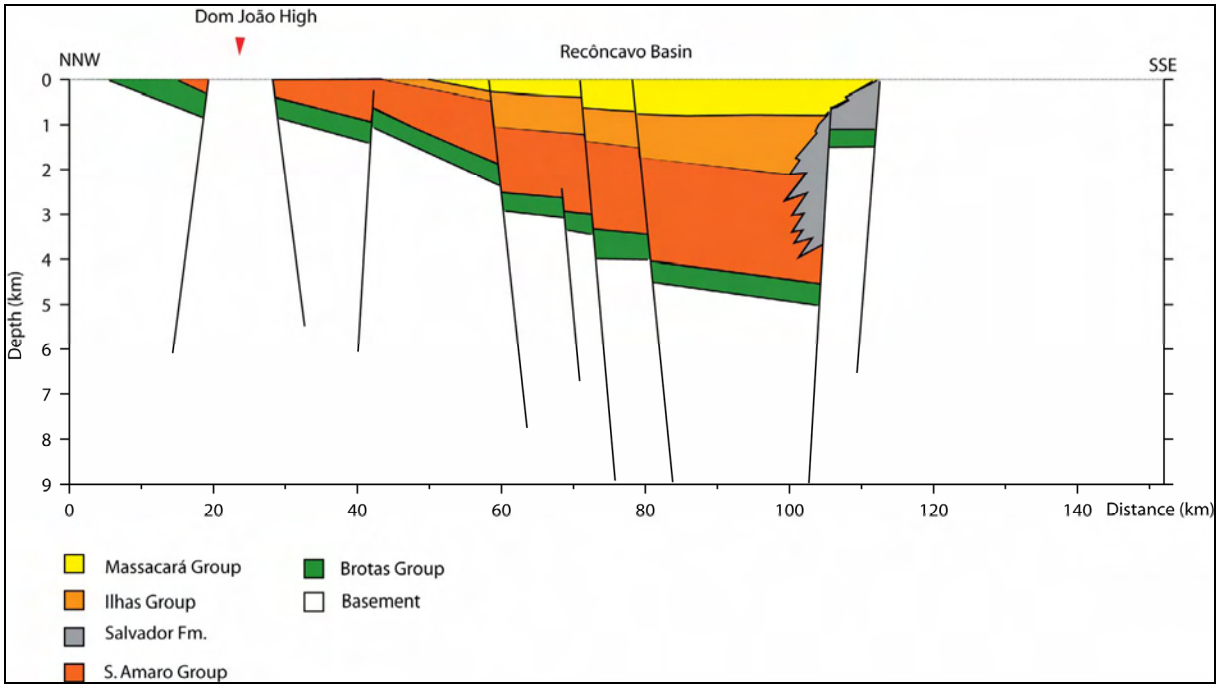

Fig 4.8: Depth converted seismic profile B-B´ (after Milani & Davison, 1988).

4.2 Moho relief

In general, Moho is seismically defined as a velocity discontinuity, when seismic velocities abruptly increase from 6.7-7.2 km/s to velocities of 7.6-8.6 km/s, defining the crust-mantle boundary. Petrologically, Moho is defined as the transition between non-peridotitic crustal rocks and olivine-dominated mantle rocks (Evans et al., 2003).

The initial estimations of the Moho relief in this study were made utilizing two different methods: forward isostatic balancing and inverse modelling, using the "in-house" program TAMP (Breivik et al., 1990). TAMP defines polygon-models of the crust and calculates the gravity anomaly produced by the model. In this study, the simplified Earth models that were generated are described by three polygons. The first polygon represents the water column, with a density of 1.03 g/cm^3 and the input bathymetry was extracted either directly from academic ship-track or from the gridded data. The second polygon represents the crust and was modelled with different densities ranging from 2.70-2.90 g/cm^3. The third, mantle polygon was defined with a density of 3.20 g/cm^3, and its maximum depth was set to be 60 km.

4.2.1 Forward isostatic balancing

The purpose of forward isostatic balancing is to model the Moho relief along the profile in such a way that the profile is in isostatic balance. The model is based on Airy isostasy in which the crustal overburden has the same density but different thickness, inflecting that the isostatic compensation is greater where the thickness of the crust is greater.

Balancing of the model was done with a known Moho depth at a fixed point. The fixed point was chosen to be located in the oceanic crust where the depth to Moho was set to 6.5 km, approximating the global average oceanic-crust thickness (White et al., 1992). For example along line B-B´, at a distance of 435 km from the origin of the profile, the observed water depth is 4.076 km, and this value was then added to the oceanic-crust average thickness of 6.5 km giving a Moho depth of ~10.5 km. That means that for this case, Moho is constrained through a point located at a distance of 435 km from origin of the line B-B´ and at a depth of 10.5 km. In the forward gravity modelling the calculated and the observed gravity anomalies were forced to match at approximately the same fixed/anchor-point distance. Table 4.4 shows

chosen parameters for each line modelled. Figure 4.9 is illustrating the forward isostatic balancing model for line D-D´.

Modelled line	**Profile length (km)**	**Fixed Moho depth/ Anchor-point distance**
line A-A´	538	distance:530 km depth: 12 km
line B-B´	468	distance: 435 km depth: 10,5 km
line C-C´	402	distance: 400 km depth: 11 km
line D-D´	352.8	distance: 335 km depth: 11 km

Table 4. 4: Parameters used in TAMP to calculate Moho relief by forward isostatic balancing.

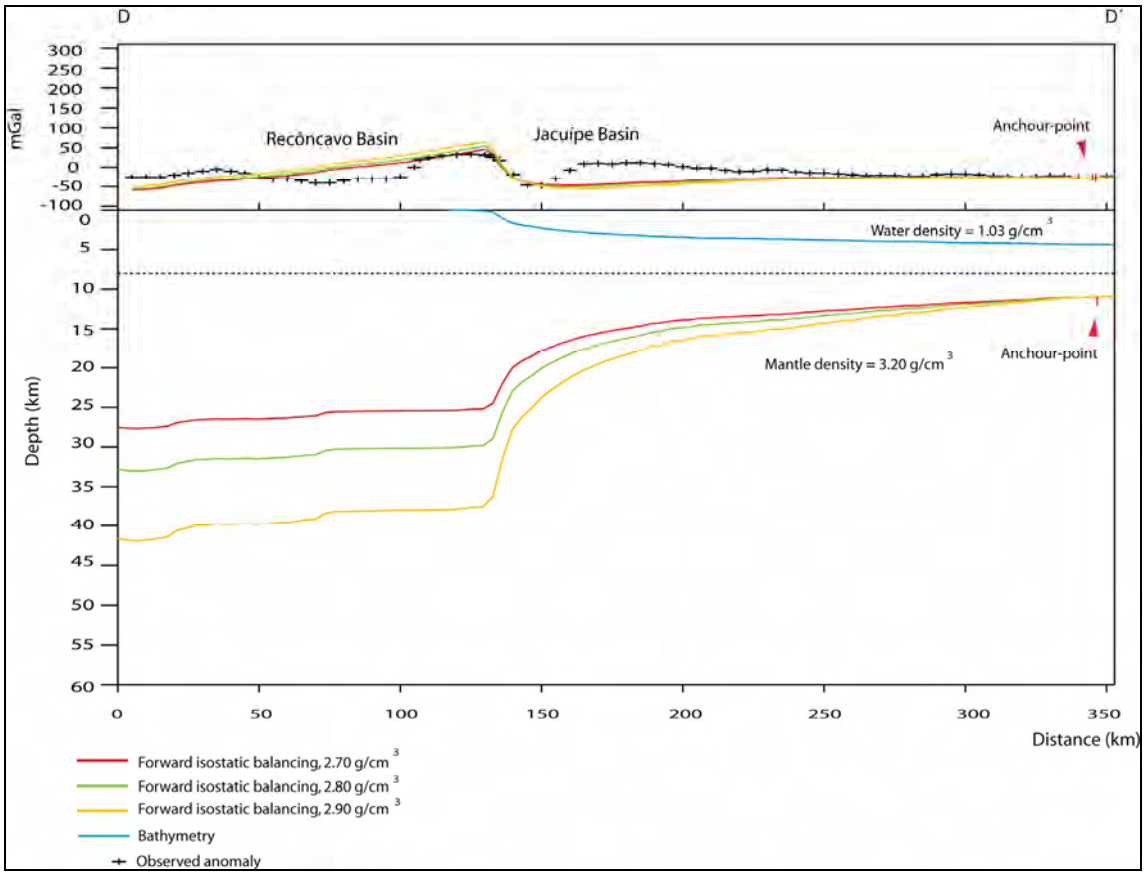

Fig. 4. 9: Moho relief calculated along line D-D´ by forward isostatic balancing. The different colours are indicating different crustal density.

4.2.2 Inverse modelling

This method is described by Cordell & Henderson (1968) and states that given a gravity anomaly a three-dimensional structure model can be calculated automatically from it by successive approximation. The causative body is assumed to be flat-bottomed, that means that the program operates with an initial planer Moho discontinuity. The gravity field of the model is calculated and the ratio between the calculated and the observed gravity is used to modify the model until a satisfactory agreement between observed and calculated gravity is obtained.

The crust in the model was divided in columns with equal widths. During the model operation, these columns were adjusted vertically, until the discrepancy between the calculated and the observed gravity was minimised. The number of iterations used, represents the amount of repeated gravity anomaly calculation done by the program (TAMP) in order to achieve acceptable discrepancies between observed and calculated gravity anomalies. The columns are extrapolated on each side of the model in order to avoid edge-effects. The modelled relief on the bottom of the columns represent the top of the mantle polygon (Moho relief) (Breivik et al., 1990).

In the inverse modelling calculations Moho was also forced through a single fixed Moho depth using the same approximations described above, and the calculated and observed gravity anomalies were similarly forced to match at approximately the same fixed/anchor-point distance. Table 4.5 shows the chosen parameters for each modelled transect. Figure 4.10 illustrates the inverse modelling approach line D-D´. The low numbers of column chosen for line B-B´ and C-C´ was necessary to constrain the model to an acceptable depth; however it will simplify the model considerably and local events will not be resolved.

Modelled line	Profile length (km)	Fixed Moho depth/Anchor-point distance	Nr. of columns	Nr. of iterations
line A-A´	538	distance: 530 km depth: 12 km	40	12
line B-B´	468	distance: 435 km depth: 10,5 km	8	6
line C-C´	402	distance: 390 km depth: 11 km	12	6
line D-D´	352.8	distance: 335 km depth: 11 km	20	8

Table 4.5: Parameters used in TAMP to model an initial Moho relief by inverse modelling.

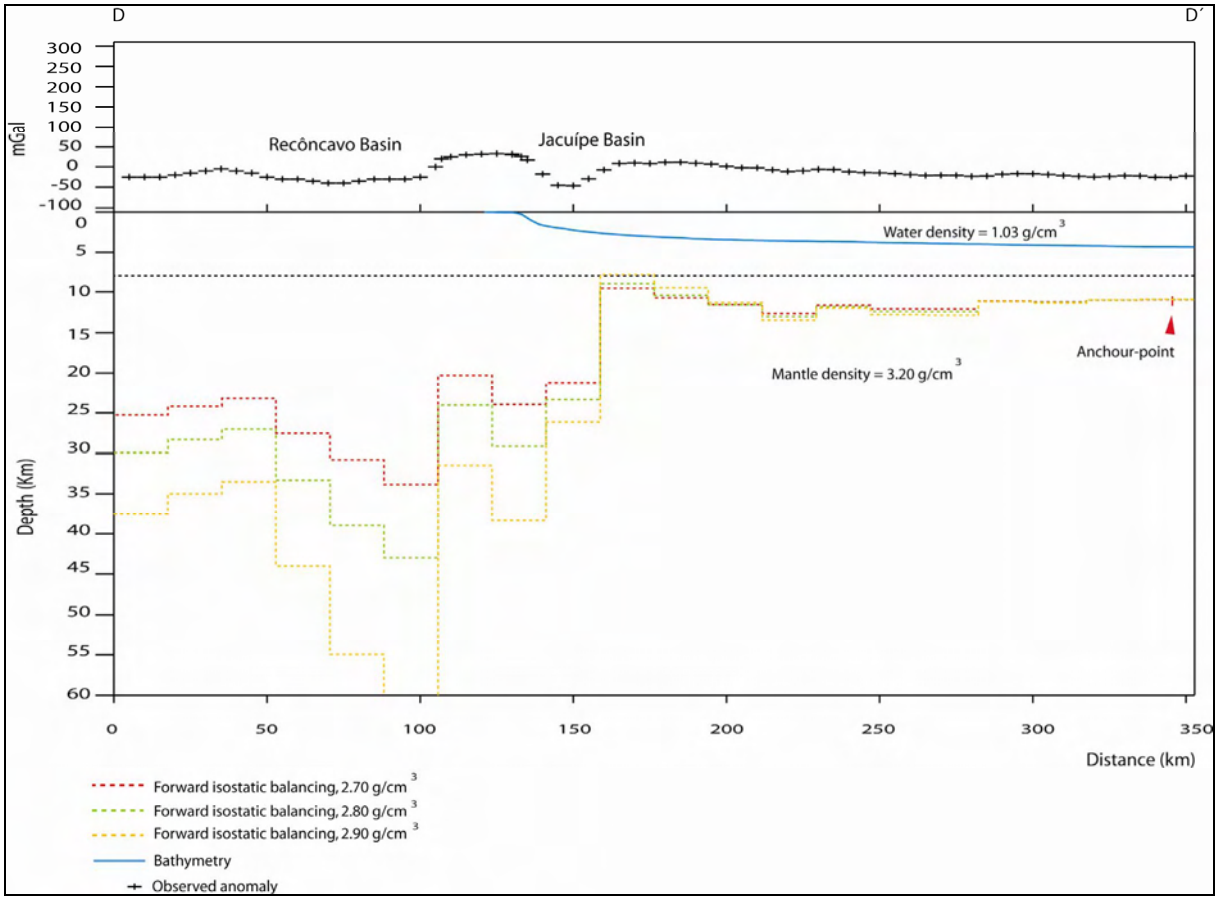

Fig. 4.10: Moho relief calculated along Line D-D´ by inverse modelling.

For a direct comparison of the two different methods (forward isostatic and inverse modelling) that provide an initial Moho relief, the results are overlapped (Fig. 4.11).

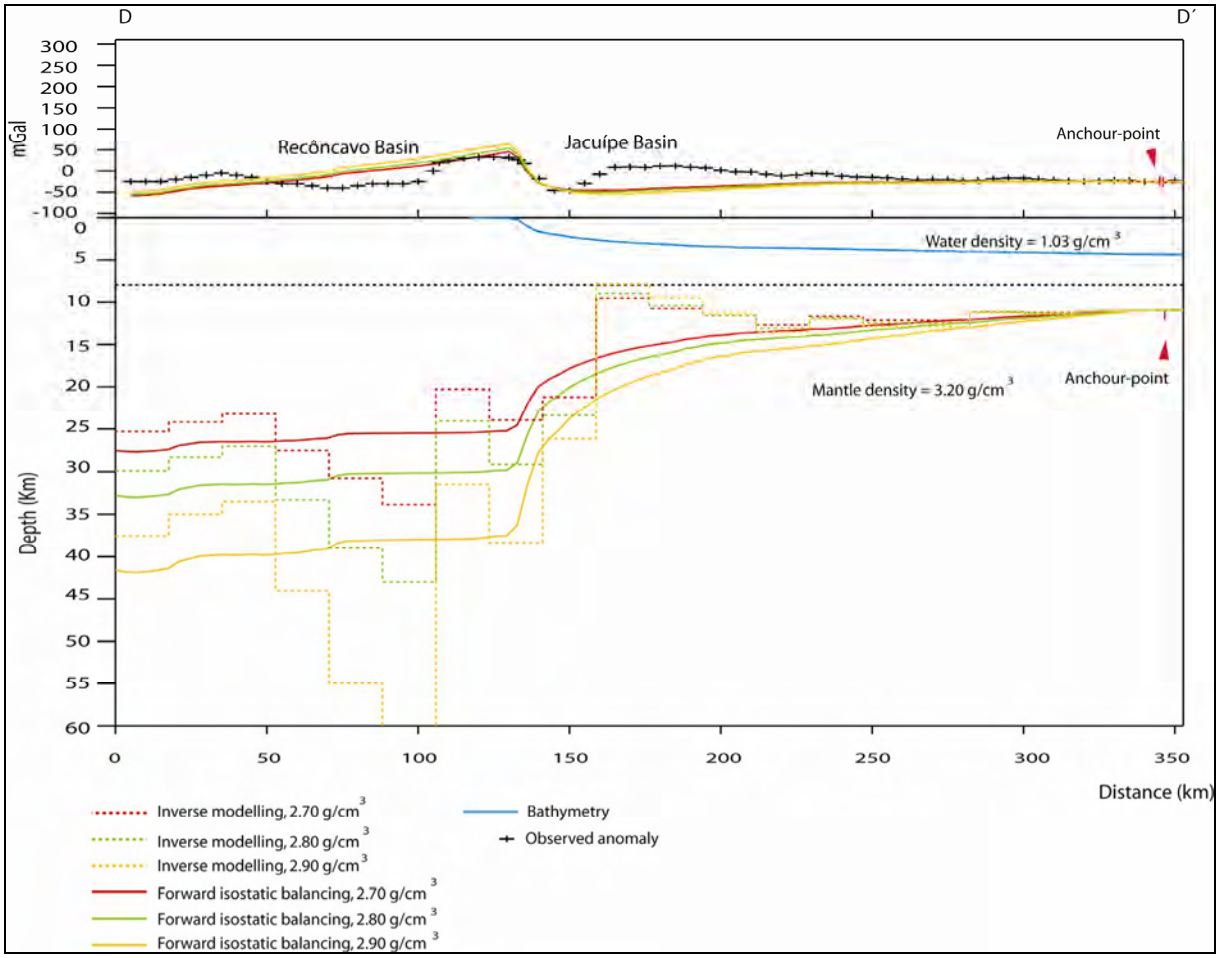

Fig. 4.11: Moho relief calculated along line D-D´ by isostatic balancing and inverse modelling.

Two local discrepancies between the output of the two methods are observed in Figure 4.11. The first is located at ~50-100 km distance and reflects a mass excess/surplus. The model shows the need of a lower density in this area explained by the sedimentary infill of the Recôncavo Basin. The second discrepancy located at ~160-220 km distance is related to a mass deficit. Here the model shows the need for locally higher densities. Initial considerations for these misfits that will be further investigated and tested by gravity modelling include a lower crustal body (underplating) and/or a local basement uplift. A deep seismic profile in this area would be needed for further investigations.

4.3 Potential field gradient and continent-ocean transition

The location of the continent-ocean boundary has obviously implications for the reconstruction of rifted continental margins since it represents the line of initial breakup. Nevertheless, it is unlikely that this boundary is characterized by an undisputed break. The extrusion of oceanic crust was probably preceded by a period of deformation of the continental crust by stretching and thinning. Implying that a complete reconstruction of the rift would not be possible by only studying this boundary, the deformed continental crust must also be considered (Talwani & Eldholm, 1973).

Early models based on Airy isostasy (zero strength during rifting) suggest that the transition between oceanic and continental crust (COT) is located at the present day shelf break, characterized by a high gravity anomaly (free-air gravity "edge effect"). These anomalies result due to of juxtaposition of thick crystalline crust and very thinned crust (due to rifting), as well as due to magmatic underplating (Watts, 2001). Talwani & Eldholm (1973) however suggested that the COT is not necessary located at the shelf break, implying that the gravity highs do not occur as a result of the location of the shelf break but rather the location of the shelf edge is predetermined by high density belts extending deep into the crust. The gravity model of line B-B´ (Fig. 5.4) provides a good example exhibiting that the COT is neither located at the shelf break nor is characterized by a steep (negative-positive) gravity gradient (Fig. 4.14). On the other hand, the gravity model of line C-C´ and D-D´ suggests a COT aligned with a distinct gravity gradient (Figs. 4.15, 4.16, 5.5 and 5.6). Furthermore, Talwani & Eldholm (1973) stressed the manifestation of a major change in the elevation at the boundary between oceanic and continental crust. In many cases, differences in elevation are not expressed in bathymetry maps due to the deposition of thick sedimentary sequences. This issue can be solved by utilising gravity anomalies both along profiles and gridded maps where the steep gradient is indicative of distinct change in basement elevation.

Karner (2000) proposed that the termination of oceanic fracture zones identified in high pass filtered free-air gravity anomaly gridded data offers an important approximation in the definition of the limits of the oceanic crust and thus the continent-ocean boundary. He also proposed that the continent-ocean boundary is broadly aligned with a steep (negative-positive) gravity gradient. However, even when filtering the free-air gravity anomaly gridded data with a high-pass filter the termination of oceanic fracture zones is very difficult to identify (Fig. 4.12). Watts (1988) developed a model based on backstripping and gravity

modelling to determine the crustal-type beneath rifted margins. The method is based on evidence from flexural studies that continental and oceanic lithosphere respond very different to long-term loads.

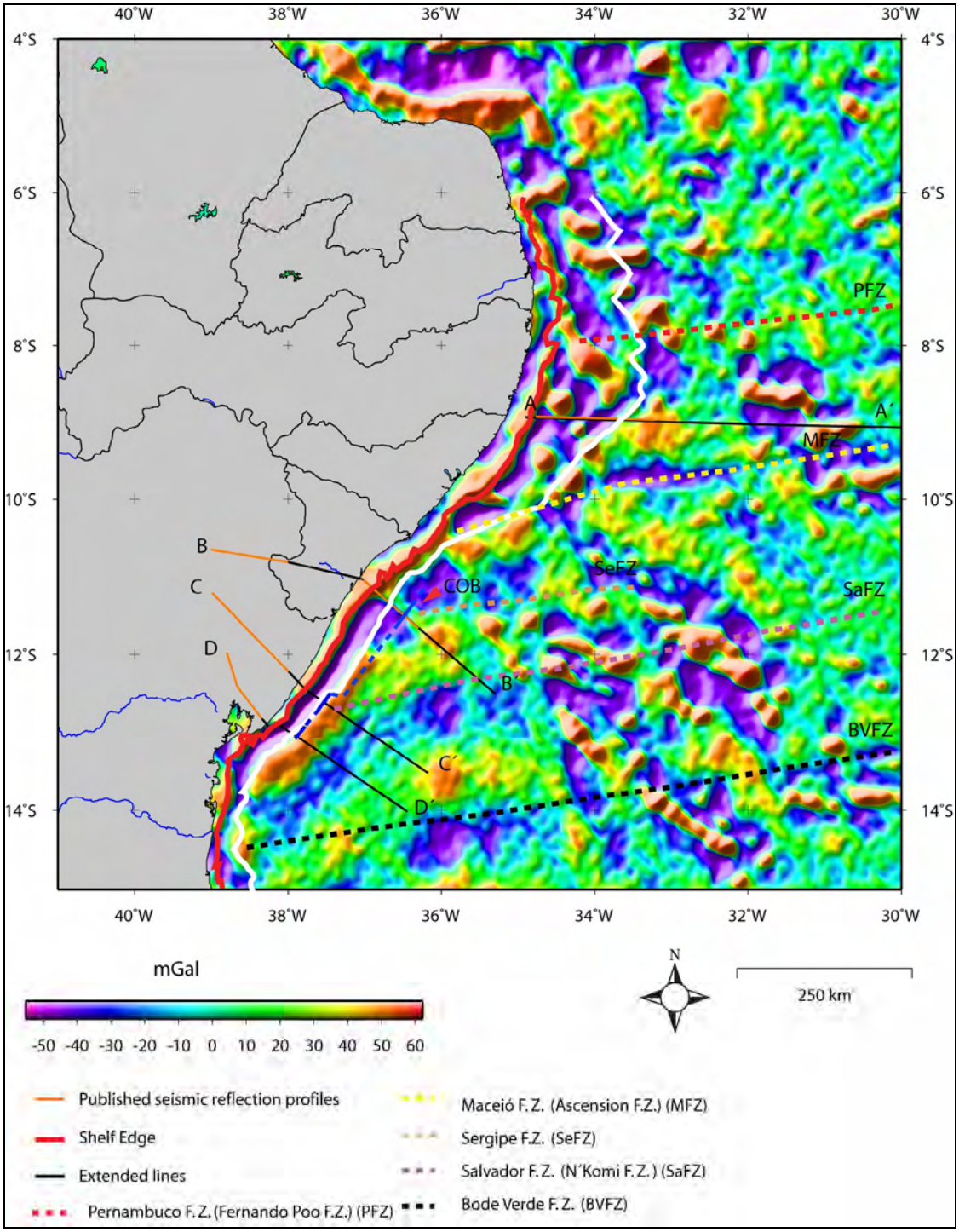

Fig. 4.12: Filtered 1x1 minute gridded satellite-radar-altimeter free-air gravity anomaly field (Sandwell & Smith, 1997; version 10.1). The filtered used was a high-pass filter, that suppressed wave-lengths >200 km. The COB interpreted by Karner & Driscoll (1999) is indicated by the white line, it shows discrepancies with COB interpreted with the use of seismic and potential data (blue line) across the line B-B´.

The COT zone is defined by a rapid crustal thinning (Tsikalas et al., 2005). This is a fact if extension occurs instantaneously and with high strain rates. However, the rheologically weakest region of the extended crust is where the region of crustal extension and mantle thinning coincides (Karner et al., 1992). The site of seafloor spreading (COT) can also be controlled by extension-induced magmatic underplating (Karner et al., 1992). As extension progresses, the rise of lithosphere mantle will imply partial melting by decompression, consequently increasing crustal temperature substantially in the region. Subsequently, the region affected by magmatic underplating becomes rheologically weaker and will probably fail becoming the site of seafloor spreading.

The COT/COB is very easy to identify along the lines C-C´ and D-D´ were it is defined by a steep gradient of the Bouguer-corrected gravity anomaly (Figs. 4.15 and 4.16).These lines/transects are located across an area that underwent rapid breakup and where the rift width is rather small. On the other hand, the rift width across line A-A´ is very extensive, indicating a prolonged rift phase before breakup. The definition of COT/COB across this line is not easily made only by observing the Bouguer-corrected gravity anomaly (Fig. 4.13), it was based mainly on observations made on seismic reflection. Across line B-B´ the width of the rift is also a little bit larger than across line C-C´ and D-D´. The use of reflection seismic data was also very crucial for placing COT/COB across this line (Fig 4.12).

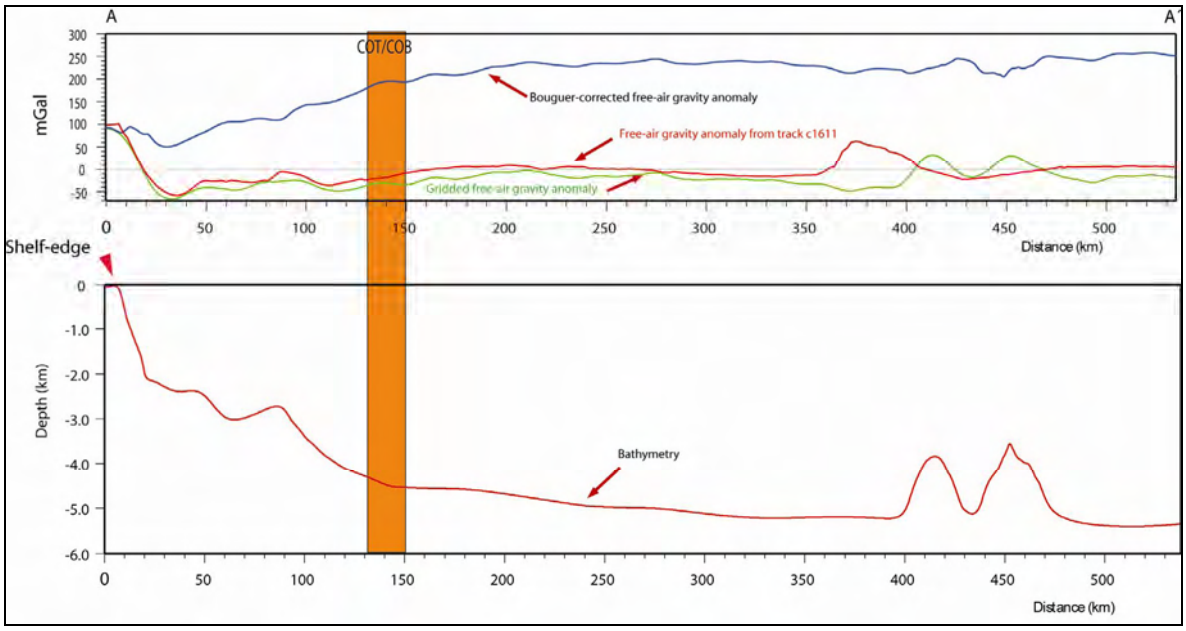

Fig. 4.13: Bouguer-corrected gravity anomaly profile (blue line) and free-air gravity anomaly from track (red line) and grid free-air gravity anomaly (green line) for line C-C´. The large discrepancy between the free-air gravity anomaly from track (red line) and the grid free-air gravity anomaly (green line) is caused by the distance of the academic track c1611 from line A-A´. The position of COT/COB is mainly based on observations made on seismic reflection profile.

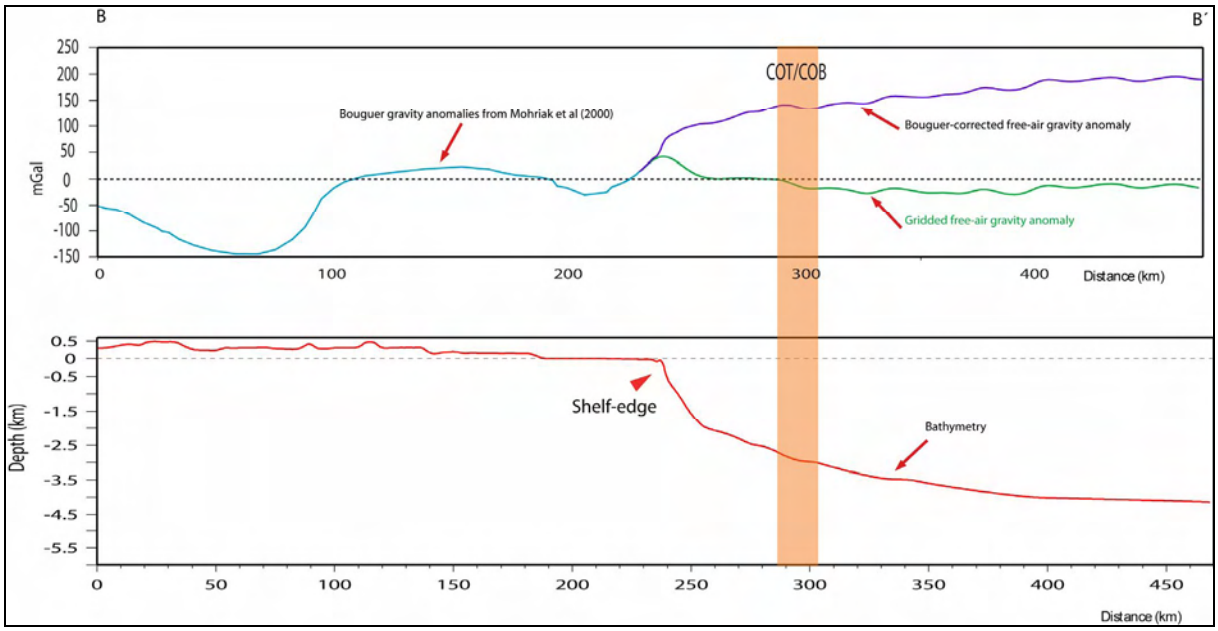

Fig. 4.14: Bouguer-corrected gravity anomaly profile (blue line) and gravity anomaly from grid (green line) for line B-B´. The COT/COB does not coincide with the location of maximum crustal extension.

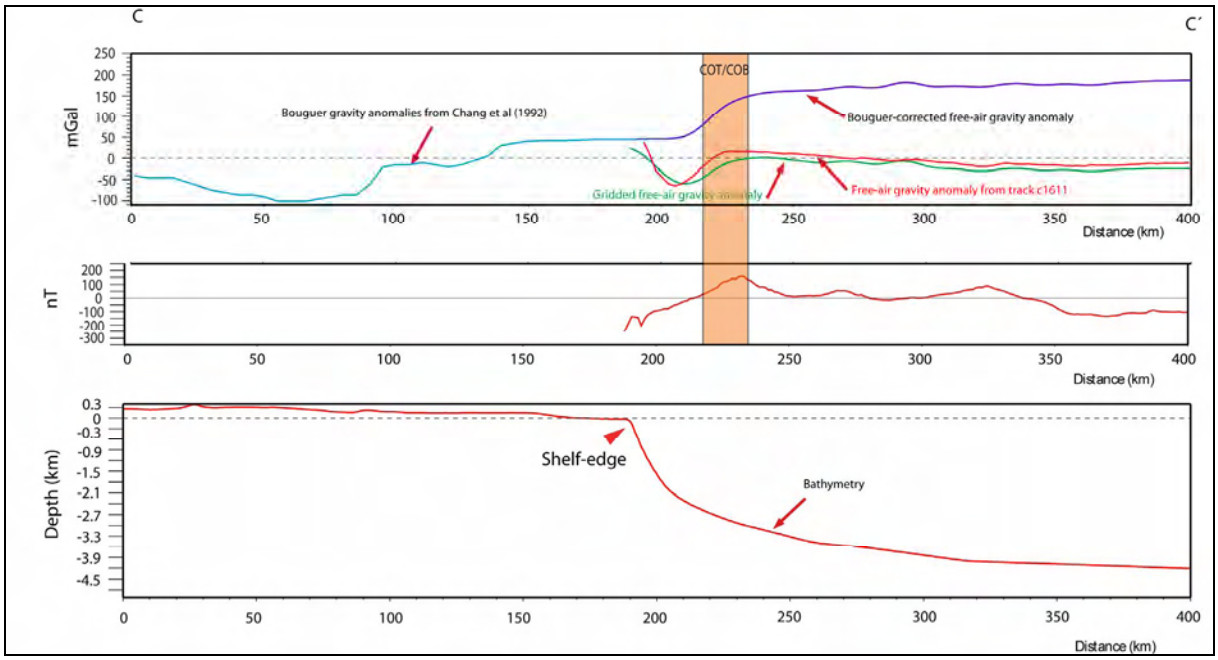

Fig. 4.15: Bouguer-corrected gravity anomaly profile (blue line) and free-air gravity anomaly from track (red line) and grid free-air gravity anomaly (green line) for line C-C´. The lower picture is showing magnetic anomaly from track. The COT/COB is positioned along a steep gradient of the Bouguer-corrected gravity anomaly, and a high magnetic anomaly.

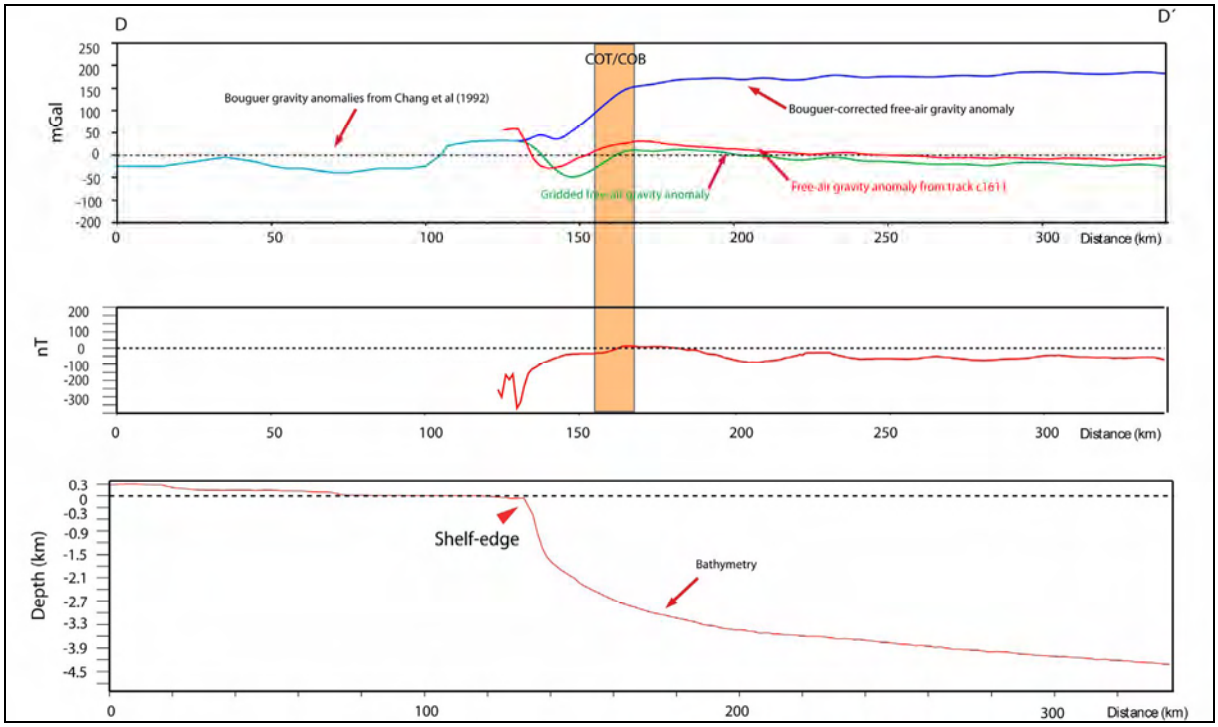

Fig. 4.16: Bouguer-corrected gravity anomaly profile (blue line) and free-air gravity anomaly from track (red line) and grid free-air gravity anomaly (green line) for line D-D´. The lower picture is showing magnetic anomaly from track. The COT/COB is positioned along a steep gradient of the Bouguer-corrected gravity anomaly.

Chapter 5
Gravity modelling

The 2-D forward gravity modelling method was applied to the depth-converted published seismic profiles combined with the results obtained in Figure 4.11. Modelling was performed utilizing the GM-SYS software (Northwest Geophysical Associates, Inc. www.nga.com). GM-SYS is an interactive gravity and magnetic modelling software where polygon-models are defined similar to TAMP, however with even greater details, representing the basin geometry and sedimentary packages better than TAMP. For gravity modelling with GM-SYS, each of the defined polygons is provided with representative density values. The polygons defined in the model are extended ±30000 km on each side of the model in order to avoid edge-effects. The calculated gravity anomaly resolved by the model is based on the Talwani et al. (1959) algorithm, where "expressions are derived for the vertical and horizontal components of the gravitational attraction due to a 2-D body of arbitrary shape by approximating it to an n-side polygon". GM-SYS is a robust software because it allows interactive manipulation of the geological model, meaning that the model can be tested for different solutions (geometries and density values) and improved until the discrepancy (residual error) between the calculated and observed gravity anomaly is acceptable small. GM-SYS provides also the possibility of 2.5 D modelling, meaning that additional densities information can be given to polygons located outside the modelled line/profile. However, in this study the 2-D modelling was satisfactory.

One important issue to keep in mind while performing gravity modelling is the inherited non-uniqueness effect of gravity anomalies concerning the causal body depth and shape determination. The non-uniqueness effect in gravity modelling implies that many different and even unrealistic models will produce acceptable small residual errors. Since many models can be unrealistic, the modelling results will depend greatly on the quality of the start model, i.e. the depth converted seismic profiles. If the wrong or not well constraned velocity-depth functions are used during depth-conversion of the seismic profiles, the uncertainty will propagate during modelling and the result will not be representative.

The purpose in performing gravity modelling is three-fold, namely to construct a representative crustal structure, to test the validity of the initial Moho relief modelled with the use of TAMP (Fig. 4.11) and to test the validity of the interpretations done in the seismic profile. By holding most parameters constant a more realistic model can be achieved. The parameters are densities, geometry of the polygons, depth of the basin and depth to Moho. The regions along the modelled lines/transects that enclosed reflection seismic data provided satisfactory information to hold most parameters constant. Depth to Moho and densities were the only parameters to be revised on these regions, whereas geometry and depth of the basin were kept constant. However, in the regions where seismic reflection data were not available all parameters were subjected to improvement. The 2-D gravity model results for these areas are expected to be less realistic since there are no seismic constraints. In this study, the models were kept very simple, with homogeneous density for the oceanic and continental crystalline crust.

5.1 Velocity to density conversion

The modelling densities derived mainly from the Nafe and Drake velocity-density empirical relationship (Nafe & Drake, 1957; Ludwig et al., 1970) (Fig. 5.1) and from publications mentioned on Table 3.1. In addition, velocity-density relationships used on similar rifted continental margin settings were taken into consideration, e.g. regional wide-angle velocity studies and gravity modelling along the Lofoten-Vesterålen and SW Barents Sea margins off Norway (Tsikalas et al., 2005; and Mjelde et al., 2002). The Nafe and Drake velocity-density empirical relationship is based on laboratory studies using data from geological formations in North America, therefore it is not certain that it is applicable to other areas. Tsikalas (1992), however, obtained a good fit to the Nafe and Drake curves by using seismic velocity and bulk density data from the Barents Sea. The uncertainty in using this relation is expressed by the minimum and maximum curve (Fig. 5.1).

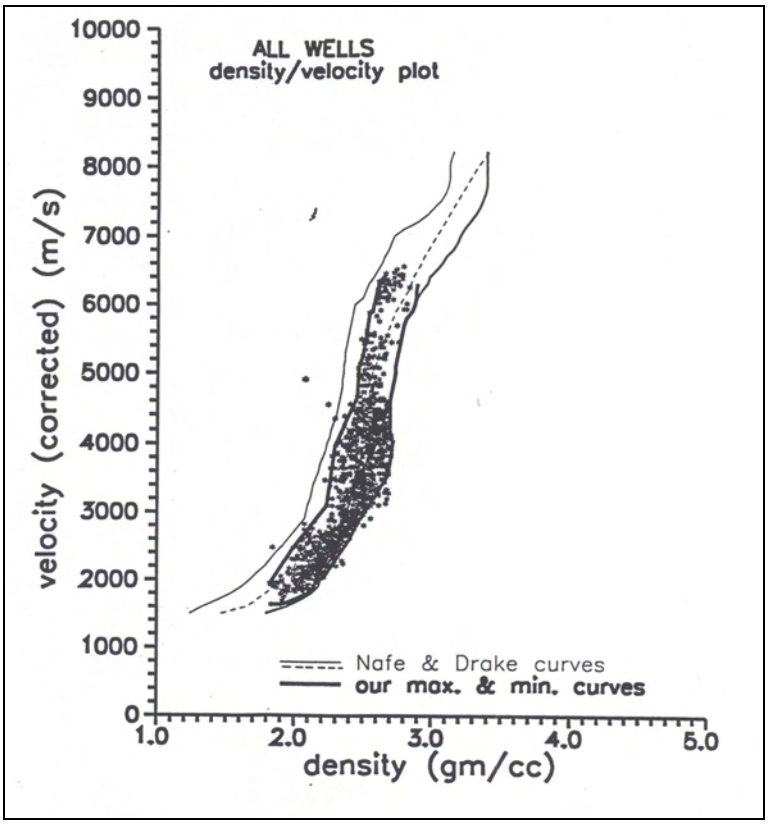

Fig. 5.1: Density versus velocity plot for data from Barents Sea wells (Tsikalas, 1992). The plot is also showing the Nafe and Drake curves (Ludwig et al., 1970).

5.2 Modelling results

Modelling results were improved by "trial and error" until the discrepancy between the observed and calculated gravity anomaly was reduced to an acceptable level. The gravity modelling results are discussed individually for each modelled line/transect.

5.2.1 Line A-A´

As mentioned earlier, the input gravity anomaly along this line used in gravity modelling is extracted from the 1x1 minute free-air gravity anomaly grid that is based on satellite-radar-altimetry (Sandwell & Smith, 1997; version 10.1).

The observed gravity anomaly across line A-A´ reflects very well the basement geometry, as it exhibits a ~90 mGal gravity high at the origin of the profile where the crystalline basement is at shallow depth. At the depocenter, where the sediment thickness reaches ~4.5 km the anomaly drops to a value of ~-65 mGal. The gravity anomaly remains negative across the

sedimentary basin, however it clearly shows a general increase in level towards the east. This gradual level increase in the long-wavelength gravity anomaly component is interpreted to be caused by a progressive shallowing of the Moho relief towards the eastern part of the profile (~26 km Moho depth at the origin and ~14 km Moho depth at ~160 km distance) accompanied by a gradual thinning of the crystalline crust (Fig. 5.2). The progressive shallowing of the Moho relief is characteristic for areas that underwent slow-rate crustal thinning during breakup. There are no indications for volcanic activity in this region, and actually this area (Pernambuco-Paraiba Basin) has even been proposed as a possible non-volcanic rifted margin (Gomes et al., 1997). It has been postulated that the rate of crustal thinning may have considerable influence on the volcanic activity of passive margins (Gomes et al., 1997).

Furthermore, the two prominent gravity anomaly highs at ~400 km distance (Fig. 5.2) are probably related to seamounts on oceanic crust domain. The crystalline crust thickens abruptly across the seamounts as a result of a surface volcanic load flexing an elastic plate. The insertion of the seamounts causes a local isostatic instability which is slowly compensated by Moho deepening underneath the seamounts. Watts et al. (1985) suggest that flexed oceanic crust beneath the Hawaiian-Emperor seamount chain is underlain by a 4 km-lower crustal body (LCB) (underplating). When inserting an underplating to the model, the isostatic compensation of the oceanic crust is represented by a more regional flexure (Fig. 5.3) instead of a very local one (Fig. 5.2). The Figures 5.2 and 5.3 illustrate very well the non-uniqueness effect of gravity anomalies by the fact that different solutions can produce same residual error.

The initial Moho relief provided by forward isostatic and inverse modelling using TAMP shows an overall good fit with the modelled Moho relief with GM-SYS. Nevertheless there are some discrepancies, that were most probably caused by the simplified uniform crustal model used in TAMP.

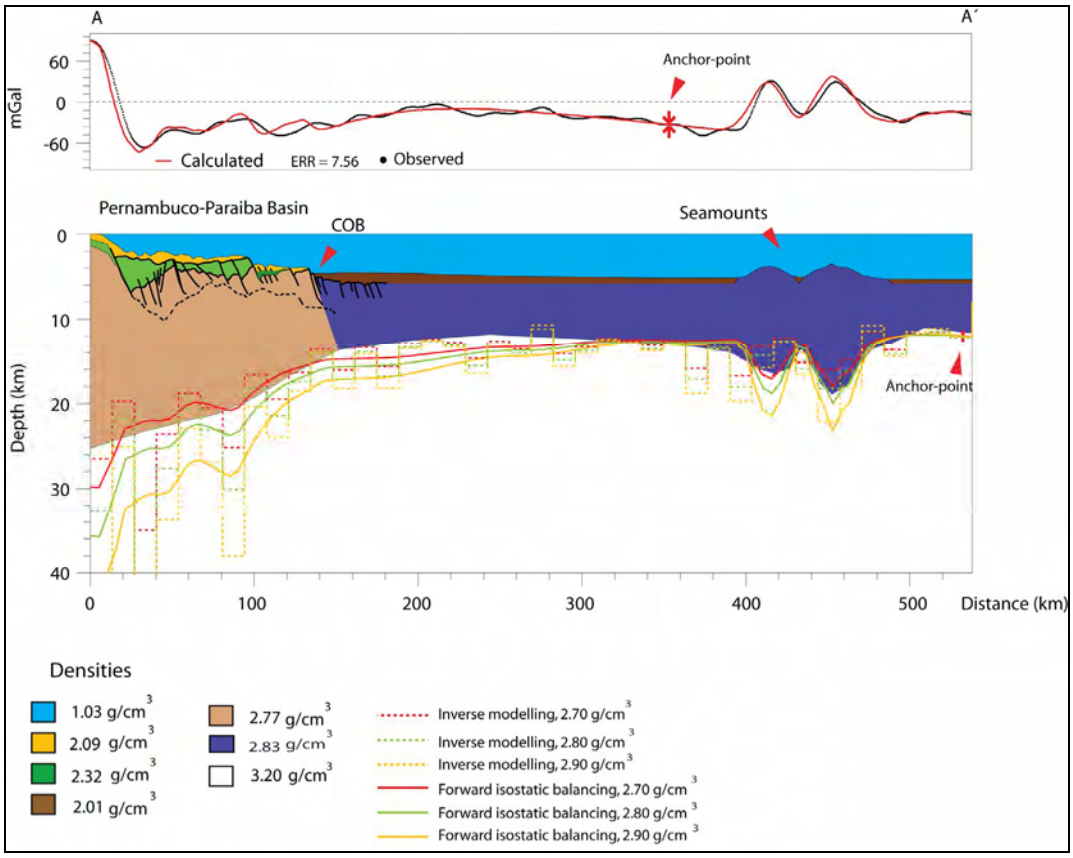

Fig. 5.2: 2-D gravity model of line A-A´. Abbreviations: COB, continent-ocean boundary.

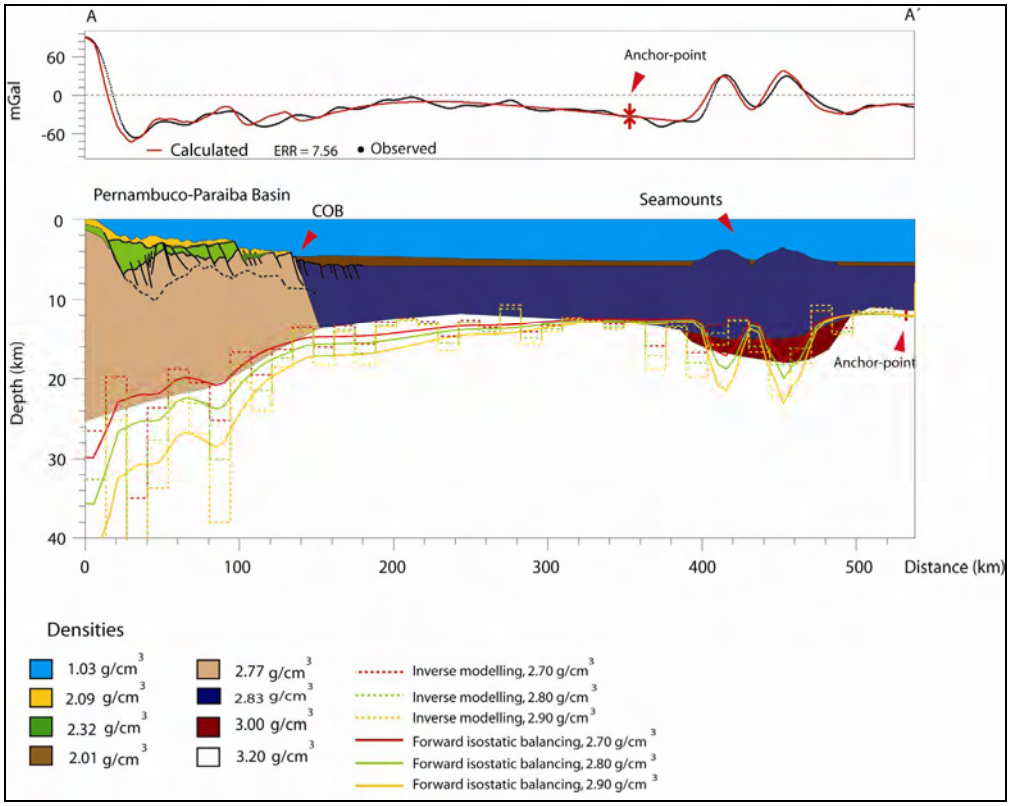

Fig. 5.3: Final 2-D gravity model of line A-A´ with LCB interpreted beneath the seamounts. Abbreviations: COB, continent-ocean boundary.

5.2.2 Line B-B´

As mentioned earlier, the input gravity anomaly along this line used in gravity modelling is extracted from the 1x1 minute free-air gravity anomaly grid that is based on satellite-radar-altimetry (Sandwell & Smith, 1997; version 10.1). For the onshore part (0-220 km distance), Bouguer gravity anomalies (Mohriak et al., 2000) was used and extracted along the line/transect

One remarkable observation is the contrast between the Bouguer gravity anomaly across the onshore rift (Central Tucano Basin) and the free-air gravity anomaly across the offshore rift (Sergipe-Alagoas Basin) (Fig. 5.4). The prominent Bouguer gravity anomaly low (up to -150 mGal) observed across the depocenter of the onshore rift indicates that the rift was not compensated by a mantle uplift and that this basin was filled with sediments of comparatively low density (Fig. 5.4) (Mohriak et al 2000). On the other hand, the lower amplitude gravity anomaly low across the Sergipe-Alagoas Basin reflects that, during rifting, the flexural strength of the lithosphere was significantly smaller across this area in comparison with the Recôncavo, Tucano and Jatobá basins. There is, however, a rise in Moho topography starting in the eastern portion of the Central Tucano Basin and forming a local apex at the footwall of the rift boundary fault.

The Bouguer gravity anomaly attains positive values and forms a small amplitude, wide high at ~110-190 km distance along the line (Fig. 5.4). This high coincides with a Precambrian horst corresponding to the Aporá and Jacuípe highs (Figs. 2.3 and 5.4). The prominent gravity anomaly high observed at about 240 km distance is a characteristic free-air gravity “edge effect” anomaly that characterizes the shelf-break of passive continental margins. These anomalies result due to the juxtaposition of thick crystalline crust and thinned crust (due to rifting), as well as due to magmatic underplating (Watts, 2001).

The gravity model (Fig. 5.4) indicates that a very rapid crustal thinning takes place at the Sergipe Basin, with Moho topography shallowing from ~35 km depth (at 200 km distance) to less than 20 km depth (at 260 km distance).

The local discrepancies between the output of forward isostatic and inverse modelling using TAMP (240-300 km distance) are accounted for in the final gravity model of Figure 5.4 by the introduction of a high-velocity (+7 km/s) LCB (underplating). Such a lower crustal body

is consistent with the interpretations of Mohriak et al. (2000). The initial Moho relief provided by forward isostatic and inverse modelling using TAMP shows an overall good fit with the modelled Moho relief with GM-SYS. Discrepancies located on the extremities of the model are probably caused by “edge-effects”.

.

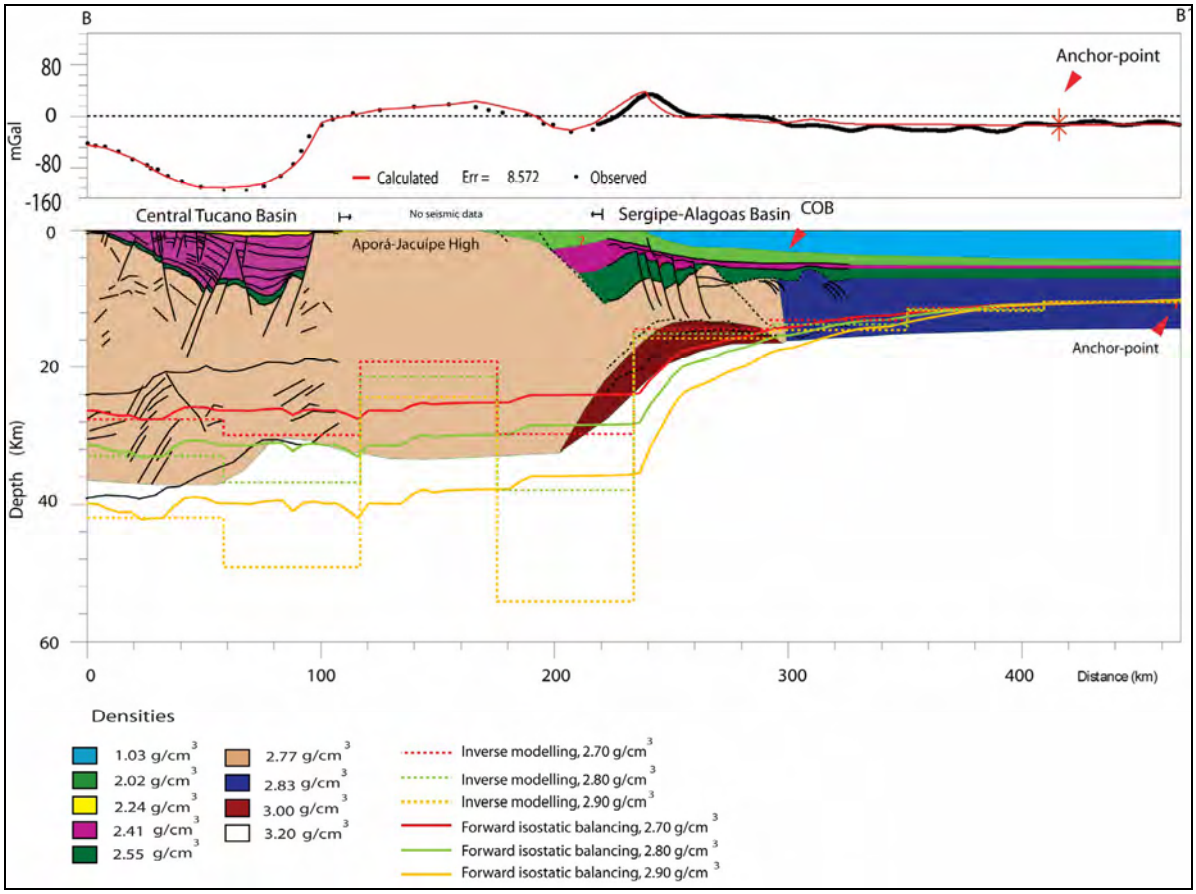

Fig. 5.4: Final 2-D gravity model of line B-B´. Abbreviations: COB, continent-ocean boundary.

The same deep seismic reflector (at 40 km distance and 14 km depth, Fig. 5.5) interpreted by Mohriak et al. (2000) as representing LCB (underplating) was interpreted by Pontes et al, (1991) as representing the transition between a thick syn-rift sedimentary sequence and Precambrian basement. By applying the gravity modelling approach, it is clear that Mohriak et al. (2000) interpretation of this deep reflector as being related to LCB is the most likely one. The large discrepancy (residual error) observed at ~40 km distance (Fig. 5.5) is indicative for the need of higher densities across this area (Fig. 5.4).

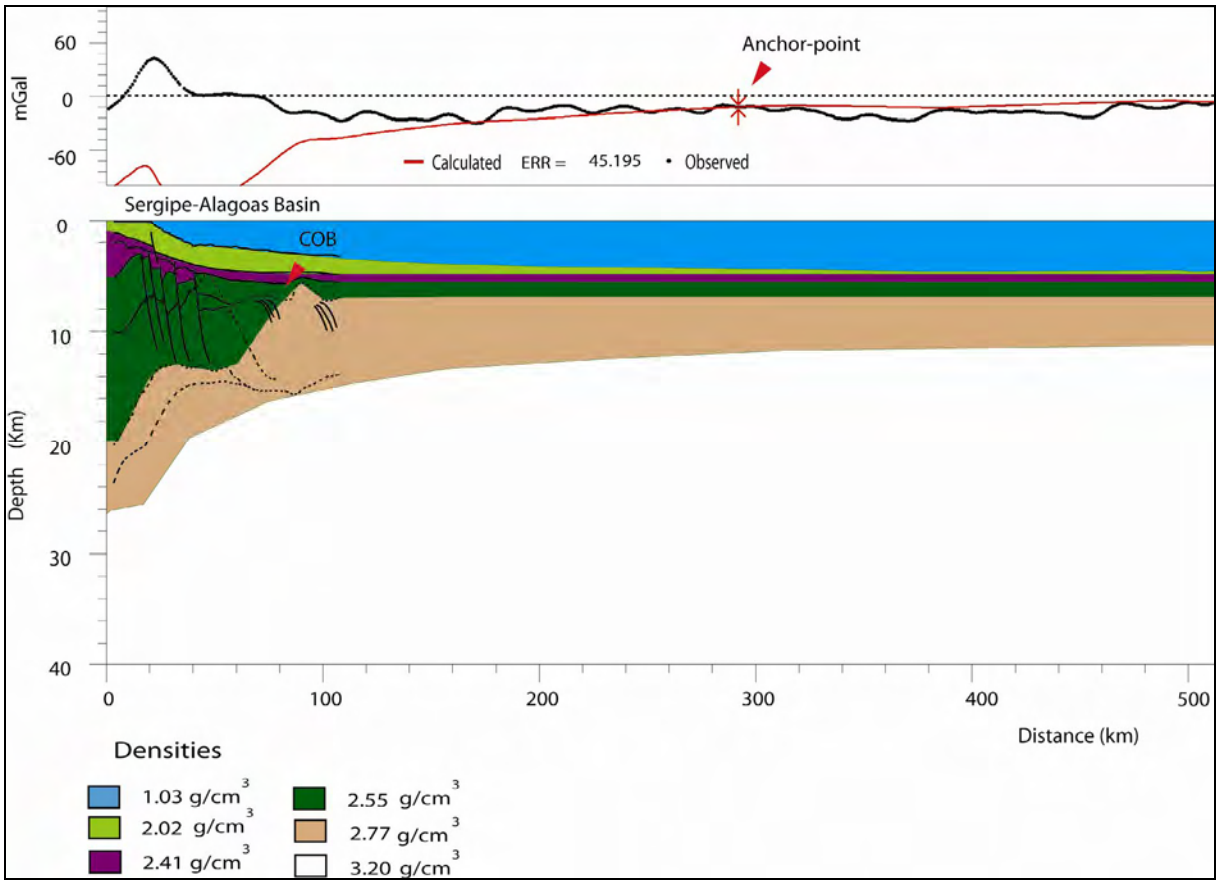

Fig. 5.5: 2-D gravity model along the offshore part of line B-B´. The interpretation is after Pontes et al, (1991), that proposed a very thick syn-rift sedimentary sequences. Abbreviations: COB, continent-ocean boundary.

5.2.3 Line C-C´

The input gravity anomaly used in gravity modelling along the offshore part of line C-C´ is extracted from academic track c1611 (Fig. 3.1). For the onshore part, Bouguer gravity anomalies (Chang et al., 1992) were used and extracted along the line/transect (Fig. 2.5).

A prominent Bouguer anomaly low (up to -100 mGal) is also observed in the depocenter of the South Tucano Basin (Fig. 5.6). Once again the anomaly low is indicative of the lack of both mantle uplift and thinning of the crystalline crust in this area. The Bouguer anomaly low is not so pronounced in the depocenter of the Recôncavo Basin; in this area rifting is indeed compensated by mantle uplift and thinned crystalline crust. The higher amplitude anomaly located in between the South Tucano and Recôncavo basins coincides with the Boa União

high (Figs. 2.4 and 5.6). The broad, high-amplitude gravity anomaly (up to 40 mGal) located around 160 km distance (Fig. 5.6) is caused by the Salvador and Jacuípe highs (Fig. 2.3).
There is no available seismic profile for the Jacuípe Basin in this area, leaving the model very simple and with no further constraints; however it is possible to make some observations based only on the gravity model. The gravity anomaly low observed at ~200 km distance (Fig. 5.6) is probably caused by a rotated fault-block, causing a depression filled with sediments. The gravity anomaly lows located between the shelf edge and continent-ocean boundary appear to be diagnostic of the extended and subsided continental crust, and is caused by the juxtaposition of thick continental crust and thinned oceanic crust (Talwani & Eldholm, 1973). There is a very rapid crustal thinning in the Jacuípe Basin, where Moho shallows from ~30 km depth (at 180 km distance) to ~16 km depth (at 240 km distance) (Fig. 5.6).

The final gravity model for line C-C´ (Fig. 5.6) also requires introduction of an LCB (underplating) located at the region that underwent rapid crustal thinning. An interesting observation is the shallowing of Moho at the origin of line C-C´. This shallowing can simply be caused by an edge-effect or it can be explained by multiple crustal detachment surfaces as suggested by Castro (1987) (Fig. 2.10). In the latter model, the Moho upwarping coincides with the termination of the detachment surface.

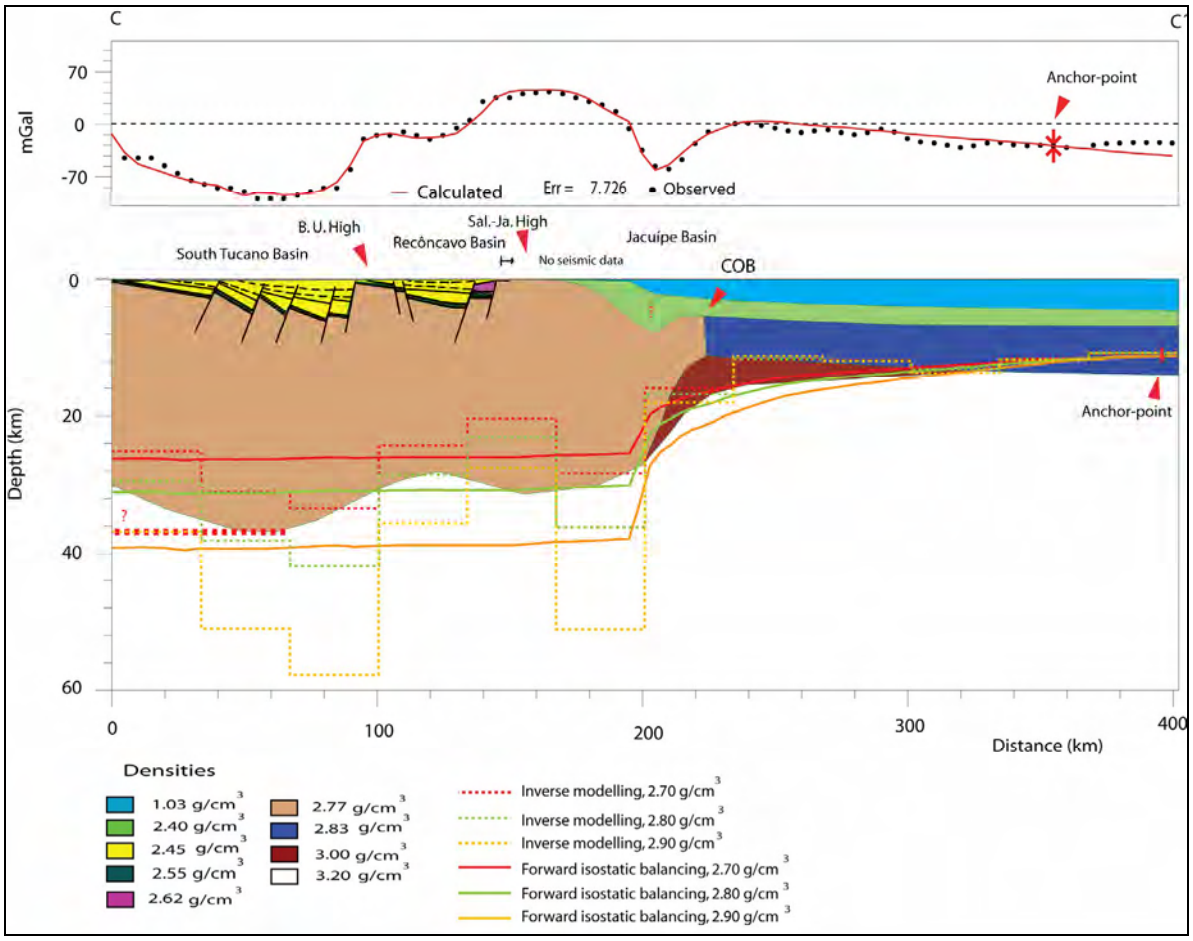

Fig. 5.6: Final 2-D gravity model of line C-C´. Abbreviations: B. U., Boa União; Sal.-Ja., Salvador-Jacuípe; COB, continent-ocean boundary.

5.2.4 Line D-D´

The input gravity anomaly used in gravity modelling along the offshore part of line D-D´ is extracted from academic track c1611 (Fig. 3.1). For the onshore part, Bouguer gravity anomalies (Chang et al., 1992) were used and extracted along the line/transect (Fig. 2.5).

Similar to line C-C´, a gravity anomaly low characterizes the Recôncavo Basin (Fig. 5.7), however, in this line the low is more prominent. This is again indicative of a rift not being compensated by mantle uplift and thinned crystalline crust. The locally higher-amplitude anomaly observed at ~40 km distance is most probably caused by high density Atlantic granulites at this location (Figs. 2.4 and 5.7). The dislocation of the anomaly may have been caused by a 3-D effect explained by the fact that the Bouguer gravity anomaly in the Recôncavo, Tucano and Jatobá basins has an overall N-S orientation. As for its first ~70 km, the profile is orientated sub-parallel to the orientation of the Bouguer gravity anomaly contour lines (Fig. 2.5) and therefore, the extracted along-profile anomaly will not be totally

representative for the gravity anomaly trend in the area. This anomaly might also simply be caused by the Dom João High (Figs. 2.4 and 5.7). If this is the case, anomaly high expected to be caused by Atlantic granulites are not captured due to the 3-D effect explained above. Furthermore, the large discrepancy between the observed and calculated gravity anomaly located at 120 km distance is probably caused by misinterpretation of the anomaly amplitude. This is probably due to the manual reading and extraction of the anomaly values and due to the fact that the Bouguer anomaly gradient is very steep in this area hindering the proper distinction between the contour lines (Fig.2.5).

Moho is almost flat underneath the Recôncavo Basin lying at a depth of ~30 km and shallows very rapid at the Jacuípe Basin reaching depth <20 km. Therefore, the crystalline crust in this area underwent rapid thinning. The discrepancy between isostatic balancing and inverse gravity modelling done with the use of TAMP is discussed in chapter 4.2.2.

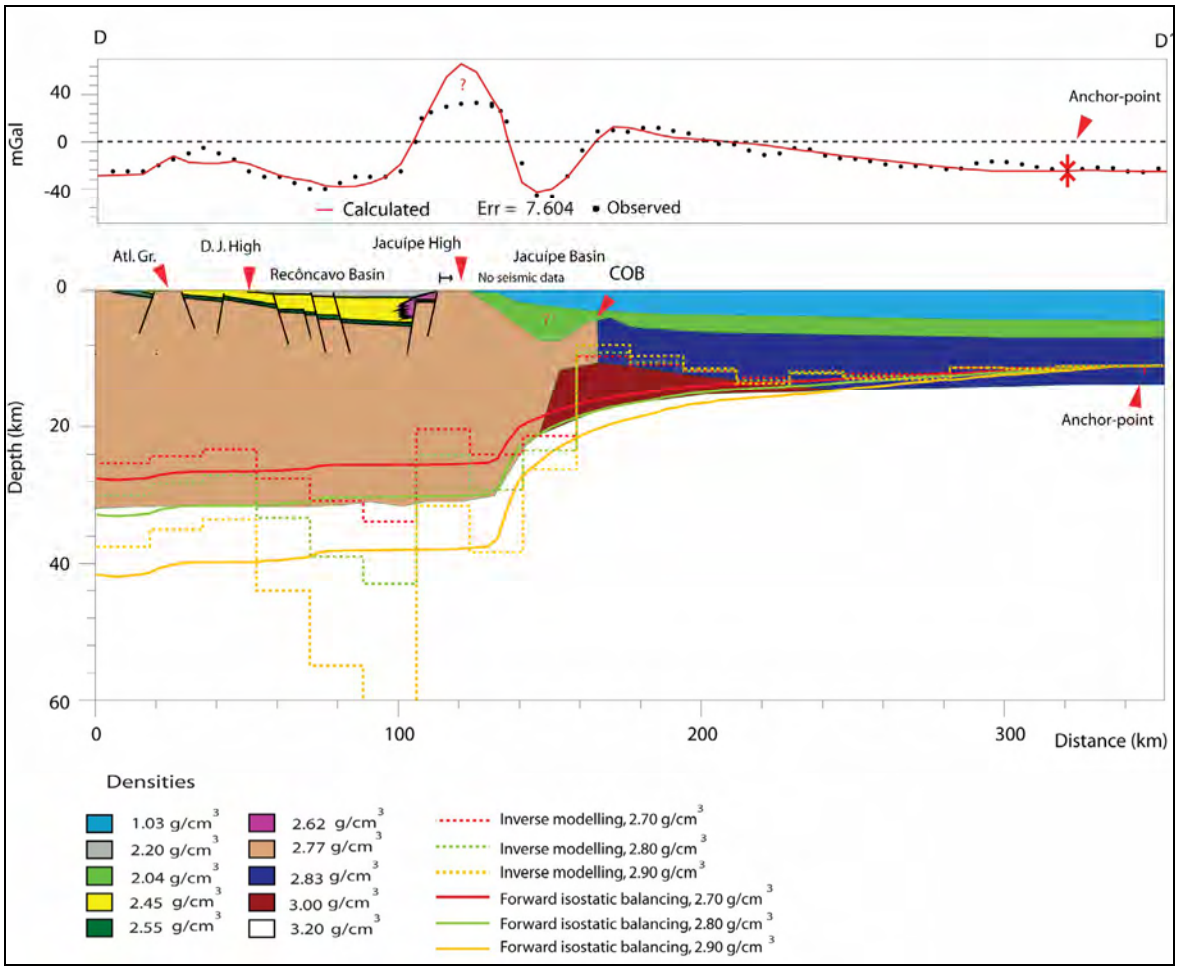

Fig. 5.7: Final 2-D gravity model of line D-D´. Abbreviations: Atl. Gr., Atlantic Granulites; D. J., Dom João; COB, continent-ocean boundary.

Chapter 6
Discussion

Several geological/geophysical models have been proposed for the formation and evolution of the Northeastern Brazil basin systems (e.g.Austin & Uchupi, 1982; Ussami et al., 1986; Castro, 1987; Milani & Davison, 1988). In the light of the performed analysis, the aim of the discussion chapter is to evaluate the existing models and come up with an integrated structural model for the formation and evolution of the Tucano, Recôncavo, Sergipe-Alagoas, Jacuípe and the conjugate Gabon basins. The focus area discussed in this chapter is the “corridor” formed by lines B-B´, C-C´ and D-D´ (Fig. 6.4).

6.1 Basin formation and evolution of the Northeastern Brazilian margin

The final gravity models (Fig. 6.1) show that Moho is shallows considerably more across the Sergipe-Alagoas/Jacuípe basins than across the South Tucano and Recôncavo basins. This implies that crustal thinning is much more accentuated across the Sergipe-Alagoas/Jacuípe than across South Tucano and Recôncavo basins. In addition, the Moho shallowing across the Sergipe-Alagoas/Jacuípe, Pernambuco-Paraiba and Recôncavo, Tucano and Jatobá basins is located eastward of the deepest part of the basins. Furthermore, the boundary between upper brittle crust and the lower ductile crust can represent a physical boundary that separates zones with different deformation characteristics, i.e. crustal heterogeneities. Intracrustal detachment and décollements zones may develop often at such heterogenic boundaries as high-angle planar normal faults can easily evolve into listric normal faulst following the dip of the detachment instead of dying out in a plastic deformation regime. The observations on the Northeastern Brazilian margin (Fig. 6.1) will be discussed and evaluated in the framework of simple shear and pure shear crustal extension models. An integrated structural model is further proposed.

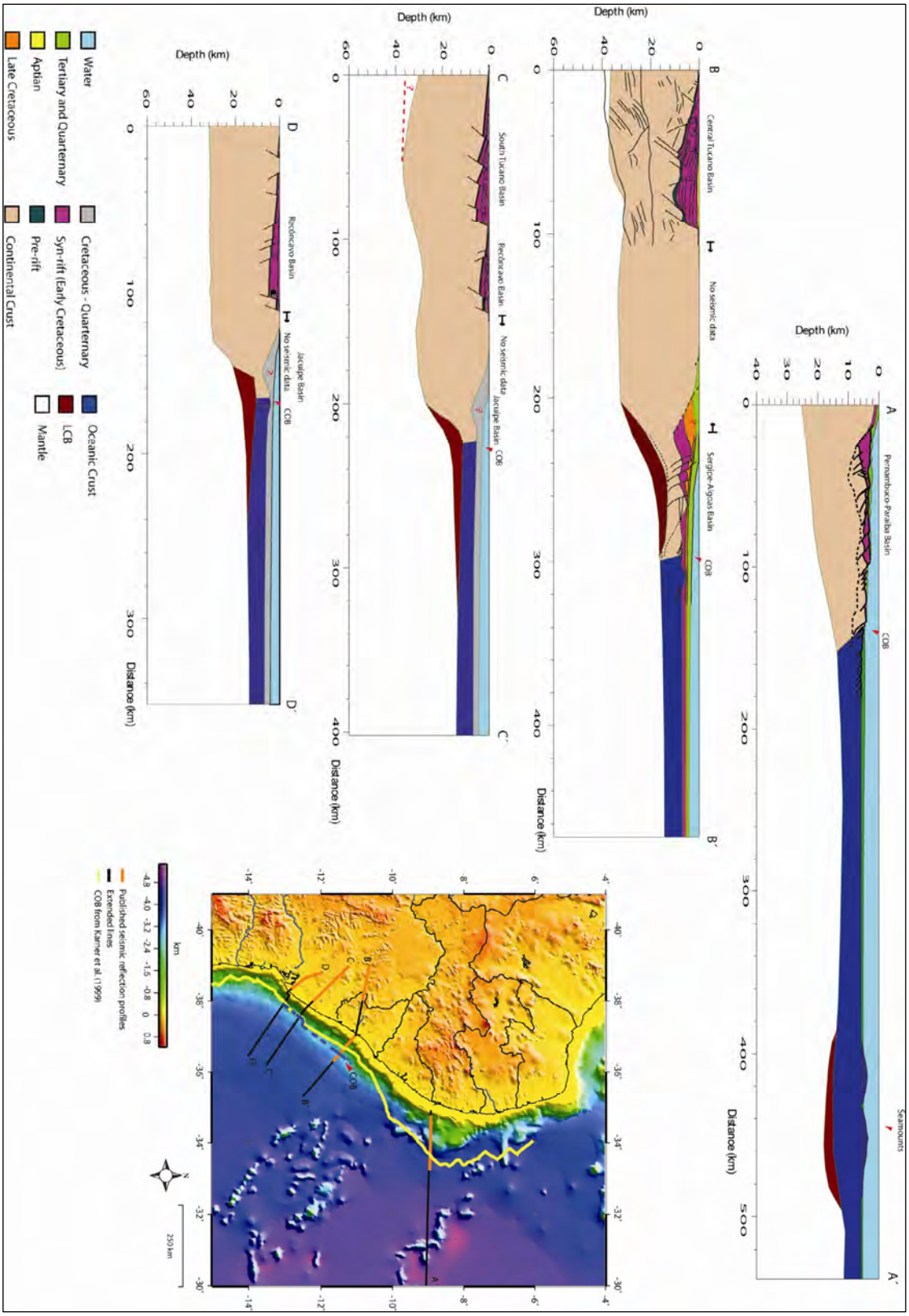

Fig. 6.1: Final 2-D gravity models of all profiles. Bathymetry map (left figure) shows the location of the profiles as well as the COB defined by Karner et al. (1999) (yellow line) and COB defined in this study (blue line).

Simple Shear

The simple shear model has been proposed by Wernicke (1985). In this model, the basal detachment cuts down all the way through the crustal lithosphere until it reaches the Moho discontinuity (Fig. 6.2). The detachment can be subhorizontal for a large distance before it ramps down cutting the lower crust. This model can explain a dissimilar extension between the crust and the lithospheric mantle, where extension is not uniform with depth. The detachment acts as the fundamental boundary that separates the crust in an upper plate and a lower plate. Moreover, in this model, the zone of maximum crustal extension is not necessarily located directly over the region of maximum lithosphreric mantle extension (Fig. 6.2). This model can also account for the asymmetry observed in many rift systems.

Pure shear

The pure shear model has been proposed by McKenzie (1978). In this model, the detachment defines the base for upper crustal normal faulting and the transition between brittle/ductile deformation (Fig. 6.2). The crust and mantle lithosphere will be deformed uniformly across a broad zone beneath the detachment by ductile strain or movement on an array of anastamosing shear zones. The model implies uniform extension with depth, i.e. a square becomes a rectangle when extension is imposed. In addition, the pure shear model implies that lithospheric mantle extension and lithospheric mantle upwarping will find place directly below the region of maximum crustal stretching and thinning (Fig. 6.2).

Combined shear-hybrid model

Barbier et al. (1986) proposed a hybrid model, where extension is partial uniform with depth, meaning that the detachment accounts for a limited separation between the upper plate and lower plate. Furthermore, the shear zone of the simple shear model may merge at depth with a zone of uniform deformation (Fig. 6.2).

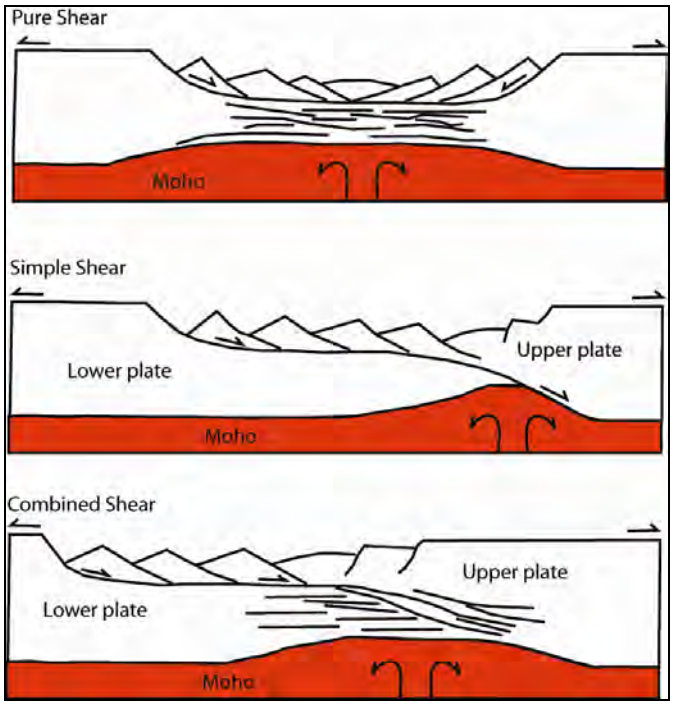

Fig. 6.2: Models of rifting and lithospheric stretching at the crustal scale (modified after van der Pluijm & Marshak, 1997).

Integrated structural model

According to McKenzie's (1978) pure shear model, the lithospheric extension will usually be succeeded by post-rift sedimentation that will reach thicknesses approximately equal to that of the syn-rift sedimentary deposits. If this concept is applied to the Northeastern Brazilian margin, it implies that ~6 km of post-rift sediments were deposited across the Tucano Basin, burying pre-rift sediments to a depth of ~12 km. Since post-rift sediments are not observed in the Recôncavo, Tucano and Jatobá basins (Chang et al., 1992), it means that ~ 6 km of post-rift sediments must have been removed by erosion across the basins. However, observed sandstone porosity values of the pre-rift sequences (Sergi Formation of the Brotas Group) (Figs. 2.11 and 2.14) beneath the Tucano Basin, indicate primary values typically ranging 10-20 % at 2.5-2.6 km depth (Karner et al., 1992). The remaining high porosities exclude the deep burial of these sediments and imply that extensive erosion is not a likely explanation for the absence of post-rift sediments across the Recôncavo, Tucano and Jatobá basins.

Based on kinematic modelling, Karner et al. (1992) suggested that the crustal extension responsible for both the Tucano and Sergipe-Alagoas basins was similar and coexisting in time. Furthermore, it was suggested that the weakest region in an extending lithosphere is

where the maximum crustal thinning coincides with the region of maximum lithospheric mantle thinning. This means that the eventual continental breakup and onset of oceanic crust formation should occur where crustal thinning and lithospheric mantle thinning is greatest. (Karner et al., 1992). The Tucano Basin has approximately the same depth as the Sergipe-Alagoas Basin (Fig 6.1) implying that the amount of crustal extension and deformation was probably similar for both basins. If the above assumptions are taken into consideration, then the fact that continental breakup, as evidenced by the occurrence of the continent- ocean boundary took place in the Sergipe-Alagoas Basin and not in the Tucano Basin can only be accounted for the fact that extension was not uniform with depth. The dissimilar extension between the crust and the lithospheric mantle requires the existence of an intracrustal detachment (Karner et al., 1992).

The large gravity anomaly amplitude difference observed across the Tucano and Sergipe-Alagoas basins (Fig. 6.3) also indicates that lithospheric mantle extension was considerable larger across the Sergipe-Alagoas Basin in comparison to the Recôncavo, Tucano and Jatobá basins. These observations also support the need to introduce a detachment separating the crust into upper and lower plate.

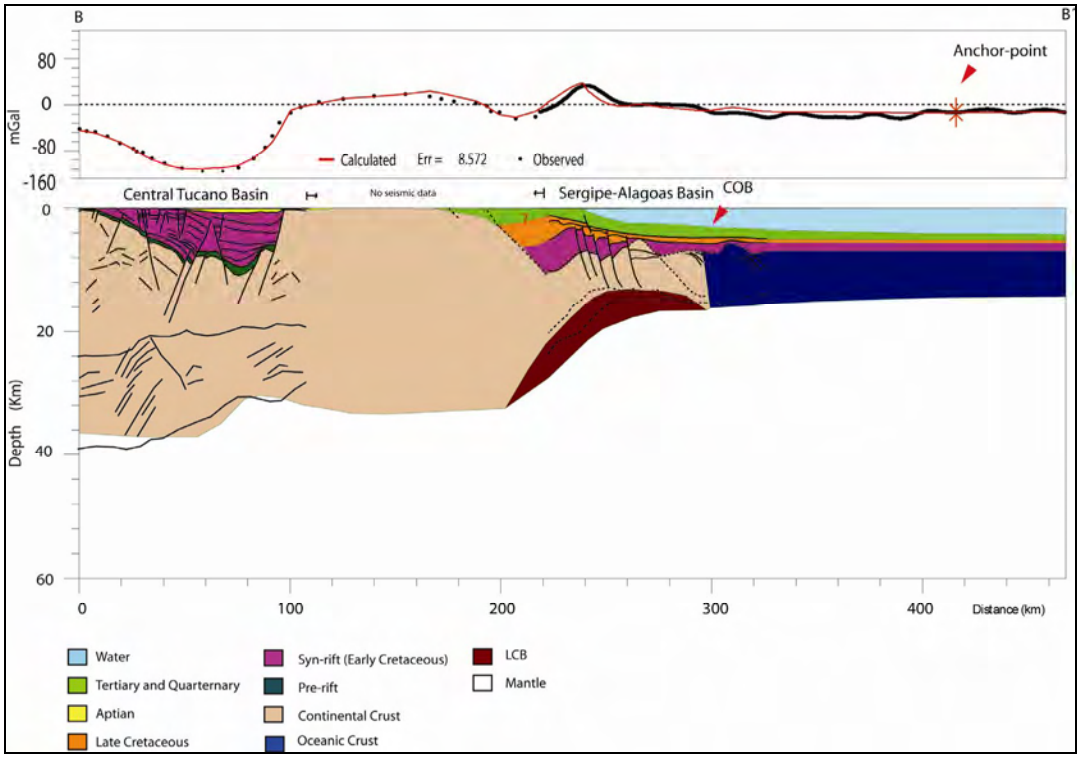

Fig. 6.3: 2-D gravity model of line B-B´. The model shows that lithospheric mantle extension was considerable larger across the Sergipe-Alagoas basin, indicating a dissimilar extension between the crust and the lithospheric mantle.

Based on the gravity model results (Fig. 6.1) and on the structure map provided by Milani & Davison (1988) (Figs. 2.3 and 2.4), a simplified structure map (Fig. 6.4) and a structural model (Fig. 6.5) were created to illustrate the possible involvement of detachments during the South Atlantic rifting and the formation of Recôncavo, Tucano and Jatobá /Sergipe-Alagoas and Jacuípe basins. It appears that the upper crustal extensional deformation in this area was strongly influenced by a pattern of structural inheritance. In particular, a complex Proterozoic inheritance has been proposed where crustal heterogeneities are controlled by the complex network of shear zones and by two different kinds of terrains, namely Proterozoic granulites and Proterozoic metasediments (Darros De Matos, 1999) (Fig. 2.3). The detachments proposed on the structure map (Fig. 6.4) are located on these zones characterized by different kinds of terrains.

The zone across the Recôncavo Basin was probably influenced by pure shear crustal extension in the early stage of rifting followed by simple shear. This assumption is based on the observed shallowing of Moho across profile C-C´ and on the geometry of the Recôncavo Basin (Fig. 6.5). A zone of simple shear crustal extension is proposed for the Central and South Tucano Basin.

The COB location proposed by Karner & Driscoll (1999) is defined from potential field data and is subjected to uncertainties. Using potential field data and available reflection seismic profiles, the COB is redefined across Jacuípe Basin (Figs. 6.4 and 4.12).

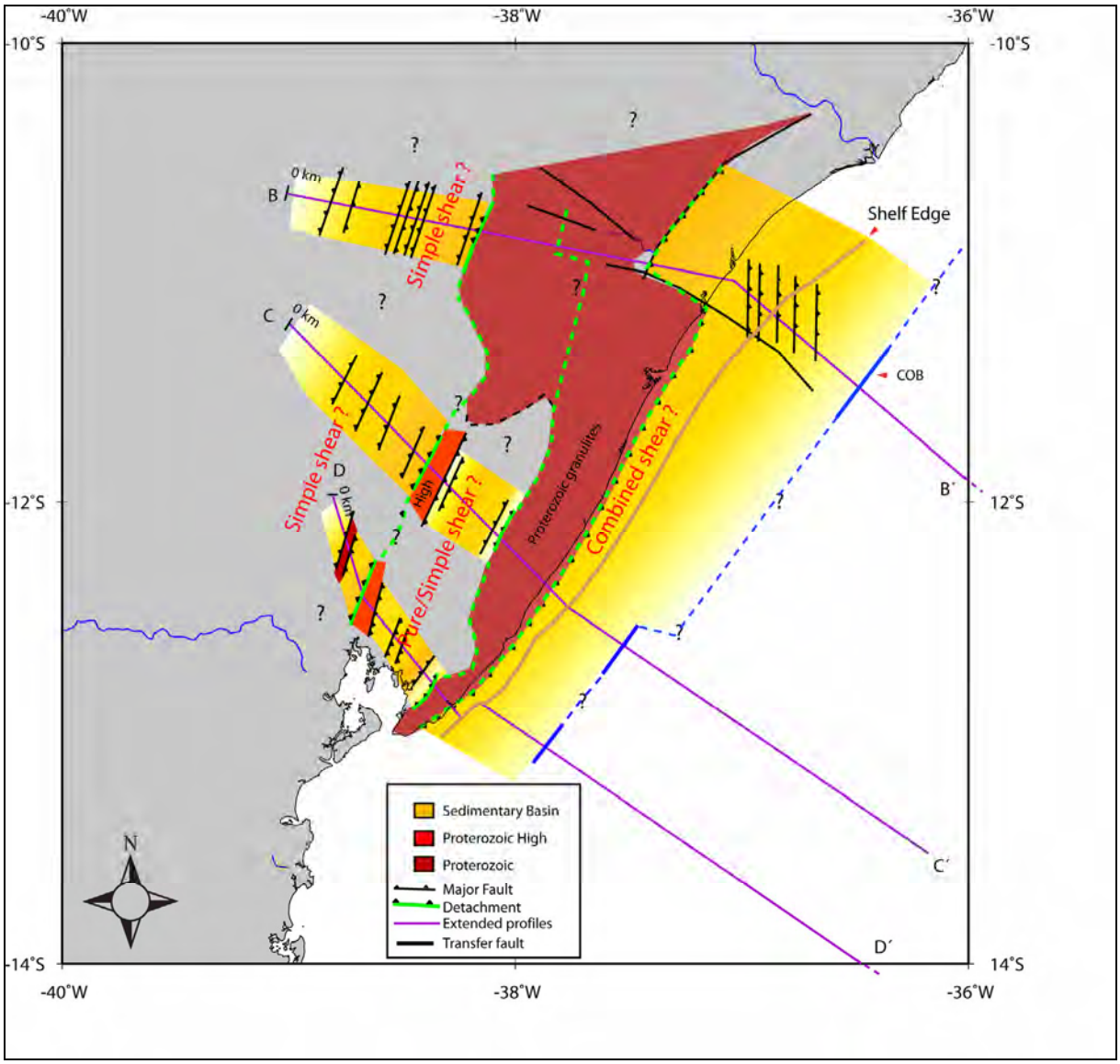

Fig. 6.4: Simplified structure map, indicating a possible deformation regime acting during the South Atlantic rifting and basin formation.

The proposed structural model (Fig. 6.5) exhibits some similarities with the model proposed by Castro (1987) (Fig. 2.10). However, the lithospheric mantle compensation observed both on line B-B´ (~80–120 km distance, Fig. 6.5) and C-C´ (~80–130 km distance, Fig. 6.5), across the Tucano and Recôncavo basins were not proposed by the Castro, (1987) model. Furthermore, a different dip for the detachment located across the Sergipe-Alagoas/Jacuípe basins is now proposed (Figs. 2.10 and 6.5). The thinning of the crust and Moho shallowing observed across the Tucano and Recôncavo basins (lines B-B´ and C-C´, Fig. 6.5) are interpreted to be possibly caused during a period of pure shear regime preceded by the simple

shear detachment establishment. The lack of crustal thinning observed on line D-D´ may be related to sensitivity problems during gravity modelling.

The dip of the detachment was interpreted based on the geometry of the basins, i.e. where the depocenter indicating the area of greatest subsidence is likely to be located at the onset of the detachment. The most likely model of rifting that separated Africa from Brazil is the combined shear model (Fig. 6.2). This assumption is substantiated by the fact that the maximum crustal thinning is not placed directly bellow the maximum depocenter depth of Sergipe-Alagoas/Jacuípe basins but also not so far from it as it would have happened in the case of a simple shear crustal extension model.

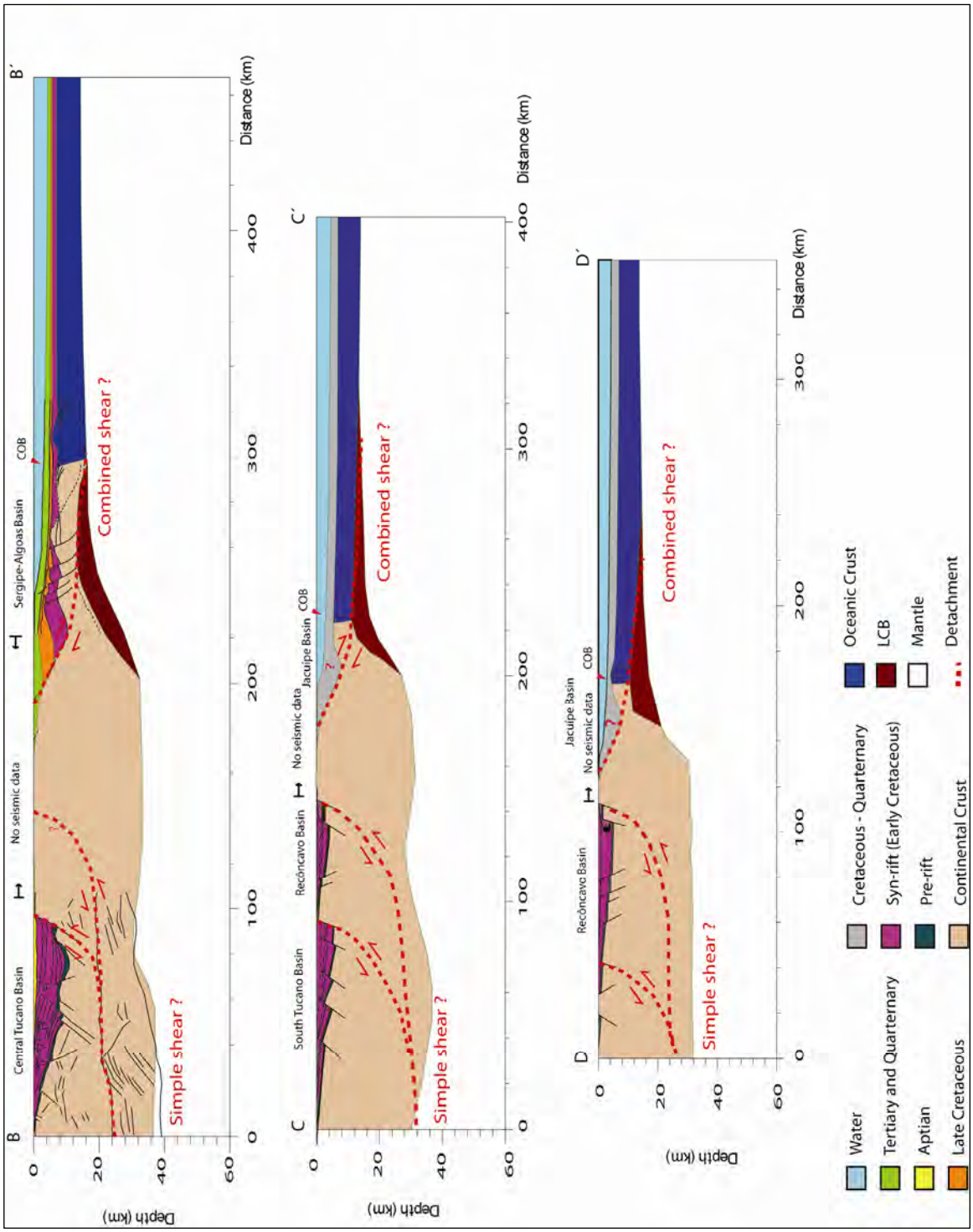

Fig. 6.5: Proposed evolution for the Recôncavo, Tucano and Jatobá /Sergipe-Alagoas and Jacuípe basins.

6.2 Oblique transform margin

Mohriak & Rosendahl (2003) postulated that the depocenters of purely extensional rift basins are parallel to the spreading centre (Mid-Atlantic Ridge) and are located between major transform offsets. The detailed structure map of the Sergipe-Alagoas Basin (Fig. 6.6) clearly shows that the sub-basins exhibit an overall en-echelon fault arrangement. This N-S arrangement is sub-parallel to the Mid-Atlantic Ridge (Fig. 6.9), suggesting that this margin segment was produced by extension. However, there is evidence that breakup of the South Atlantic cannot be modelled by a simple rotational opening as proposed by Rabinowitz & La Brecque (1979) (Milani & Davison, 1988). In particular the involvement of transform fault dislocations along the subequatorial South Atlantic prior to final rupture.

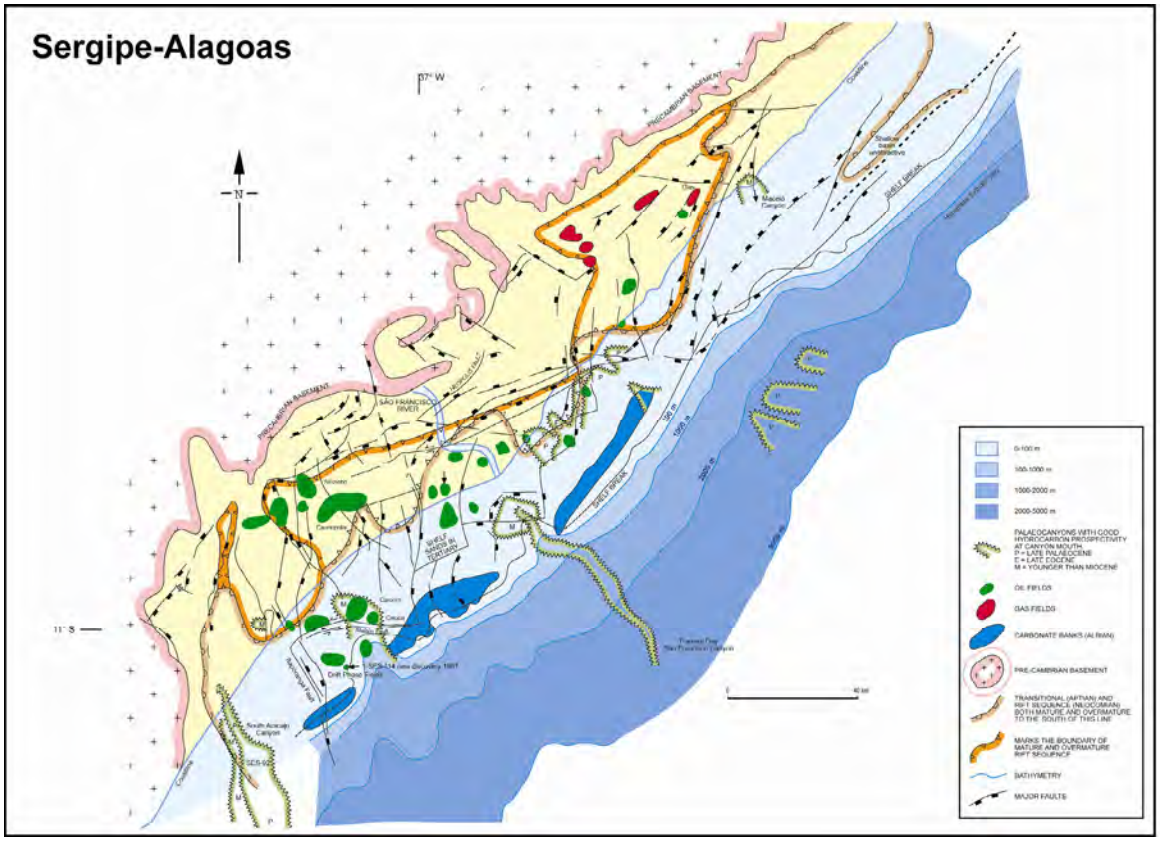

Fig. 6.6: Major tectonic and structural features of the Sergipe-Alagoas Basin. An overall en-echelon fault arrangement is clearly shown on this figure (Davison, 1999).

On sheared continental margins, elevated continental crust is juxtaposed against subsided oceanic crust across a transform fault (Mohriak & Rosendahl, 2003). The seismic profile C

(Fig. 6.7) exhibits some typical characteristics of a sheared continental margin. In particular the elevated continental crust, observed at ~120 km (Fig. 6.7), is juxtaposed against subsided oceanic crust, and shallowing of Moho across this line (line A-A´) is gradual which is characteristic for areas that underwent slow-rate of crustal thinning during breakup (Fig. 6.1). In addition, the absence of SDRs along this profile indicates the close proximity to a transform margin (Gomes et al., 1997). These observations leave open the possibility for an dominantly transform zone located northward of the Maceió-Ascencion F.Z. This means that the opening of the South Atlantic was affected by two very different regimes: one extensive (with some oblique component), affecting areas located south of the Maceió-Ascencion F.Z. and another dominantly shear/transform matter affecting areas north of the Maceió-Ascencion F.Z.

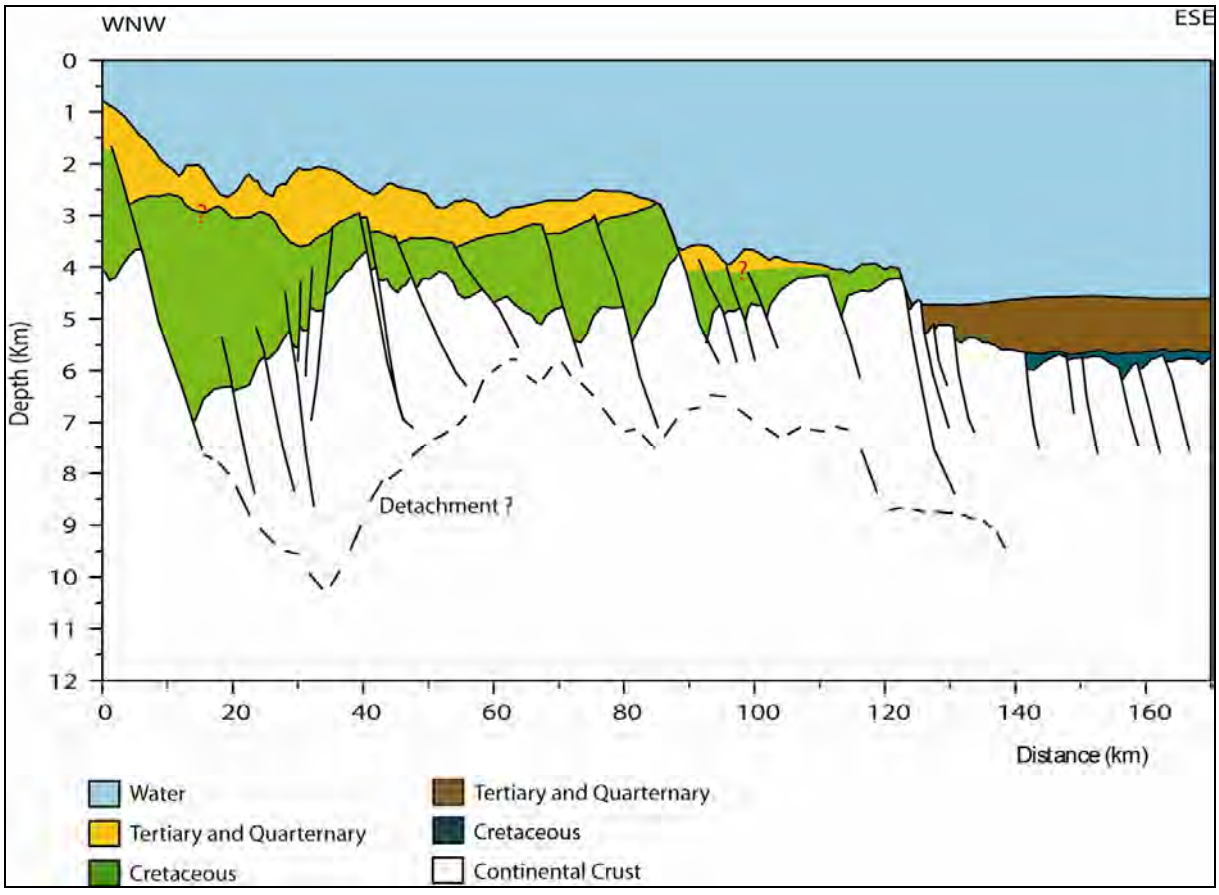

Fig. 6.7: Depth-converted reflection seismic profile C. Seismic interpretations are based on Gomes et al, (1997).

The amount of stretching prior to drift and consequently the width of the rift in a given locality is not only dependent on the pre-rift strength of the lithosphere but also on the coincidence in space and time between maximum crustal thinning and maximum lithospheric mantle thinning. The rift width is changing abruptly across the Brazilian and African margins.

In the Gabon Basin, the rift width is considerable extensive southward of the N´Komi-Salvador F.Z. and narrows abruptly towards the north (Fig. 6.9). On the other hand, the rift width on the conjugate Brazilian margin is very small southward of the N´Komi-Salvador F.Z. and enlarges northwards. However, it is only northward of the Maceió-Ascencion F.Z. that the rift becomes considerable wide. In the margin segment between the Maceió-Ascencion and N´Komi-Salvador fracture zones there are no accentuated differences on the rift width (Fig. 6.9).

Based on the above observations it is tempting to classify the different segments in accordance with the rift models indicated on Figure 6.2. The different segments can be interpreted as being evolved with different detachment dips and with different rift symmetries. The margin segments located southward of the N´Komi-Salvador F.Z. can be interpreted as having a westwards-dipping detachment. The structural evolution of this segment is easier explained with the simple shear model, where the line of continental breakup was located closer to the Brazilian margin. The segments located northward of the Maceió-Ascencion F.Z. can be interpreted as having an eastward-dipping detachment (Fig. 6.8). Similarly, the structural evolution of this segment is explained easier with the simple shear model, however, breakup probably took place in an oblique sense and is located closer to the African margin. The segment sandwiched between the Maceió-Ascencion and N´Komi-Salvador fracture zones can be interpreted as having an eastward-dipping detachment. The structural evolution of this segment is easier explained with the combined shear model, where the rift width is similar on both conjugated margins (Fig. 6.9). A tectonic reconstruction model was only attempted for the segment located between the Maceió-Ascencion and N´Komi-Salvador fracture zones since it is the focus area for the thesis (line E-E´, Figs. 6.9 and 6.10). Note that the discussion presented here is just a first attempt to understand the structural evolution of the other margin segments since there was limited amount of studied data on these regions.

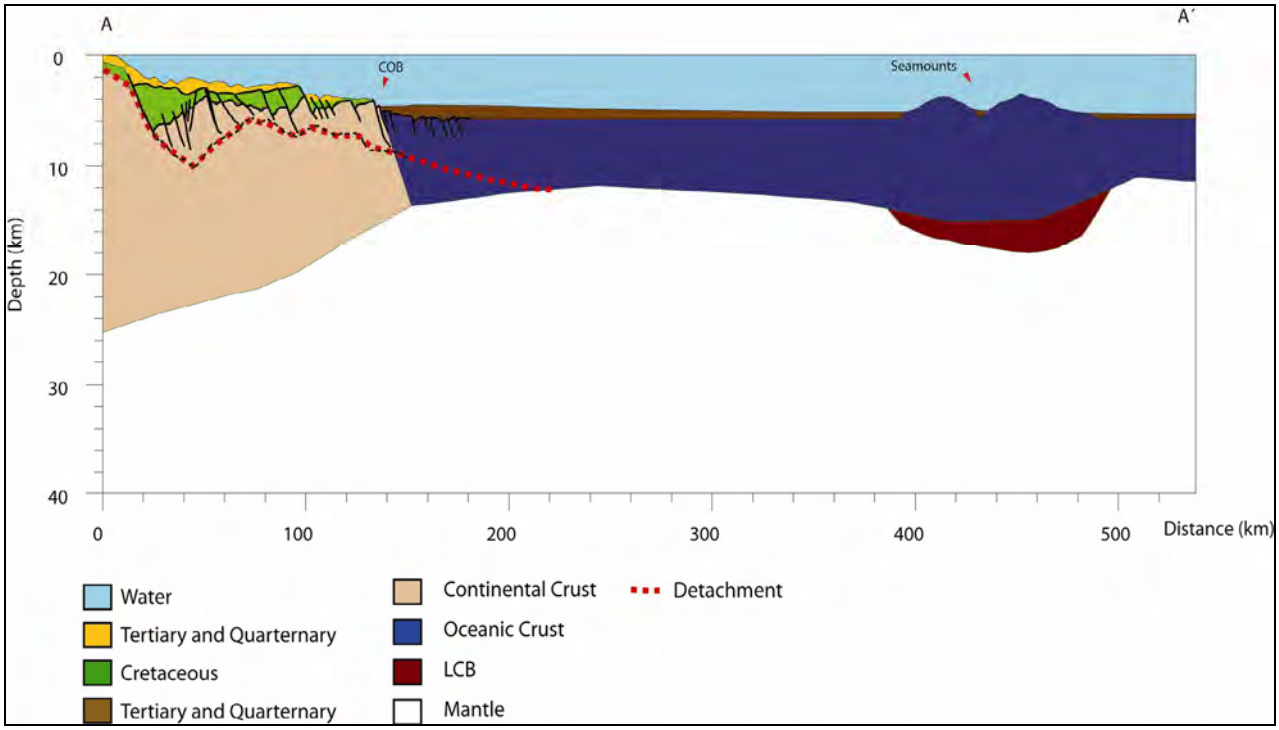

Fig. 6.8: Final 2-D gravity model of line A-A´. A detachment surface is interpreted to dip eastwards.

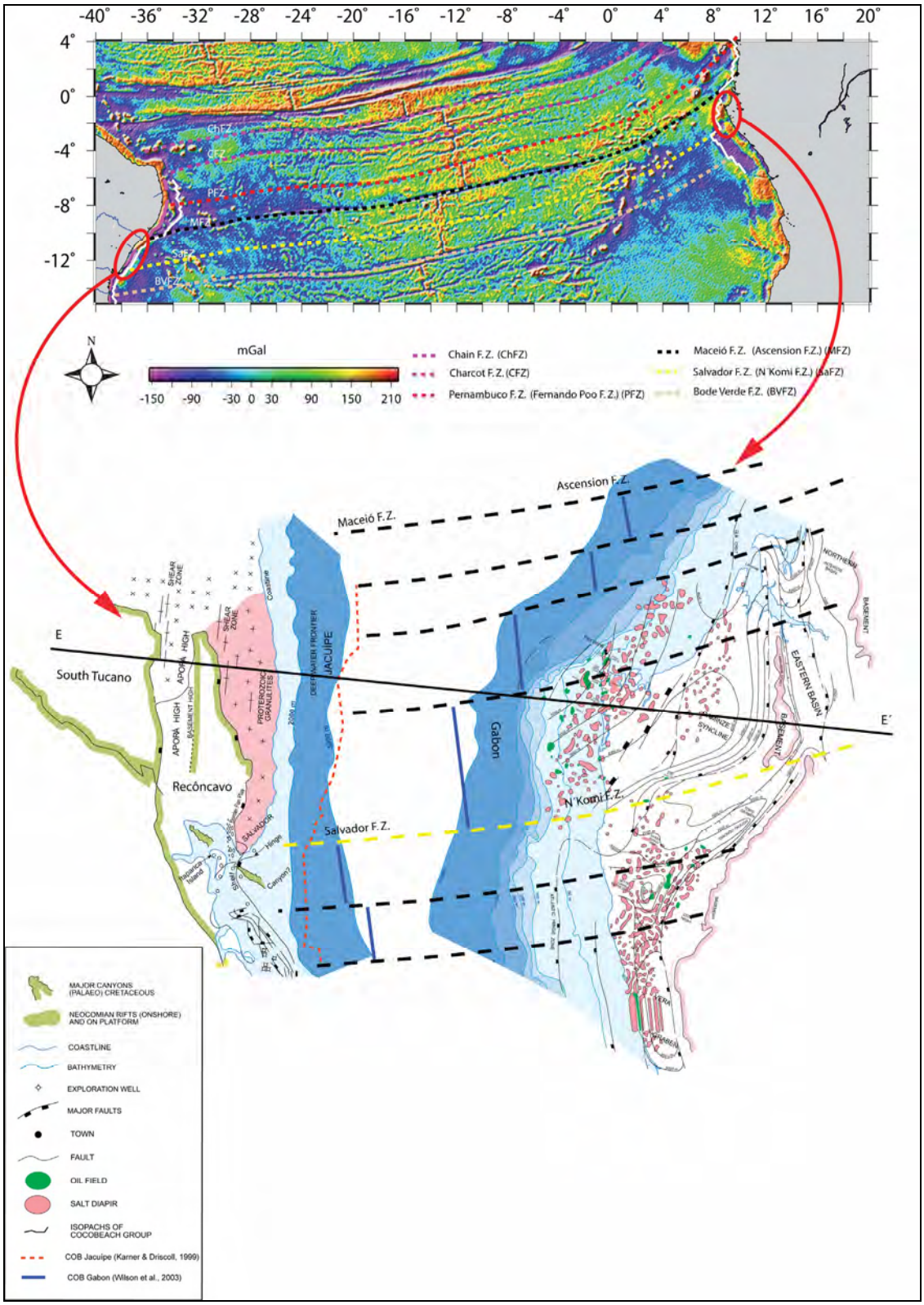

Fig. 6.9: Top: map showing current position of the continent Brazilian and African margins with the main fracture zones. The COB (white line) on the Brazilian side is from Karner & Driscoll (1999) and on the African side from Wilson et al. (2003). Bottom: Plate reconstruction showing the main fracture zones and the position of the conjugate margins during breakup (modified from Davison, 1999). Here, the COB on the Brazilian side (dashed red line) is from Karner & Driscoll (1999), and on the African side (blue line) from Wilson et al. (2003).

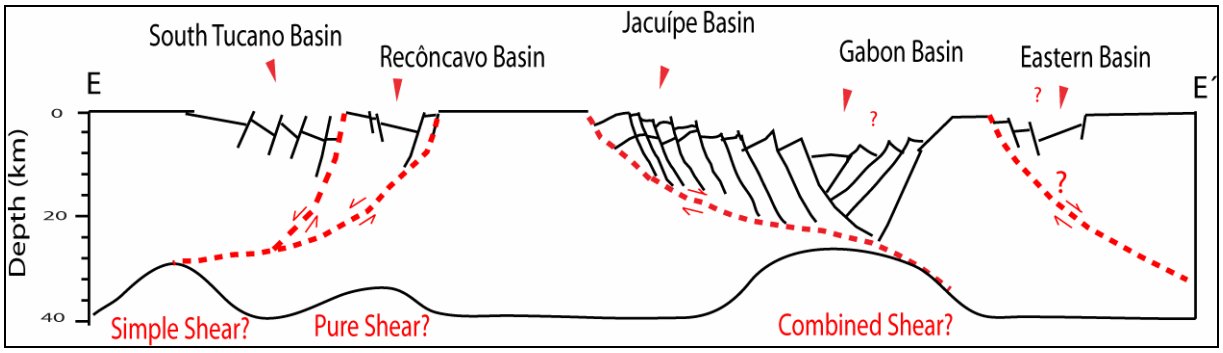

Fig. 6.10: Suggested pre-breakup structural model for the conjugate Tucano-Gabon basin system.

6.3 Breakup related magmatism

With the purpose of discussing more closely breakup related magmatism one more profile is introduced to this thesis (Fig. 6.11). The seismic reflection profile (profile C) was published by Mohriak et al. (1998). Profile C is a deep seismic reflection profile located across the Jacuípe Basin (Fig. 6.12). The seismic section shows sigmoidal reflectors dipping seaward located between ~45-70 km (between 6.0 and 7.5 s TWT) on Figure 6.11. These sigmoidal features were attributed by Mohriak et al. (1998) to impedance contrasts between magmatic layers formed during emplacement of oceanic crust (SDR´s). The high impedance deep seismic reflectors observed across the entire seismic section (from 7.5-9.5 s TWT on Fig. 6.11) may correspond to the crust-mantle transition in the deep water region, although it can also represent the top of a lower crustal body (LCB).

In order to accomplish for an acceptable 2-D gravity model, it was necessary to introduce high density bodies (LCB) on profiles B-B´, C-C´, D-D´ (Fig. 6.1). All profiles are marked by very rapid crustal thinning. These facts indicate magmatic activity during emplacement of oceanic crust. Moreover, SDR´s were observed across seismic reflection profile A-2 (Fig. 4.6) and C (Fig. 6.11) again indicating that this part of Brazilian margin was influenced by intense magmatic activity during breakup. However, across profile A-A´ there was no need for LCB during 2-D gravity modelling neither there was observed SDR´s (Figs. 4.1 and 5.3). This

profile is marked by gradual crustal thinning. These facts indicate that this part of the rifted Brazilian margin was probably absent of magmatic activity during breakup.

Summarizing these observations it is likely that areas northward of the Maceió-Ascencion F.Z evolved as a non-volcanic rifted margin, whereas areas southward of the Maceió-Ascencion F.Z. evolved as a typical volcanic margin.

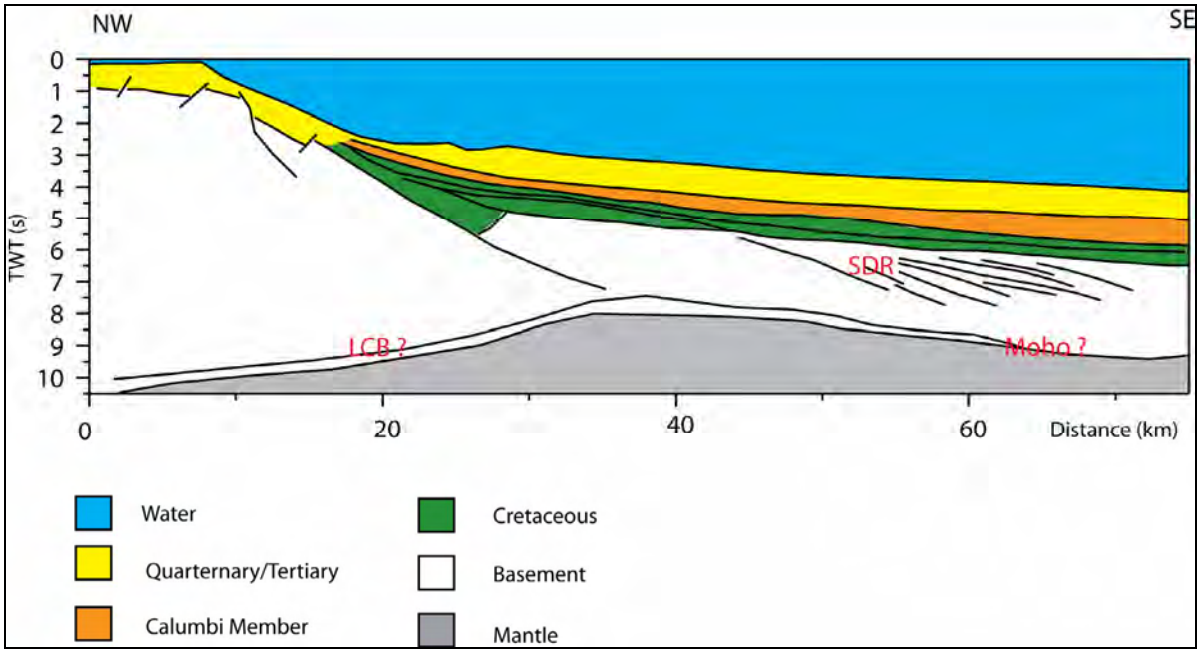

Fig. 6.11: Digitised published profile C in TWT showing interpretations based on Mohriak et al. (1998).

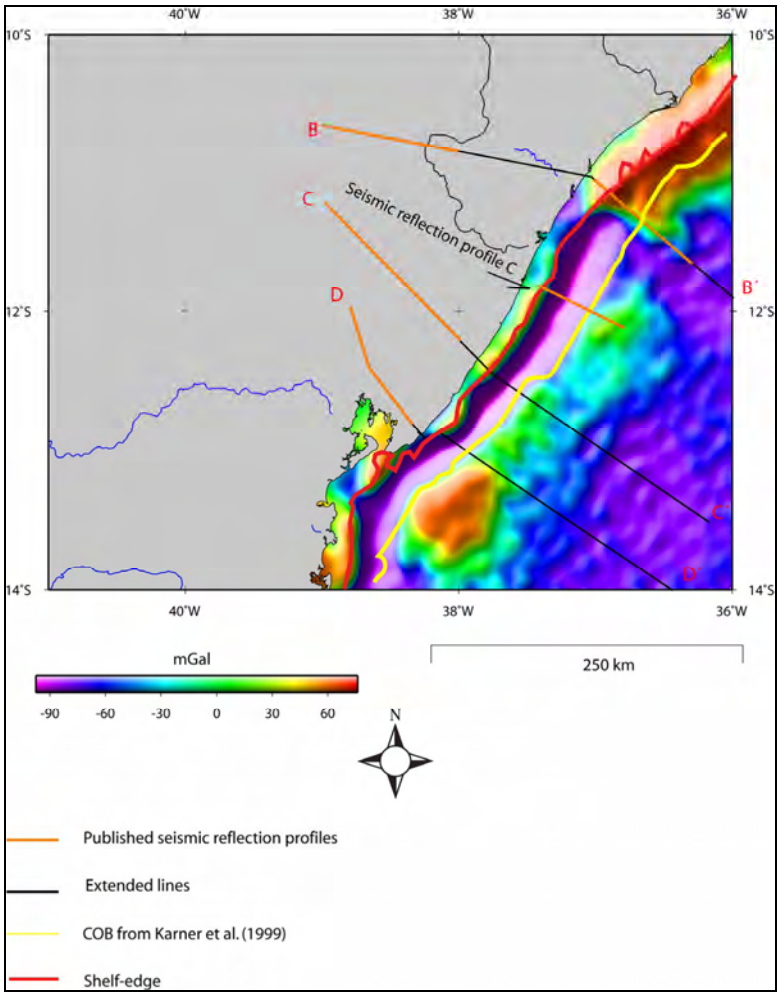

Fig. 6.12: 1x1 minute gridded satellite-radar-altimeter free-air gravity anomaly field (Sandwell & Smith, 1997; version 10.1) indicating the location of published profile inclusive seismic profile C.

6.4 Structural inheritance

Several studies on South Atlantic margins have postulated a pattern of structural inheritance, indicating that early Precambrian continental lineaments and transfer zones exerted influence on the development of the Mesozoic rifting, breakup and early oceanic crust (McConnel, 1974; Guazelli & Carvalho,1978; Meyers et al, 1996). Within the study area, the Vaza-Barris transfer zone may reflect an inherited Precambrian zone of crustal weakness that separated tectonic provinces during the Braziliano/Pan-African orogeny. It seems that this transfer zone is of deep-crustal origin and it is spatially related to the Sergipe F. Z. (Fig. 6.13). The Rio Muni-Gabon basins also exhibits transfer zones that apparently continue basinwards and join with oceanic fracture zones (Meyers et al., 1996). Furthermore, the Arcoverde Fault and Pernambuco Lineament, located on the Brazilian margin (Figs. 6.13 and 6.14) seems to be closely connected to and to define the onset of the Pernambuco Fracture Zone. These

transform systems are probably conjugate to the Sanaga Fault and Adamoua Fault system on the African margin (Fig. 6.14).

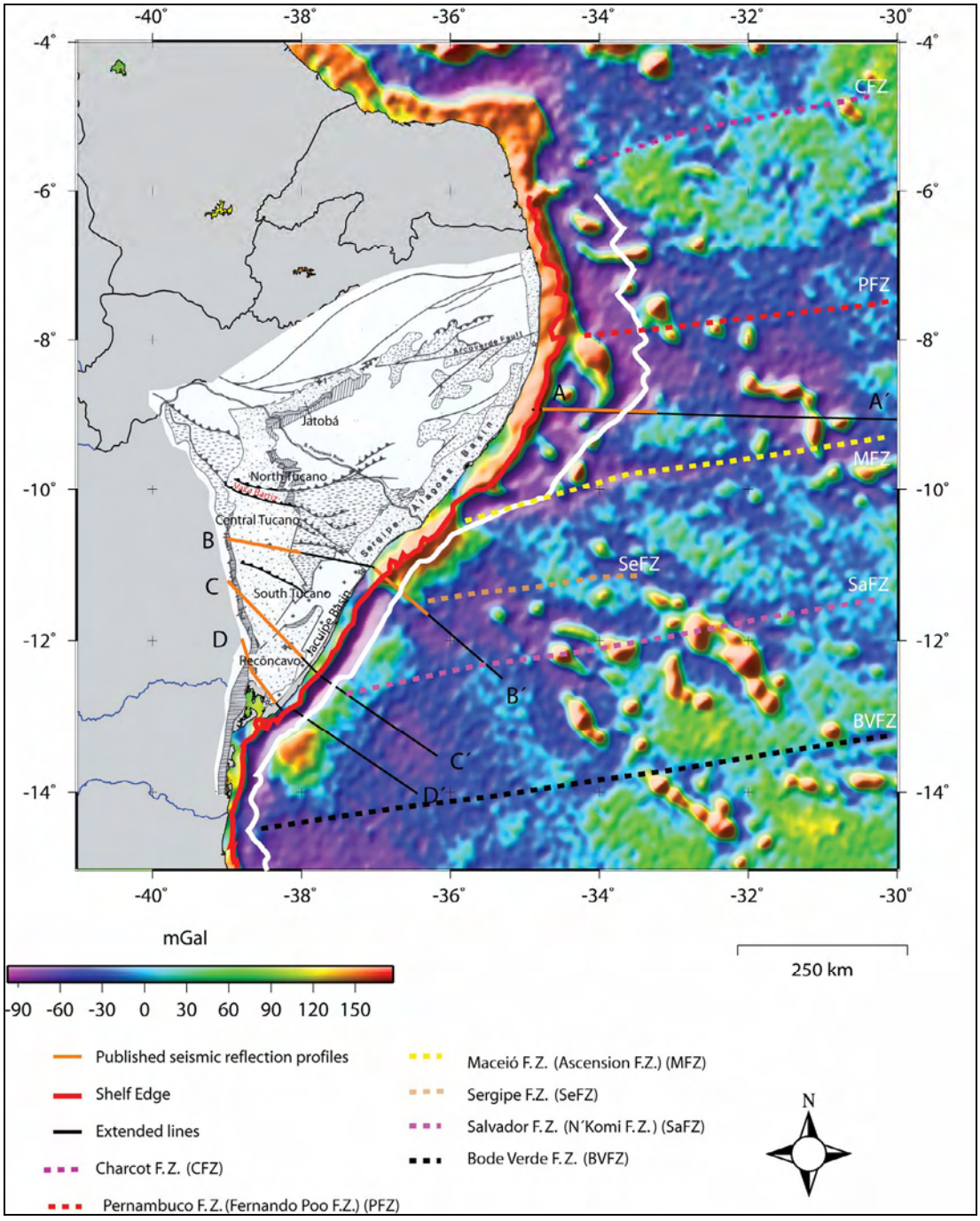

Fig. 6.13: Free-air gravity anomaly map with regional main tectonic elements along the northeastern Brazilian margin. The onset of the Sergipe F.Z. seems to have been determined by the transform fault system of Vaza-Barris. The published profiles and extended lines are also indicated. Structure map is modified from Ussami et al. (1986). The COT/COB is indicated by a white line and is based on Karner & Driscoll (1999).

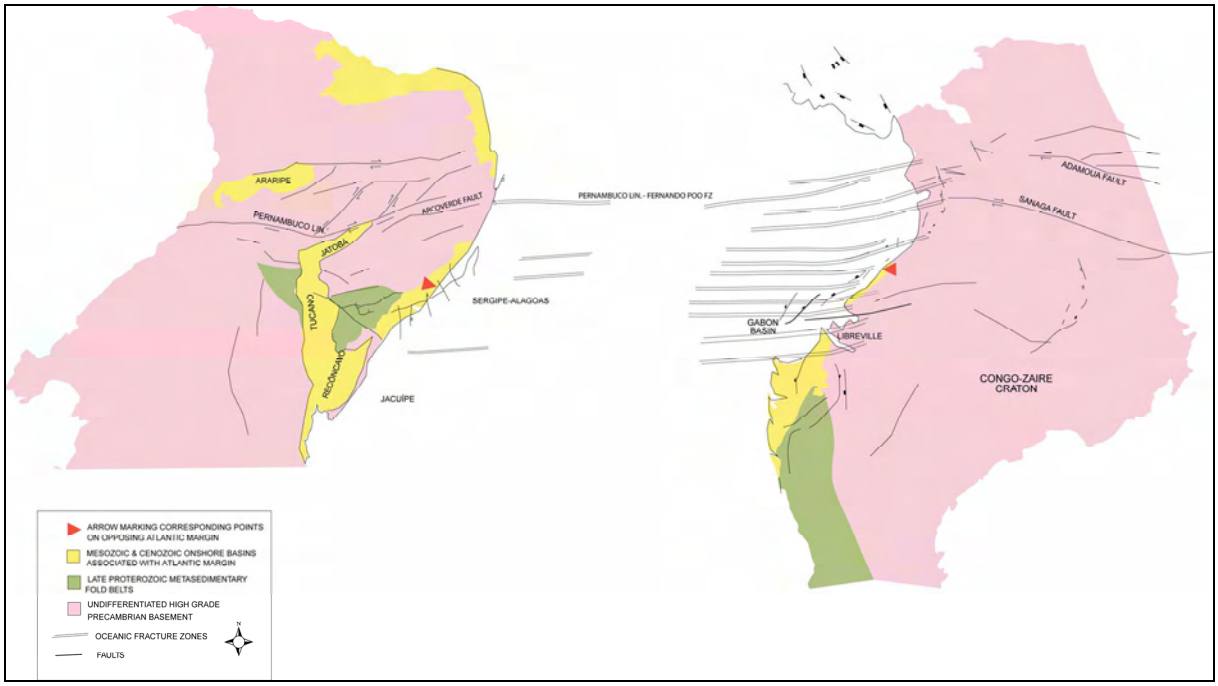

Fig. 6.14: Structural map of the Brazilian margin and its conjugate. The map show structural trends that are very similar on both conjugate margins (modified from Davison, 1999).

Chapter 7
Summary and conclusions

The integration of seismic reflection and potential field data has proven to be very useful in the study of crustal structure, continent-ocean boundary/transition, margin segmentation and plate reconstruction. The result of this work are presented in basemaps and in profiles located perpendicular to the continental margin.

The potential field basemaps present good information on the overall geological setting of the study area. The lines/profiles present detailed information on the Moho relief, crustal thickness, presence of LCB and the structural trend across the study area. Combined, they offer good information on the structural evolution of the region and tectonic setting during breakup and drift.

From the 2-D gravity modelling results (Fig. 6.1) it is observed that rifting and breakup of Africa and South America in the northern part of the study area (north of Maceió/Ascension F.Z.) occurred in an oblique setting, characterized by a gradual shallowing of Moho (slow rate of crustal thinning) and lack of SDR´s. This area probably evolved as a non-volcanic rift margin. The segment located between the Maceió/Ascension and Salvador/N´Komi fracture zones is characterized by rapid crustal thinning (rapid shallowing of Moho) and magmatic activity (SDR´s) indicating that rifting and breakup occurred in a more extensive setting. This segment evolved as a typical volcanic rift margin.

Continent-oceanic transition/boundary (COT/COB) was easily interpreted with the use of Bouguer-corrected gravity anomaly profile across line C-C´and D-D´ where the rift width is very small, indicating a short-lived rifting before breakup (Figs. 4.15 and 4.16). COT/COB is placed along a steep gradient of the Bouguer-corrected gravity anomaly. However, across line B-B´ and specially across A-A´ where the rift width is extensive, indicating prolonged rifting before breakup, the use of reflection seismic was crucial for defining COT/COB (Figs. 4.13

and 4.14). This observation stresses the importance of having an integration of seismic reflection and potential field data.

The offshore part of line C-C´ and D-D´ are lacking seismic reflection profiles, consequently these areas are lacking one important parameter used in this study. Moreover, it is important to keep in mind the fact that some of the data used in this work were based on published papers, meaning that some results will be constrained to the published paper. For example, the seismic reflection profile and Bouguer gravity anomalies used along the line B-B´ were based on publications from Mohriak et al. (2000), meaning that the result will be much influenced by the authors interpretations.

In the future it would have been very interesting to make a more profound study of the South Atlantic margins. With new/original data available, in particular deep seismic reflection and wide-angle refraction data, a better constrained study of the Brazilian margin would be achieved. The use of marine gravity and aeromagnetic data would also provide better constrain for the study. Moreover, studying additional segments of the Brazilian margin and extending the study to the conjugate margin off Africa would provide a broader understanding of the tectonic and structural setting of the South Atlantic rift system, making it possible for a complete study on the evolution and tectonic events influencing the opening of the South Atlantic Ocean. A plate tectonic reconstruction study would also help to determining and refining the timing of tectonic events.

References

Alan, E. M., and M. A. Khan, 2000. Looking into the Earth: an introduction to Geological Geophysics.

Alkmim, F. F., 2004. O que faz de um Cráton um Cráton? O Cráton do São Francisco e as revelacões Almeidianas ao delimitá-lo. Geologia do Continente Sul-Americano: Evolucão da obra de Fernando Flávio Marques de Almeida, p. 17-34.

Austin, J.A., and E. Uchupi, 1982. Continental-oceanic crustal transition off Southwest Africa. Am.Assoc.Pet.Geol.Bull., 66, v. 2, p. 1328-1347.

Barbier, F., J. Duvergé, and X. Le Pichon, 1986. Structure profonde de la marge Nord-Gascogne. Implications sur le méchanisme de rifting et de formation de la merge continentale. Bull. Cent. Rech. Explor.-Prod. Elf-Aquitaine, v. 10, p. 105-121.

Breivik, A., P. G. Granholm, B. Krokan and J. E. Rudjord, 1990. Tamp (Tyngde Anomaly Modellerings Program): A Gravity Anomaly Modelling Program. Version 3.1. Computer program/database documentation series no. 6., Geophysics Research Group, Department of Geology, University of Oslo.

Breivik, A.J., 1995. DEPTH: Depth convert seismic data. Version 1.0., Geophysics Research Group, Department of Geology, University of Oslo.

Castro, A.C.M., 1987. The northeastern Brazil and Gabon basins: a double rifting system associated with multiple crustal detachment surface. Tectonics, v. 6, no. 6, p. 727-738.

Chang, H.K., R. O. Kowsmann, A. M. F. Figueiredo, and A. A. Bender, 1992. Tectonic and stratigraphy of the East Brazil Rift system: an overview. Tectonophysics, v. 213, p. 97-138.

Cordell, L., and R. G. Henderson, 1968. Iterative three-dimensional solution of gravity anomaly data using a digital computer. Geophysics, v. 33, Issue 4, p. 596-601.

Darros De Matos, R. M., 1999. History of the northeastern Brazilian rift system: kinematic implications for the break-up between Brazil and West Africa. In: N.R.Cameron, R.H. Bate and V.S. Clure, eds., The Oil and Gas Habitats of the South Atlantic. Geological Society, London, Special Publication, 153, p. 55-73.

Davison, I., 1999. Tectonics and hydrocarbon distribution along the Brazilian South Atlantic margin. In: N.R.Cameron, R.H. Bate and V.S. Clure, eds., The Oil and Gas Habitats of the South Atlantic. Geological Society, London, Special Publication, 153, p. 133-151.

Durrheim, R. J., and W. D. Mooney, 1991. Archean and Proterozoic crustal evolution: Evidence from crustal seismology. Geology (Boulder)., 19, 6, p. 6006-6009.

Evans, D., C. Graham, A. Armour, and P. Bathurst, 2003. The Millennium Atlas: Petroleum Geology of the Central and Northern North Sea.

Gomes, P.O., B.S. Gomes, J.J.C. Palma, K. Jinno, and J.M. de Souza, 1997. Ocean-Continental Transition and tectonic Framework of the Oceanic Crust at the Continental Margin off NE Brazil: Results of LEPLAC Project. In: W.Mohriak and M.Talwani, eds., Atlantic Rifts and Continental Margins: Geophysical Monograph 115, p. 261-288.

Guazelli, W., and J. C. Carvalho, 1978. A extensao da Zona de fratura de Vitoria-Trindade no oceano, e seu possivel prolongamento no continente. In F. Carneiro, ed., Aspectos estruturais da margem continental leste e sudeste do Brasil. p. 31-38.

Guimarães, P.T.M., 1988. Basin analysis and structural development of the Sergipe-Alagoas Basin, Brazil. Ph.D. dissertation, The University of Texas, Austin, Texas, 171 p.

Jakobsson, M., 2000. Mapping of the Artic Ocean: Bathymetry and Pleistocene Paleoceanography. Ph.D. thesis. 94 p.

Katz, B.J., and M.R. Mello, 2000. Petroleum systems of South Atlantic Marginal basins-An overview, In: M.R. Mello and B.J. Katz, eds., Petroleum systems of South Atlantic margins: AAPG Memoir 73, p. 1-13.

Karner, G. D., S. S. Egan, and J. K. Weissel, 1992. Modeling the tectonic development of the Tucano and Sergipe-Alagoas rift basins, Brazil. Tectonophysics, v. 215, p. 133-160.

Karner, G.D., and N.W. Driscoll, 1999. Tectonic and stratigraphic development of the West African and eastern Brazilian Margins: insights from quantitative basin modelling. In: N.R.Cameron, R.H. Bate and V.S. Clure, eds., The Oil and Gas Habitats of the South Atlantic. Geological Society, London, Special Publication, 153, p. 11-40.

Karner, G.D., 2000. Rifts of the Campos and Santos Basins, Southeastern Brazil: Distribution and Timing. In: M.R. Mello and B.J. Katz, eds., Petroleum systems of South Atlantic margins: AAPG Memoir 73, p. 301-315.

Ludwig, G. M., J. E. Nafe, and C. L. Drake, 1970. Seismic refraction. The Sea, v. 4, p. 53-84, Maxwell, A. E. (red.), Wiley, New York.

McConnel, R. B., 1974. Evolution of taphrogenic lineaments in continental platforms. Geologische Rundschau, Stuttgart. v. 63, p. 389-430.

McKenzie, D., 1978. Some remarks on the development of sedimentary basins. Eath and Planetary Science Letters. v. 40, p. 25-32.

Meyers, J. B., B. R. Rosendahl., B. H. Groschel ., J. A. Jr. Austin, and P. A. Rona,1996. Deep penetrating MCS imaging of the rift-to-drift transition, offshore Douala and North Gabon basins, West Africa. Marine and Petroleum Geology. v. 13; 7, p. 791-835.

Milani, E.J., and I. Davison, 1988. Basement control and transfer tectonics in the Recôncavo-Tucano-Jatobá rift, northeastern Brazil. Tectonophysics, v. 154, p. 41-70.

Mjelde, R., A. J. Breivik., H. Elstad., A. E. Ryseth., J. R. Skilbrei., J. G. Opsal., H. Shimamura., Y. Murai, and Y. Nishimura, 2002. Geological develpment of the Sorvestsnaget Basin, SW Barents Sea, from oceanic bottom seismic, surface seismic and potential field data. Norsk Geologisk tidsskrift. v. 82, p. 183-202.

Mohriak, W.U., M. Bassetto, and I. S. Vieira, 1998. Crustal architecture and tectonic evolution of the Sergipe-Alagoas and Jacuípe basins, offshore northeastern Brazil. Tectonophysics. v. 288, p. 199-220.

Mohriak, W.U., M. Basseto, and I.S Vieira, 2000. Tectonic Evolution of the Rifted Basins in the Northeastern Brazilian Region. In: W.Mohriak and M.Talwani, eds., Atlantic Rifts and Continental Margins: Geophysical Monograph 115, p. 293-315.

Mohriak, W.U., M.R. Mello, M. Bassetto, I.S. Vieira, and E.A.M. Koutsoukos, 2000. Crustal Architecture, Sedimentation, and Petroleum Systems in the Sergipe-Alagoas Basin, Northestern Brasil. In: M.R. Mello and B.J. Katz, eds., Petroleum systems of South Atlantic margins: AAPG Memoir 73, p. 273-300.

Mohriak, W.U., and B. R. Rosendahl, 2003. Intraplate strike-slip deformation belts. Geological Society Special Publications. V. 210, p. 211-228.

Mohriak, W.U., 2004. Recursos energéticos associados à ativacão tectônica Mesozóico-Cenozóica da América do Sul. Geologia do Continente Sul-Americano: Evolucão da obra de Fernando Flávio Marques de Almeida, p. 293-318.

Mutter, J. C., 1985. Seaward dipping reflectors and the continent-ocean boundary at passive continental margins. Tectonophysics, v. 114, p. 117-131.

Nafe, J. E., and C. L. Drake, 1957. Variation with depth in shallow and deep water marine sediments of porosity, density and the velocities of compressional and shear waves. Geophysics, v. 22 Issue3, p. 523-552.

Nøttvedt, A., R.H. Gabrielsen, and R.J. Steel, 1995. Tectonostratigraphy and sedimentary architecture of the rift basins, with reference to the northern North Sea. Marine and Petroleum Geology., 12, 8, p. 881-901.

Planke, S., 1993. Section: Section plotting, digitizing, and utility program. Version 1.0. Computer program/database documentation series no. 4., Geophysics Research Group, Department of Geology, University of Oslo.

Pontes, C. E. S., F. C. C. Castro, J. J. G. Rodrigues, R. R. P. Alves, R. T. Castellani, S. F. Santos, and M. B. Monis, 1991. Reconhecimento tectônico e estratigráfico da Bacia Sergipe-Alagoas am águas profundas: Congresso Brasileiro de Geofísica, Salvador, Boletim de Resumos Expandidos, p.638-643.

Rabinowitz, P.D., and J. LaBrecque, 1979. The Mesozoic South Atlantic Ocean and Evolution of Its Continental Margins. J.Geophys. Res., v. 84, p. 5973-6002.

Sandwell, J.B., and W.H.F Smith, 1997. Marine Gravity Anomaly from Geosat and ERS-1 Satellite Altimetry. J. Geophys. Res., v. 102, p. 10039-10054.

Talwani, M., J. L. Worzel, and M. G. Landisman, 1959. Rapid gravity computations for two-dimensional bodies with application to the Mendocino submarine fracture zone (Pacific Ocean). J.Geophys. Res., v. 64, p. 49-59.

Talwani, M., and O. Eldholm, 1973. Boundary between Continental and Oceanic Crust at the Margin of Rifted Continents. Nature, v.241, p.325-330.

Tsikalas, F., 1992. A study of seismic velocity, density and porosity in the Barents Sea wells (N.Norway). Cand.Scient thesis, Department of Geology, Univ. of Oslo, pp. 169.

Tsikalas, F., O. Eldholm, and J. I. Faleide, 2005. Crustal structure of the Lofoten-Vesterålen continental margin, off Norway. Tectonophysics 404. p. 151-174.

Ussami, N., G.D. Karner, and M.H.P. Bott, 1986. Crustal detachment during South Atlantic rifting and formation of Tucano-Gabon rift system. Nature., v. 322, p. 629-632.

van der Pluijm, B. A., and S. Marshak, 1997. Earth structure: An introduction to structural geology and tectonics.

Watts, A. B., U. S. Ten-Brink, and T. M. Brocher, 1985. A multichannel seismic study of lithospheric flexure across the Hawaiian-Emperor seamount chain. Nature, 315; 6015, p. 105-111.

Watts, A. B., 1988. Gravity anomalies, crustal structure and flexure of the lithosphere at the Baltimore Canyon Trough, Earth Planet. Sc. Lett. V. 89, p. 221-238.

Watts, A. B., 2001. Gravity anomalies, flexure and crustal structure at the Mozambique rifted margin. Marine and Petroleum Geology, v. 18, p.445-455.

Wernicke, B., 1985. Uniform-sense normal simple shear of the continental lithosphere. Can. J. Earth Sci., v. 22, p. 108-125.

Wessel, P., and W.H.F Smith, 1998. New version of the Generic Mapping Tools., EOS Transactions v. 79, American Geophysical Union., p. 579., release editor http://gmt.soest.hawaii.edu/

White, R.S., and D. P. MacKenzie, 1989. Magmatism at Rift Zones: The Generation of Volcanic Continental Margins and Food Basalts. J. Geophys. Res., v. 94, B6, p. 7685-7729.

White, R.S., D. P. McKenzie, and K.R. O'Nions, 1992. Oceanic crustal thickness from seismic measurements and rare earth element inversions, J.Geophys. Res., v. 97 B13, p. 19683–19715.

Wilson, P. G., J. P. Turner, and G. K. Westbrook, 2003. Structural architecture of the ocean-continent boundary at an oblique transform margin trough deep-imaging seismic interpretation and gravity modelling: Equatorial Guinea, West Africa. Tectonophysics v. 374, p. 19-40.